UNIVERSITÀ DEGLI STUDI DI SALERNO

DIPARTIMENTO DI FARMACIA

DOTTORATO DI RICERCA IN SCIENZE FARMACEUTICHE
XIV CICLO (X-Ciclo Nuova Serie)
2008-2012

"Proteomic profiles of cultured cells stimulated with VEGFs dimers and search for natural compounds angiogenesis inhibitors"

Tutor
Prof. Fabrizio Dal Piaz
Prof. Sandro De Falco

PhD Student
Mariasabina Pesca

Coordinator
Prof.ssa Nunziatina De Tommasi

Abbreviations:

2-DE = two-dimensional gel electrophoresis
Akt = Protein Kinase B
AMD = age-related macular degeneration
Bcl-2 = B-cell lymphoma 2
BF-2 = Brain Factor 2
CAM = chicken chorioallantoic membrane
CHCl3 = Chloroform
CRC = colorectal cancer
DTT = dithiothreitol
ECD = Electronic Circular Dicroism
ECs = endothelial cells
ECM = extracellular matrix
EGF = epidermal growth factor
ELISA = Enzyme-Linked Immunosorbent Assay
eNOS = endothelial nitric oxide synthase
ERK1/2 = Extracellular Regulated Kinase 1 and 2
FDA = Food & Drug Administration
FGF = fibroblast growth factors
Flk-1 = fetal liver kinase 1
Flt-1= fms-related tyrosine kinase 1
FOXD1 = forkhead box D 1
HEK-293hFlt-1 = Human Embryonic Kidney 293 cells expressing human Flt-1
HIF= hypoxia-inducible factor
HNF3B = Hepatocyte nuclear factor 3-beta

HPLC = High Performance Liquid Chromatography

HRE = hypoxia responsive element

HSA = human serum albumin

HSCs = hematopoietic stem cells

HTS = High Throughput Screening

HUVECs = Human Umbilical Vein Endothelial Cells

HRP = enzyme horseradish peroxidase

IEF = isoelectric focusing

IL = interleukin

KDR = kinase insert domain receptor

LPLC = Low Pressure Liquid Chromatography

m/z = Mass-to-charge ratio

Mab = monoclonal antibody

MAPK = mitogen activated protein kinase

MeOH = Methanol

MBC = metastatic breast cancer

MCF-7 = breast cancer cell line

MMPs = matrix metalloproteinase

MPLC = medium pressure liquid chromatography

MS/MS = Tandem Mass Spectrometry

MTF-1 = metal transcription factor

Mw = apparent molecular weight

NF-κB = nuclear factor kappa-light-chain-enhancer of activated B cells

NIH 3T3 = Mouse embryonic fibroblast cell line

NMR = Nuclear magnetic resonance spectroscopy

NP = neuropilin

NSCLC = non-small-cell lung cancer

ORF = open reading frame

PAs = plasminogen activator system

PDGF = platelet-derived growth factor

pI = isoelectric point

PI 3-kinases = Phosphatidylinositide 3-kinases

PKC = protein kinase C

PLC = phospholipase C

PlGF = placental growth factor

PlGF/VEGF = heterodimer between VEGF-A and PlGF (also written VEGF/PlGF)

Q-TOF = quadrupole-time of flight

Ras/Raf/MEK/Map kinase pathway = a group of cellular proteins that play a key role in cellular growth and proliferation

RTKs = receptor tyrosine kinases

RTKIs = receptor tyrosine kinases inhibitors

SDS-PAGE = Sodium Dodecyl Sulphate - PolyAcrylamide Gel Electrophoresis

SPR = Surface Plasmon Resonance

Shb = SH2 domain-containing adapter protein B

sFlt-1 = soluble Flt-1

TGF = transforming growth factors

TSAd = T cell specific adapter

VEGFs = vascular endothelial growth factors

VEGFR = vascular endothelial growth factors receptor

VHL = von Hippel-Lindau

VPF = vascular permeability factor

Y = phosphorylated tyrosine residues.

ABSTRACT

Some members of the vascular endothelial growth factor (VEGF) family, such as VEGF and PlGF, and related receptors (KDR and Flt-1) play a key role in the modulation of angiogenesis, both physiological and pathological. For this reason they are considered valid therapeutic targets. Anti-angiogenesis therapy, despite the scientific efforts and promising results, is still suffering of some limitations.

In the attempt to produce a research that can facilitate the future development of new antiangiogenic therapy strategies, we realized these goals: 1) carry out an expression proteomic study of cell coltures, after their treatment with some dimers of VEGF family; 2) identify new natural compounds able to inhibit the axis of interaction VEGF/Flt-1 and PlGF/Flt-1.

We used gel-based proteomics to detect the differentially expressed proteins by VEGF, PlGF and VEGF/PlGF, in HUVECs and HEK-293-hFlt-1. Gels variability was also determined by principal component analysis (PCA). Statistically significant spots were enzimatically digested and analyzed by nano-LC-ESI-MS/MS analysis, allowing to achieve protein identifications.. Different treatments shared the modulation of a number of proteins. This aspect was particularly marked in HUVECs. This implies that in HUVEC, more biological events, due to the presence of both receptors involved in angiogenesis, might be found. For some of identified proteins, few data were already reported in the literature thus confirming the reliability of all the collected data. The functional annotation clustering evidenced the different physiology between the two cell cultures, and the different endothelial roles exerted by the selected VEGF dimers and related receptors. All the achieved data will pave the way for future studies on understanding the functional

mechanism of endothelial cells in response to different vascular endothelial growth factors.

In order to identify plant compounds able to interfere in the VEGFs/VEGFR-1 (Flt-1) recognition by VEGFs family members, we screened a small libraries of plant extracts. By using this bioassay-oriented approach five proantocyanindins, including the new natural compounds (2S)-4',5,7-trihydroxyflavan-(4β→8)-afzelechin (**1**) and (2S)-4',5,7-trihydroxyflavan-(4β→8)-epiafzelechin (**2**), and the known geranin B (**3**), proanthocyanidin A2 (**4**), and proanthocyanidin A1 (**5**), were also isolated. The study of the antiangiogenic activities of compounds **1**-**5** using ELISA and SPR assays showed compound **1** as being the most active. The antiangiogenic activity of **1** was also confirmed in vivo by the chicken chorioallantoic membrane (CAM) assay. Our results indicated **1** as a new antiangiogenic compound inhibiting the interaction between VEGF-A or PlGF and their receptor VEGR-1.

Publications

1. Malafronte N, Pesca MS, Bisio A, Escobar LM, De Tommasi N. New flavonoid glycosides from *Vernonia ferruginea.* Natural Product Communications (2009), 4(12), 1639-1642.
2. Cioffi G, Pesca MS, De Caprariis P, Braca A, Severino L, De Tommasi N. Phenolic compounds in olive oil and olive pomace from Cilento (Campania, Italy) and their antioxidant activity. Food Chemistry (2010), 121(1), 105-111
3. Olivieri S, Conti A, Iannaccone S, Cannistraci CV, Campanella A, Barbariga M, Codazzi F, Pelizzoni I, Magnani G, Pesca M, Franciotta D, Cappa SF, Alessio M. Ceruloplasmin oxidation, a feature of Parkinson's disease CSF, inhibits ferroxidase activity and promotes cellular iron retention. Journal of Neuroscience (2011), 31(50), 18568-18577.
4. Lepore L, Pesca M, De Tommasi N, Carputo D, Dal Piaz F. Studio dei metaboliti secondari di varietà precoci di *Solanum tuberosum*. Minerva Biotecnologica (2012), 24 , 43-50
5. Pesca M, Dal Piaz F, Sanogo R, Vassallo A, Bruzual de Abreu M, Rapisarda A, Germanò MP, Certo G, De Falco S, De Tommasi N, Braca A. Bioassay-Guided Isolation of Proanthocyanidins with Antiangiogenic Activities. Journal of Natural Products (2012) Manuscript ID: np-2012-00614u, accepted.
6. Vassallo A, Pesca M, Ambrosio L, Malafronte N, Dekdouk Melle N, Dal Piaz F, Severino L. Antiproliferative Oleanane Saponins from *Dizygotheca elegantissima*. Natural Product Communications (2012), 7(11), 1427-30

Participation in Conferences

1. L. Lepore, M. Pesca, N. Malafronte, D. Carputo, F. Dal Piaz, N. De Tommasi. *Solanum tuberosum* metabolic fingerprint using spectroscopic and spectrometric techniques. *XVIII Congreso Italo-*

Latino Americano De Etnomedicina, Ciudad de La Habana, Cuba, (14-18 settembre 2009)

2. M. J. Gualtieri, N. Malafronte, M.S. Pesca, F. Dal Piaz, N. De Tommasi. Studio fitochimico della *Polyscias Guilfoylei* (W.BULL) L.H.BAILEY. *XIX Congresso SILAE*, Cagliari, Italia, (6-10 settembre 2010)
3. A.Conti, N. Riva, M. Pesca, A. Quattrini, S. Previtali, S. Iannaccone, M. Alessio. Proteomic differential analysis of human muscle biopsies of ALS patients versus healthy controls. *HSR SCIENTIFIC RETREAT* Stresa, Italy (February 11th-13th, 2011)
4. F. Dal Piaz, M. Alessio, S. De Falco, A. Conti, N. De Tommasi, M. Pesca. Clarifying the signal network of antiangiogenic amentoflavone using proteomic approach. *Trends in natural products research a PSE young scientists' meeting,* Kolymvari, Crete (June 12-15, 2011)
5. M. Pesca, L. Ambrosio, L. Tudisco, A. Vassallo, R. Sanogo, F. Dal Piaz, S. De Falco, N. De Tommasi. Effetti antiangiogenici di *Feretia Apodanthera* Del. *Congresso Interdisciplinare sulle Piante Medicinali,* Cetraro (CS), Italia (31 Maggio - 2 Giugno, 2012)
6. M. Pesca, V. Hernández, N. Malafronte, F. Mora, F. Dal Piaz, A. Vassallo, P. Meléndez, N. De Tommasi. Biological activity of 1,2,3,4,6-pentagalloyl glucose from A*stronium graveolens. XXI Congresso SILAE,* Paestum, Italia (26-29 settembre 2012)
7. M. Pesca, F. Dal Piaz, N. Malafronte, S. De Falco, N. De Tommasi. Analisi del proteoma della linea cellulare HUVEC trattata con amentoflavone. *Scuola di Fitochimica "P. Ceccherelli",* Paestum, Italia (5-7 Ottobre 2012)

INDEX

CHAPTER 1:

Introduction

1.1 Formation of blood vessels

In vertebrates, transport of nutrient, oxygen and cells is mediated by extensive and highly organized tubular network that is mainly formed by endothelial cells (ECs).

Blood vessels are responsible for systemic circulation, while the lymphatic vasculature drains extravasated plasma, proteins, particles, and cells from the interstitium. In particular, blood vessels supply oxygen and nutrients and produce instructive signals to promote organ morphogenesis and allow haematopoietic cells to patrol the organism for immune surveillance (Carmeliet and Jain, 2011).

The three known processes aimed to blood vessels formation and remodeling are: “vasculogenesis”, “angiogenesis” and “arteriogenesis” (figure 1) (Carmeliet, 2004). The term “vasculogenesis” identifies *de novo* blood vessels formation. During embryogenesis, endothelial progenitor cells migrate to sites of vascularization and differentiate into ECs forming the initial vascular plexus (Semenza, 2007). Already at this stage capillaries are endowed with an arterial and venous character, thus showing that vascular-cell specification is genetically programmed and not only determined by haemodynamic factors. During angiogenesis, the vascular plexus progressively expands by means of the formation of new blood vessels starting from the pre-assembled ones. Pericytes and smooth muscle cells cover the nascent endothelial-cell channels committed to the arterial fate allowing the vessels perfusion. This process is named “arteriogenesis”(Carmeliet, 2005).

The lymphatic system develops differently, as most lymphatic vessels transdifferentiate from a subset of veins (Alitalo et al., 2005).

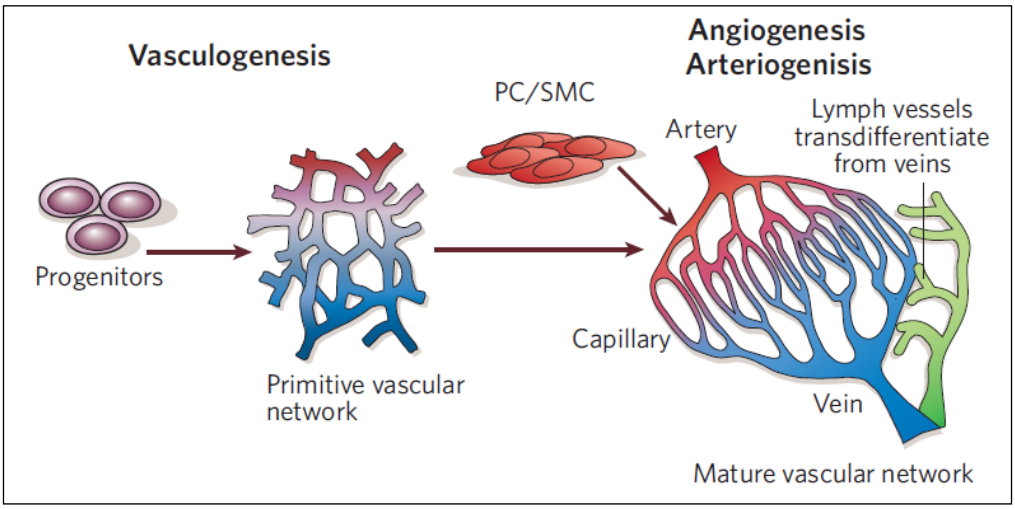

Fig. 1. Development of the vascular systems: during vasculogenesis, endothelial progenitors give rise to a primitive vascular labyrinth of arteries and veins; during subsequent angiogenesis, the network expands, pericytes (PCs) and smooth muscle cells (SMCs) cover nascent endothelial channels, and a stereotypically organized vascular network emerges. Lymph vessels develop via transdifferentiation from veins (adopted and modified by Carmeliet, 2005).

1.2 Basic aspects of angiogenesis

Angiogenesis is a complex multistep process that requires an extensive interplay between a variety of cells, soluble factors, and extracellular matrix (ECM) components.

At the onset of sprouting, endothelial cells of existing blood vessels degrade the underlying basement membrane and invade into the stroma of the neighboring tissue. This process requires the cooperation of the plasminogen activator system (PAs) and the matrix metalloproteinases (MMPs). These activate plasmin, an important enzyme present in blood that degrades several ECM components. Angiogenic growth factors, cytokines and other proteins control the activity and the expression of both PAs and MMPs. PAs and MMPs are secreted together with their inhibitors, ensuring a strict control on local proteolytic activity, thus preserving the tissue structure (Mignatti and

Rifkin, 1996; Bikfalvi et al. 1997; Blasi 1997; Westermarck et al., 1999). Following proteolytic disintegration of basement membrane, a variety of growth factors stimulates ECs migration and proliferation. These angiogenesis inducers can be divided into three classes: the first one consists of the vascular endothelial growth factors (VEGFs) family and the angiopoietins, specifically acting on ECs; the second class includes many direct-acting molecules, such as cytokines, chemokines, and angiogenic enzymes that activate many target cells; the third group of angiogenic molecules is represented by the indirect-acting factors, whose effect on angiogenesis is the release of direct-acting factors from macrophages, endothelial or tumor cells.

The processes of ECs invasion, migration, and proliferation not only depend on angiogenic enzymes, growth factors and their receptors, but also on cell–cell contacts and cell–ECM interactions, mediated by specific adhesion molecules. These are classified on the base of their biochemical and structural characteristics into four families as follows: the selectins, the immunoglobulin supergene family, the cadherins, and the integrins (Liekens et al., 2001).

1.3 Physiological and pathological angiogenesis

After birth, angiogenesis contributes to organ growth but during adulthood most of the blood vessels remain quiescent. However, ECs keep their remarkable ability of dividing rapidly and under some conditions, such as the cycling ovary, the pregnancy, the physical exercise, the wound healing, or in response to a specific stimulus (for example hypoxia); therefore angiogenesis can be reactivated. The normal and healthy body controls angiogenesis through a series of “on” switches, known as angiogenesis factors (cytokines) and “off” switches, known as endogenous angiogenesis inhibitors (table 1).

	Stimulators	Inhibitors
Growth Factors	Angiogenin Angiotropin Epidermal growth factor (EGF) Fibroblast growth factor (acidic and basic) (FGF) Granulocyte colony-stimulating factor (G-CSF) Hepatocyte growth factor/scatter factor (HGF/SF) Placental growth factor (PlGF) Plateled-derived endothelial cell growth factor (PD-ECGF) Platelet-derived growth factor-BB (PDGF-BB) Transforming growth factor alpha and beta (TGF-alpha/beta) Tumor necrosis factor-alpha (TNF-alpha) Vascular endothelial growth factor/Vascular permeability factor (VEGF/VPF)	Transforming growth factor beta (TGF-beta) Tumor necrosis factor-alpha (TNF-alpha)
Proteases and Protease Inhibitors	Cathepsin Gelatinase A, B Stromelysin Urokinase-type plasminogen activator (uPA)	Heparinases Plasminogen activator-inhibitor-1 (PAI-1) Tissue inhibitor of metalloprotease (TIMP-1, TIMP-2)
Endogenous Modulators	Alpha v Beta 3 integrin Angiopoietin-1 Endothelin (ETB receptor) Erythropoietin Follistatin Hypoxia Leptin Midkine (MK) Nitric oxide synthase (NOS) Platelet-activating factor (PAF) Pleiotropin (PTN) Prostaglandin E Thrombopoietin	Angiopoietin-2 Angiostatin Caveolin-1, caveolin-2 Endostatin Fibronectin fragment Heparin hexasaccharide fragment Human chorionic gonadotropin (hCG) Interferon-alpha, beta, gamma Interferon inducible protein (IP-10) Isoflavones Kringle 5 (plasminogen fragment) 2-Methoxyestradiol Placental ribonuclease inhibitor Platelet factor-4 Prolactin (16 Kd fragment) Proliferin-related protein (PRP) Retinoids Tetrahydrocortisol-S Thrombospondin Troponin-1 Vasculostatin
Cytokines	Interleukin-1 Interleukin-6 Interleukin-8	Interleukin-10 Interleukin-12
Signal Transduction Enzymes	Thymidine phosphorylase Farnesyl transferase Geranylgeranyl transferase	
Oncogenes	c-myc , ras , c-src , v-raf, c-jun	p53, Rb

Tab. 1. Endogenous positive and negative regulators of angiogenesis.

In many disorders, the perfect balance between angiogenesis modulators is compromised; angiogenesis has been implicated in more than 70 disorders so

far and the list is ever growing. In particular, when angiogenic growth factors are produced in excess over angiogenesis inhibitors, the balance is moved in favor of blood vessels growth. Vice versa, when inhibitors exceed stimulators, angiogenesis is stopped. Persistent and up-regulated angiogenesis is often a diagnostic factor of severe pathologies such as cancer, atherosclerosis, and diabetic retinopathy. Instead, insufficient angiogenesis is a characteristic of coronary artery disease (CAD), cardiac failure, tissue injury, etc. Angiogenesis has been implicated in more than 70 disorders so far and the list is ever growing. (Carmeliet 2003; Carmeliet, 2005).

1.4 VEGF family

New vessels growth and maturation require the sequential activation of a series of receptors by means of numerous ligands. However, among these VEGF signaling represents the key rate-limiting step (Ferrara et al., 2003).
In mammalians, five VEGF ligands (occurring in several different splice variants and processed forms) have been identified:

- ✓ VEGF-A
- ✓ VEGF-B
- ✓ PlGF (placental growth factor)
- ✓ VEGF-C
- ✓ VEGF-D

All these factors are secreted as dimeric and glycosilated proteins of approximately 40 kDa. Structurally (figure 2) they are characterized by a common motif represented by eight cysteine residues specifically spaced in a conserved domain. This is called “cysteine –knot motif”. The crystal structure of VEGF-A shows that the dimer is formed by two monomers ordered in an anti-parallel fashion, with the receptor-binding site located at each pole of the

dimer. The VEGFs form also heterodimers if co-expressed in the same cell. Proteins that are structurally related to the VEGFs exist in parapoxvirus (VEGF-E) and snake venom (a group of proteins known as VEGF-Fs).

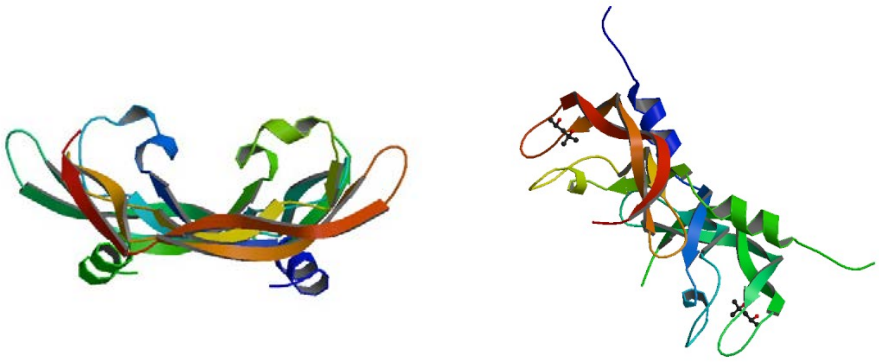

a) b)

Fig. 2. a) Structure of human Vascular Endothelial Growth Factor (PDB code: 1VPF); b) The crystal structure of human Placenta Growth Factor-1 (PLGF-1), an angiogenic protein at 2.0a resolution (PDB code: 1FZV)

The VEGF family presents different biological and physical properties. VEGF-A, VEGF-B and PlGF are mainly involved in the angiogenesis, while VEGF-C and VEGF-D in the lymphangiogenesis. Their biological activities are due to the interactions with the extracellular domains of receptor tyrosine kinases (RTKs) (figure 3). These receptors are known as:

- ✓ VEGFR-1 (also known as Flt-1, fms-like tyrosine kinase)
- ✓ VEGFR-2 (also named KDR, kinase domain receptor, in human and Flk-1, Fetal liver kinase-1, in mouse)
- ✓ VEGFR-3 (also known as Flt-4)

Some ligand isoforms are able to bind also co-receptors such as neuropilins (NP-1 and NP-2), other than heparin sulphate proteoglycans (HSPGs). The binding induces the RTKs dimerization. Each protein kinase monomer phosphorylates a distinct set of tyrosine residues in the cytosolic domain of its dimer partner (a process termed autophosphorylation) and finally a cascade of

downstream proteins is activated. Through this fine mechanism, diverse angiogenic signals, including cell migration, survival and proliferation, are propagated. Thus, VEGRs play a key role in the signal transduction aimed at the formation of the new vessels and the regulation of vascular permeability (Rahimi , 2006; Roy et al., 2006; Otrock et al., 2007; Koch et al., 2011).

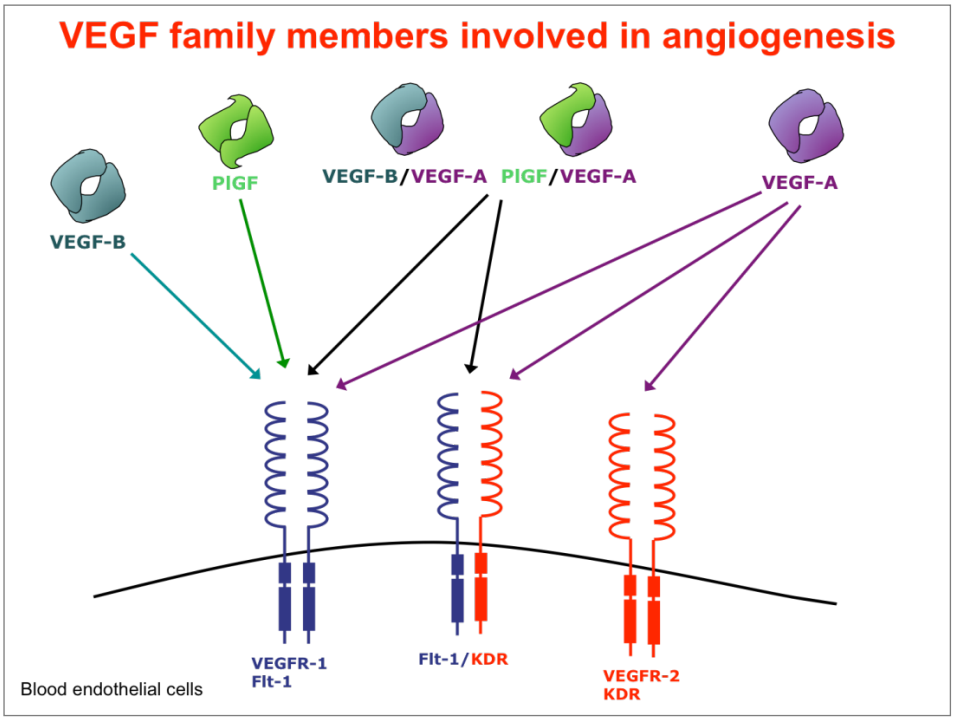

Fig. 3. Schematic representation of the Vascular Endothelial Growth Factors family members involved in angiogenesis.

A detailed description of some members of VEGF family is here after reported.

1.5 VEGF-A

VEGF-A (also known as VEGF) is the the most studied member of VEGF family. It plays a key role in the onset of angiogenesis, vasculogenesis and

lymphangiogenesis. The *vegf* gene is located in the short arm of chromosome 6, formed by approximately 14 kb and containing 8 exons and 7 introns.

VEGF-A transcription is up-regulated in hypoxia condition through a fine mechanism. In particular, hypoxia-inducible factor–1α (HIF–1α) binds to the hypoxia responsive element (HRE) in the VEGF-A gene promoter region, which in turn increases the transcription of VEGF-A. Through the same mechanism, the transcription of other genes implicated in glucose transport, glycolysis and angiogenesis is also activated. Recent studies report the role of von Hippel-Lindau (VHL) tumor suppressor gene in HIF-1-dependent hypoxic responses. Also other pathways involving different growth factors can increase the expression of VEGF-A (Semenza, 2002; Mole at al. 2001). For instance, epidermal growth factor (EGF), transforming growth factors (TGF-α, TGF-β), keratinocyte growth factor, insulin-like growth factor-1, fibroblast growth factors (FGF) and platelet-derived growth factor, are able to up-regulate VEGF mRNA expression. This suggests that paracrine or autocrine systems deal with local hypoxia by regulating VEGF release. Some inflammatory cytokines (IL-1α, IL-6α) also induce VEGF-A gene expression supporting the hypothesis that VEGF-A is a mediator of permeability in inflammatory disorders. Finally, it has been also demonstrated that VEGF-A is up-regulated by mutations or amplification of Ras (Rat sarcoma) (Neufeld et al., 1999; Ferrara et al., 2003; Otrock at al., 2007).

VEGF exists in four different isoforms (comprising 121, 165, 189 and 206 amino acids in humans), which are generated by alternative splicing of a single pre-mRNA species. Among these, VEGF165 is the predominant isoform. However, isoforms that are expressed at lower extent were also identified (VEGF145 and VEGF183). Isoforms differ in their ability to bind to heparin sulfate and extracellular matrix (ECM) (Park et al., 1993; Ferrara et al., 2003).

VEGF-A exerts its biologic effects through interaction with the receptors Flt-1 and KDR/Flk-1 and with the co-receptors NP-1 and NP-2. It is the most potent

pro-angiogenic protein. VEGF-A induces proliferation, sprouting and tube formation of endothelial cells (ECs) and exerts many effects on a broad range of not-ECs types. It is also a potent survival factor, both *in vitro* and *in vivo*. In ECs it induces the expression of antiapoptotic proteins (Bcl-2 and A-1). VEGF-A was originally described as vascular permeability factor (VPF) but it is also involved in vascular leakage (a key process in inflammation and other pathological conditions) through the formation of intercellular gaps, vescico-vascular organelles, vacuoles and fenestration in some vascular beds. Furthermore, it increases the hydraulic conductivity of isolated microvessels, through an accentuation of calcium influx. This growth factor causes vasodilatation through the release of nitric oxide by inducing the endothelial nitric oxide synthase (eNOS). VEGF-A promotes the mobilization of hematopoietic stem cells (HSCs) from the bone marrow, monocyte chemotaxis, osteoblast-mediated bone formation and neuronal protection. Furthermore, it stimulates inflammatory cell recruitment and the expression of proteases implicated in pericellular matrix degradation in angiogenesis.

VEGF-A is essential mainly during embryonic and early postnatal development. The loss of a single *vegf* allele is lethal in the mouse embryo between days 11 and 12. These embryos present some developmental anomalies, not well-vascularized organs and a low number of nucleated red blood cells. Inhibition of VEGF during early postnatal life, increases mortality, stunts the body growth and impairs organ development and skeletal growth. In juvenile primates it results in abnormalities in physiological angiogenesis. On the other hand, transgenic mice with over-expression of VEGF-A in the skin, develops a psoriasis-like skin condition and accelerates experimental tumor growth. In humans, VEGF-A is expressed in most of all solid tumors as well as in some hematological malignancies. VEGF is also implicated in the pathogenesis of diabetes mellitus, having a major role in the onset of vitreous hemorrhages, retinal detachment, neovascular glaucoma and blindness

correlated with this pathology. Recent studies showed the presence of VEGF in choroidal neovascular membranes of age-related macular degeneration (AMD) patients. It has been reported that this presence is correlated to neovascularization and vascular leakage that cause AMD. Finally, VEGF is involved in many inflammatory disorders and it cooperates in induction of angiogenesis associated to polycystic ovary syndrome, endometriosis and preeclampsia. (Ferrara et al., 2003; Tammela et al., 2005; Otrock et al., 2007; Roy et al. 2006).

1.6 PlGF

The human *plgf* gene is located on chromosome 14q24 and is formed by 7 exons spanning on 12 qD. Using alternative splicing processe, PlGF can be expressed in four isoforms, named PlGF-1, -2, -3 and -4 composed by 131, 152, 203 and 224 amino acids, respectively. They differ in the ability to bind heparan sulfate proteoglycans (Maglione et al., 1993a; DiPalma et al., 1996).
Although some reports indicated an upregulation of PlGF in cells exposed to hypoxia, the analysis of promoter/enhancer region of PlGF did not show active HRE sequence as observed also for VEGF-A (Green et al., 2001; Oura et al., 2003; Selvaraj et al., 2003). However, PlGF gene promoter includes many recognition sequences for metal transcription factor 1 (MTF-1) and for NF-κB. These sequences are typically involved in the modulation of PlGF expression in hypoxic condition (Green et al., 2001). Moreover, overexpression of HIF-1α in endothelial cells or in primary cardiac and vascular cells up-regulates the expression of PlGF. Moreover, PlGF expression is modulated also by the forkhead/winged helix transcription factor FoxD1 (BF-2) in the developing kidney stroma. This is possible given the presence of a conserved HNF3b binding site on PlGF promoter region (Zhang et al., 2003). Finally, PlGF

expression is also post-transcriptionally regulated by other growth factors and oncogenes (Maglione et al., 1993b).

The pro-angiogenic activity of PlGF is exerted through the binding and the activation of VEGFR-1. This growth factor shows the highest affinity if compared to those of the other members of the same family.

PlGF may also activate VEGFR-2 indirectly, using one of the following mechanisms:

- ✓ VEGFR-1, once activated by PlGF, can transphosphorylate VEGFR-2
- ✓ PlGF, upon binding to VEGFR-1, makes VEGF-A available for the binding and activation of VEGFR-2
- ✓ PlGF and VEGF-A, if co-expressed from the same cells, can form heterodimers able to activate VEGFR-1 or to induce VEGFR-1/VEGFR-2 heterodimerization.

Furthermore PlGF-2 is able to bind the two coreceptors NP1 and NP2 (Autiero et al., 2003).

PlGF was originally discovered in placenta. It is also expressed in throphoblastic giant cells associated with the parietal yolk sac, during early embryonic development. At cellular level, the expression of PlGF was demonstrated in endothelial cells, thyroid transformed mouse embryonic fibroblast, NIH 3T3 cells and a limited number of tumor-derived cell lines.

PlGF knockout mice do not have an evident phenotype. They born at medelian frequency, are healthy and fertile but present an impaired angiogenesis when pathological conditions are induced such as tumor growth, heart or limb ischemia, choroid neovascularization. This strongly indicates that PlGF is involved only in pathological angiogenesis and not in physiological angiogenic process. Overexpression of PlGF in the skin of transgenic mice results in a significant increase in the number and size of skin blood vessels, in number of mature smooth muscle-coated vessels and in enhanced vascular permeability. Accordingly, adenovirus-mediated PlGF transfer in the ischemic

heart and limb was able to induce a strong angiogenic response, forming numerous larger vessels, with an efficacy almost comparable to that of VEGF-A (Luttun et al., 2002). The same approach used in xenograft tumors did not show an increase of tumor volume and vessel density, however it generated an increment of the vessel lumen, of the inflammatory infiltrate and of the vessel maturation (Tarallo et al., 2010). Recombinant PlGF homodimer or PlGF/VEGF heterodimer significantly promoted angiogenesis in ischemic conditions (Luttun et al., 2002; Autiero et al., 2003).

Futher studies demonstrated that PlGF promoted pathological angiogenesis by stimulating vessel growth and maturation. In particular, it acts on the growth, migration and survival of endothelial cells, increases the proliferation and recruitment of smooth-muscle cells and supports the proliferation of fibroblasts. Finally, PlGF is crucial for the recruitment and maturation of bone marrow derived progenitors and the differentiation and activation of monocyte-macrophage (De Falco, 2012).

1.7 VEGFR-1 and VEGFR-2

Human VEGFR-1 and VEGFR-2 are transmembrane glycoproteins of 180 and 200 kDa, respectively. They are structurally related to the platelet-derived growth factor (PDGF) receptor family and contain (figure 4):

- ✓ an extracellular domain of 7 extracellular immunoglobulin (Ig) like domains
- ✓ a single transmembrane region
- ✓ a regulatory juxtamembrane domain
- ✓ an intracellular tyrosine kinase domain, interrupted by a kinase insert domain.

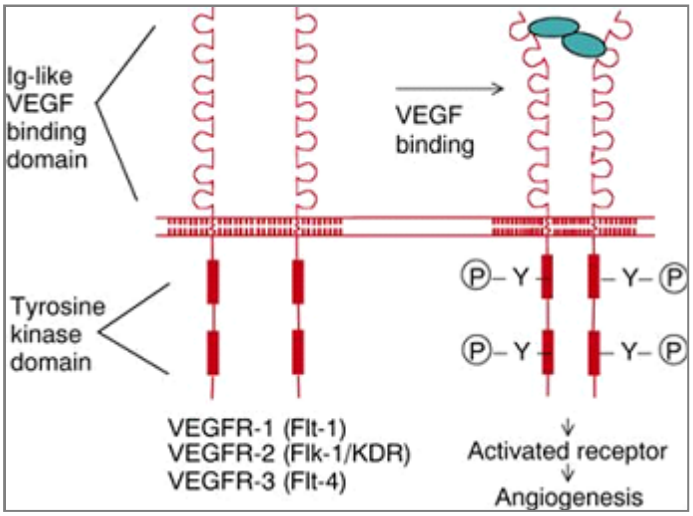

Figure 4. Representative structure of vascular endothelial growth factor (VEGF) tyrosine kinase receptors. The VEGF receptor family is represented by seven immunoglobulin-like loops in the extracellular domain, which binds VEGF. Ligand induces the formation of receptor dimer to activate autophosphorylation of tyrosine residues on the cytoplasmic domain. Ig = immunoglobulin; VEGF = vascular endothelial growth factor; Y- = phosphorylated tyrosine residues.

Both the receptors bind VEGF with high affinity. The ligand-binding region is localized within the second and third Ig domains, while the fourth Ig domain is essential for dimerization of VEGF receptors. In addition, Flt-1 also acts as a receptor for VEGF-B and PlGF, whilst KDR also binds to VEGF-C and VEGF-D and the viral homolog VEGF-E.

Upon ligand binding, the tyrosine kinase activity of VEGFR1 is ten-fold weaker than that of VEGFR-2. This information prompts further investigations to understand at molecular level the different biological roles of these receptors.

VEGFRs undergo alternative splicing to generate soluble forms of the receptors. Soluble VEGFR-1 (sFlt-1) is composed by the first six domains of extracellular portion of the receptor. This form binds VEGF-A and PlGF with the same affinity of the full length receptor, it functions as an endogenous VEGF inhibitor (Tugues et al., 2011; Shibuya, 2013). As recently reported, it plays a pivotal role to maintain cornea avascularity. However, when an injury

of cornea occurs with an increase of VEGF-A level, it titles sFlt-1 and binds to Flk-1 inducing angiogenesis (Ambati et al., 2006; Shibuya, 2013). Similarly, soluble VEGFR-2 (sKDR) is important in ocular lymphoangiogenesis context (Pavlakovic et al., 2010).

KDR and Flt-1 are both expressed in endothelial cells. VEGFR1 is also expressed in monocyte/macrophages, dendritic cells, osteoclasts, pericytes, trophoblasts, in mesangial cells, smooth muscle cells and also in bone marrow stem/progenitors derived cells. Its transcription is up-regulated by hypoxia, via a HIF-1-dependent mechanism and upon activation of macrophages. Non endothelial expression of VEGFR-2 has been observed in vascular endothelial progenitors, retinal progenitor cells, hematopoietic stem cells, neuronal cells, osteoblasts, pancreatic duct cells, and megakatyocytes.

VEGFR-1 knock out mices die at embryonic day 8.5-9.0, due to the over-growth and disorganization of blood vessels. This suggested that VEGFR-1, trapping VEGF-A and preventing activation of VEGFR-2, plays a negative regulatory role during the development of primitive vascular network.

Several tyrosine residues in VEGFR-1 intracellular domain have been identified as autophosphorylation sites using various experimental approaches. For instance, phosphorylation of Y1169 allows the binding and in turn the activation of phospholipase C (PLC)γ1 regulating endothelial cell proliferation via the mitogen activated protein kinase (MAPK) pathway. It is worth noting that VEGF-A and PlGF don’t induce the same autophosphorylations in VEGFR-1. This suggests that the two ligands stabilize two distinct conformations of the receptor intracellular domain in the activated VEGFR1 dimer or induce distinct modes of association with accessory molecules, such as heparin sulfated proteoglycans or neuropilins,. As a result, the availability of VEGFR-1 tyrosine residues as substrates for the kinase is different in response to the diverse ligand bound (Shibuya 2006). Finally, it has been

demonstrated synergy between VEGFR-1 and VEGFR-2, by a “cross-talking mechanism” (Tjwa et al., 2003).

VEGFR-2 null mices die at embryonic day 8.5-9.0, due a lack of vasculogenesis and very poor hematopoietic development. This means that VEGFR-2 plays an essential role in survival, growth and differentiation of endothelial cell progenitors.

Thus, during early embryogenesis, the two VEGFRs have opposite roles in angiogenesis: VEGFR-2 is a positive signal transducer, whereas VEGFR-1 is a suppressor. It is necessary a coordinated signaling between the two receptors to obtain a balanced expansion and differentiation of the endothelial precursor pool.

VEGFR-2 activity is also important for migration of ECs during adulthood. Several studies have been carried out in order to clarify the signal transduction by VEGFR-2. Therefore some autophosphorilation sites have been identified. Y951 mediates the binding to T cell specific adapter (TSAd), which in turn binds to Src, thus regulating actin cytoskeleton and cell migration. Phosphorilation of Y1175 induces the activation of PLCγ that in turn stimulates the protein kinase C(PKC) pathway leading to inositol phosphate formation and calcium mobilization. Furthermore, Raf-MEK-MAP kinase pathway and subsequent DNA synthesis are regulated through the phosphorylation at this site. Y1175 also binds to the adapter molecule Shb, that is also implicated in the activation of PI3-kinase and its downstream effector Akt and MAPK p38 via VEGFR-2. This site is also involved in the differentiation of hemangioblasts. (Shibuya 2006, Shibuya 2013)

Recent studies give the first indications about the role of heterodimerization between VEGFR-1 and VEGFR-2 in the regulation of endothelial cell homeostasis. According to this research VEGFR1 − 2 activation mediates VEGFR phosphorylation, endothelial cell migration, sustained *in vitro* tube formation and vasorelaxation via the nitric oxide pathway, but not

proliferation or endothelial tissue factor production, confirming that these functions are controlled by VEGFR-2 homodimers. Moreover VEGFR1 − 2 inhibits VEGF-A-induced prostacyclin release, phosphorylation of ERK1/2 MAP kinase and mobilization of intracellular calcium from primary endothelial cells. These findings indicate that VEGFR-1 subunits modulate VEGF activity predominantly by forming heterodimer receptors with VEGFR-2 subunits and such heterodimers regulate endothelial cell homeostasis (Cudmore et al., 2012).

1.8 Anti-angiogenic therapy in cancer

Expanding tumor tissues rapidly exhaust the available oxygen supply and become hypoxic. As described partially above, the activation of hypoxia-inducible factor (HIF) signaling triggers VEGF expression, not only in tumor cells but also in tumor-associated stromal cells. VEGF, meets the tumor's oxygen requirements and promotes therefore tumor growth and metastasis, by stimulating vascular growth. For this reason tumor tissue is often characterized by a superficial dense vascular network (Kubota, 2011).

With the aim of suppressing tumor progression and metastatic spread, in the last years anti-angiogenic therapy has been developed. Most current anti-cancer chemotherapeutic drugs, used in the clinical setting, indiscriminately target all rapidly dividing cells (e.g., at the level of DNA replication and protein synthesis) and therefore cause severe adverse effects, such as immunosuppression, intestinal problems and hair loss. Also if anti-angiogenic agents theoretically may have fewer side effects, the clinical practice has evidenced the appearance of important side effects such as bleeding, thrombotic events, hypertension, proteinuria, leucopenia, lymphopenia, hypothyroidism. They are due to physiological angiogenesis blockage.

Blocking VEGF appeared immediately a reasonable anti-angiogenic modality. Several studies of angiogenesis inhibition by administration of VEGF blockers have demonstrated significant tumor-suppression effects in various types of cancers. Treatment of mice carrying human tumors with an anti-VEGF neutralizing Mab (monoclonal antibody) significantly inhibited xenograft tumor growth. In 2003, the Food & Drug Administration (FDA) approved Bevacizumab (Avastin; Genentech Inc.), a humanized variant of a VEGF neutralizing Mab, as the first anti-angiogenic agent for combination treatment with chemotherapeutic agents in metastatic CRC (colorectal cancer) and subsequently for treatment of NSCLC (non-small-cell lung cancer) or MBC (metastatic breast cancer). VEGF-TrapR1R2 (Aflibercept; Regeneron Inc.), a chimeric soluble receptor that neutralizes circulating VEGFs, is currently in clinical trials. Additionally, blockade of VEGF receptors inhibits tumor growth. Receptor tyrosine kinases inhibitors (RTKIs), such as sunitinib (SU11248; Sugen), pazopanib (Votrient; GSK), sorafenib (Bay 43-9006; Nexavar) vendatanib (Caprelsa; AstraZeneca), cabozantinib (XL184; Exelixis), axitinib, tivozatinib and linifanib have recently been developed, for the treatment of many types of cancer. A number of studies have reported their significant therapeutic efficacy (Shojaei, 2012).

Recently also PlGF becomes an interesting target. An antibody against placental growth factor (PlGF) inhibits growth of VEGF-resistant tumors without affecting healthy vessels; interestingly, targeting PlGF not only inhibits vessel growth but also the recruitment of angiogenic macrophages (Fischer, 2007).

Despite the encouraging conditions, it is well to report that anti-angiogenesis therapy is facing three major challenges nowadays (figure 5):

- ✓ inherent/acquired resistance
- ✓ enhanced invasiveness during treatment with AIs

- ✓ lack of validated predictive biomarkers to select patient population and to monitor tumors responses to the therapy

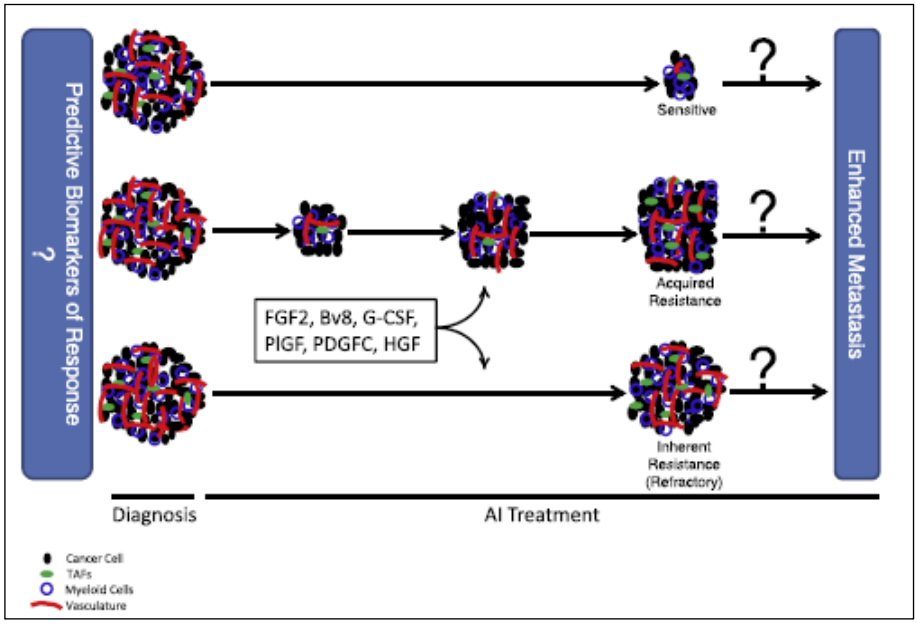

Fig. 5. Three major challenges of antiangiogenic therapy

Many patients show a lack of response to inhibitors of angiogenesis . Certainly, this is in part due to the very modest doses that are given to patients (5 mg/kg body weight, once every 2 weeks), compared to mice in preclinical study (10 mg/kg body weight, twice a week), to reduce possible off-target toxicities, such as hemorrhagic and thrombotic events . However, the extent of refractoriness is highly variable from one cancer to another. Mechanisms underlying resistance and/or enhanced invasiveness during treatment with AIs have been extensively studied and can be resumed in the following main points:

- ✓ both tumor and non-tumor compartments contribute to resistance to anti-angiogenic agents
- ✓ resistance to AIs may occur independent of class of agents i.e. antibodies or small molecule inhibitors

- ✓ resistance occurs independently of affinity of the anti-VEGF antibody
- ✓ limited bioavailability of therapeutic agent in tumor mass might account for lack of response to the therapy
- ✓ in absence of VEGF signaling, other mechanism (mediated for example by FGFs, angiopoietins, NRP1) can offset with their proangiogenic effects
- ✓ in tumors, some blood vessels are covered with a dense pericyte coat (whose recruitment is mainly regulated by platelet-derived growth factor (PDGF)-B/PDGF receptor-β, transforming growth factor-β (TGF-β) and angiopoietin/Tie signaling) that could represent a reason of a minor responsiveness to VEGF blockers by these vessels]
- ✓ hypoxia-tolerant cancer cells, called cancer stem cells, survive in poorly oxygenated niches and elicit tumor adaptation to anti-angiogenesis; some reports suggest that the resultant selection of tumor cells renders tumors even more invasive and metastatic
- ✓ chronic exposure of endothelial cells to anti-VEGF drugs may lead epigenetic modulation of expression of anti-apopotic genes such as *bcl-2* and *survivin.* Absence of the proapoptotic Bcl-2 homology 3 (BH3)-only Bcl-2 family member *Bim* in endothelial cells completely abolishes the effect of VEGF blockade macrophages are also involved in vascular development, independently of VEGF signaling; histological test of various cancer tissues reveals a vast accumulation of macrophages, that coordinate various aspects of tumor angiogenesis

Given and modest responses observed to antiangiogenesis therapy in the clinic, it is essential to identify a set of biomarkers to select populations of likely responders and/or to monitor disease progression and response over the course of treatment in the clinic. From some studies, CD31 expression has been proposed as biomarker of response in breast cancer patients treated with bevacizumab and chemotherapy. Quantification of circulating endothelial

progenitor cells, cytokines and/or growth factor in serum could also be another strategy to monitor response to angiogenesis inhibitors. Because of VEGF inhibition results in a reduction in NO (nitric oxide) synthesis, leading to vasoconstriction and increase in blood pressure, hypertension is another biomarker of response to these drugs.

In conclusion, in order to surmount several challenges associated with anti-angiogenesis therapy, advances in understanding the molecular and cellular bases of tumor angiogenesis are required, as well as new drugs are required to pave the path towards a more efficient and successful clinical application (Tonra and Hicklin, 2007; Hsu and Wakelee, 2009; Shojaei, 2012).

CHAPTER 2:

Project aims and approaches

2.1 Project aims

The work presented in this thesis was aimed to support a rational design of new antiangiogenic drugs or treatment strategies. To this end, the whole work was focused on the following objectives:

- Performing an expression proteomic study of cell cultures treated with some dimers of VEGF family. In particular, following the incubation of Human Umbilical Vein Endothelial Cells (HUVECs) and Human Embryonic Kidney 293 cells, over-expressing stably human Flt-1, (HEK-293hFlt-1) with VEGF, PlGF, VEGF/PlGF, we meant to identify the proteins and differentially modulated following each treatment. Information relating to functional genomics can represent a valuable contribution to the further understanding of the molecular bases of angiogenesis and for the development of therapeutic strategies more effective and safer than those currently approved.
- Identifying novel putative inhibitors of angiogenesis, performing a small library of natural compounds screening. On the basis of the experimental evidence reported in the literature on their involvement in pathological angiogenesis, we chose the axis VEGF/Flt-1 and PlGF/Flt-1,as target for this study.

2.2 Proteomic approach

“Proteomic” (term coined in 1994) is the science that describes the entire set of proteins expressed by the entire genome of a cell in the lifetime or, in a less universal sense, at any one time, under specific conditions. Providing these informations, proteomic promises to bridge the gap between our understanding

of genome sequence and cellular behavior (Wilkins et al., 1996; Patterson et al., 2003).

The completion of human genome sequencing represented undoubtedly one of the most exciting biological achievement. One of the interesting aspects of this effort is the finding that, though they're very different organisms from the phenotypic point of view, the number of protein-encoding genes found for humans (~30000) is not extremely different from those calculated for phylogenetically remote organism, such as a yeast cell (~6000), a fly (~13000), a worm (~18000), a plant (~26000). It's clear that the physiological complexity of an organism is not a consequence of a mere genes number. Indeed, the existence of an open reading frame (ORF) doesn't imply perforce that the gene is functional (Pandey and Mann, 2000). Many studies document the disparity between the relative expression levels of mRNA (transcriptome) and those of their corresponding proteins; in facts, through gene splicing mechanism, a single gene can code for multiple proteins and each protein can undergo numerous post-translational modifications, including phosphorylation, acetylation, ubiquitylation, SUMOylation, palmitoylation, transglutamination and proteolytic cleavage (Mann and Jensen, 2003). These aspects, not predictable from genome, increase the functional diversity of a cell system. Moreover, the complexity of an organism is also due to the ability of intracellular signaling pathways to interact with each other forming complex networks. This complexity is due to the overlapping functions of some proteins, to their connections, and to their spatio-temporal relationship in the cell. Finally, many cellular processes are very often performed not by individual proteins, but by protein macromolecular complexes (Pieroni et al., 2008; Preisinger, et al., 2008).

Proteomic analysis is certainly a valid first step in functional annotating the genome. In particular, differential proteomics, that consists in the comparison of distinct proteomes (for example: normal versus diseased cells, diseased

versus treated cells and so on) is of paramount importance, in all areas of biological research (cancer research, toxicology, pharmacology and so on) (Patterson et al., 2003).

Several approaches can be used to achieve this type of study. They typically involve electrophoresis and/or chromatography combined with chemical or metabolic labeling and mass spectrometry (Gevaert and Vandekerckhove, 2000; Fuchs et al. 2005).

In this work, the proteomic profiles of cultured cells stimulated with VEGF dimers have been studied by a gel-based approach (Rabilloud, 2002; Wulfkuhle et al. 2003; Monteoliva and Albar, 2004). Classically this strategy involves the achievement of then following steps (figure 6):

1. Separation of complex protein mixtures, usually by two-dimensional gel electrophoresis, 2-DE
2. Protein visualization and image analysis
3. Excising the spots for following analyses
4. In gel digestion of proteins and pooling of the released peptides
5. Analysis of the peptide mixtures by mass spectrometry
6. Matching peptide masses against protein databases to obtain proteins identification

2-DE is a relatively simple but powerful method for high-resolution analysis of complex protein mixtures.

All proteins in an electric field migrate at a speed that is dependent on their conformation, size and electric charge. 2DE uses the latter two characteristics to allow high-resolution separation of proteins. As first described by O'Farrel and J. Klose in 1975, isoelectric focusing (IEF) separates proteins on the basis of their charge (separation in first dimension), while Sodium Dodecyl Sulphate - PolyAcrylamide Gel Electrophoresis (SDS-PAGE) on the basis of their molecular weights (separation in second dimension). The result is an array of

protein spots, characterized by precise coordinates x and y: isoelectric point (pI) and apparent molecular weight (Mw), respectively.

Separated proteins can be visualized by staining or autoradiography. Subsequently computer-based analysis is needed to detect differentially expressed proteins. The most known commercial software are: Progenesis, Nonlinear Dynamics; Image Master 2D Platinum and Melanie Software, Amersham Biosciences; PDquest, Bio-Rad.

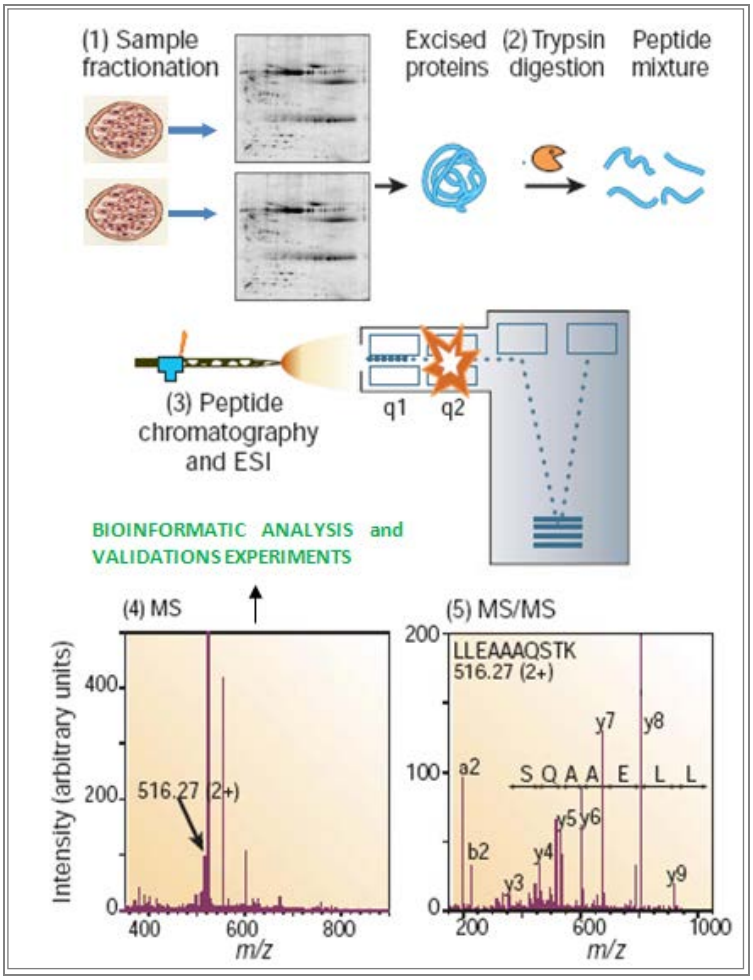

Fig. 6. Proteomic approach workflow.

A reliable protein separation by 2 DE depends on some parameters. First the choice of sample preparation protocol: it is the critical influential factor for

isoelectric focusing which in turn affects the two-dimensional gel result in terms of quality and protein species distribution (Shaw and Riederer, 2003; Monteoliva and Albar, 2004). Since immobilized ph gradient strips (IPG-strip) were developed variability in experimental conditions has greatly decreased; this is now undoubtedly the most widespread strategy for comparing distinct states of more proteomes (Weiss and Görg 2009; Görg et al., 2009).

Protein identification is based on mass spectrometry data. The starting point is a protein spot, which may be a single protein or a complex mixture of proteins. An enzyme, often trypsin, digests the proteins to peptides. Chromatography is used to regulate the flow of peptides into the mass spectrometer. Peptides selected are then induced to fragment, possibly by collision, to capture an MS/MS spectrum. For each MS/MS spectrum, software is used to determine which peptide sequence in a database of protein or nucleic acid sequences gives the best match. Each entry in the database is digested, in silico, using the known specificity of the enzyme, and the masses of the intact peptides calculated. If the calculated mass of a peptide matches that of an observed peptide, the masses of the expected fragment ions are calculated and compared with the experimental values. The result is a list of candidate proteins with different confidence levels (Fenn et al. 1989; Henzel et al. 1993; Aebersold and Mann, 2003; Roepstorff, 2012)

2.3 Natural product for drug discovery

Natural compounds have been the source of inspiration for chemists and physicians for millennia, representing the richest font of novel compound classes and an essential wellspring of drugs and drug leads (figure 7). According to a recent survey by David J. Newman, Gordon M. Cragg, and Kenneth M. Snader of the national cancer institute, 61% of the 877 small-

molecule new chemical entities introduced as drugs worldwide during 1981–2002 can be traced to or were inspired by natural products (Newman et al. 2003). These include natural products (6%), natural product derivatives (27%), synthetic compounds with natural-product-derived pharmacophores (5%), and synthetic compounds designed on the basis of knowledge gained from a natural product (that is, a natural product mimic; 23%). In certain therapeutic areas, the output is higher: 78% of antibacterials and 74% of anticancer compounds are natural products or have been derived from, or inspired by, a natural product. These numbers are not surprising since it is know that natural products evolved for self-defence. Despite that record of productivity, the use of natural products as a starting point for drug discovery was de-emphasized in many big pharmaceutical companies in 1990s, when combinatorial chemistry had place and the reasons were primarily practical. However, after several years it was clear that database of natural products have a major number of unused scaffolds, and couldn't be discarded as starting points for new drugs discovery. The differences between synthetic compounds and natural products are remarkable, especially in their structural properties (Dobson, 2004; Rosén et al., 2009). On average, natural products have higher molecular weights; incorporate fewer nitrogen, halogen, or sulphur atoms, but more oxygen atoms and are sterically more complex, with more bridgehead tetrahedral carbon atoms, rings, and chiral centres. This gives them a high "sterical complexity" due to the fact that the enzymes used for biosynthesis, as well as their molecular targets, are inherently three-dimensional and chiral. Furthermore, nature has a limited palette of building blocks at its disposal, and thus has to generate novelty by branching out common intermediates into different scaffolds.

Moreover natural compounds are a really good starting point for the set up of libraries to be tested for drug discovery (figure 7), not only for their complex and diversified chemical space but also for their ability to interact with

biomolecules. Lynn H. Caporale in her book "Darwin in the genome" (Caporale, 2002), writes: “even though natural products may not have coevolved with human proteins, they have emerged in nature to interact with biomolecules….varied genomes, based on similar chemistry, have spread across the earth. Indeed we share our gene families with other organisms. Whether inside bacteria or inside us, there is a limited number of ways that the structural components of proteins, such as -helices and -sheets, can arrange themselves in space and interact with each other and with other molecular structures”. Herbert Waldmann, from Max Planck institute for molecular physiology, offers a similar analysis, based on the premise that natural products evolved to perform a function that is achieved by binding to proteins. Therefore, natural products should be able to penetrate biological barriers and make their way to certain cells or organs in which they will exert the effect. Thus, natural products are already biologically validated to reach and bind specific proteins. Looking at all proteins and analyzing them for structural features, elements of conservatism and diversity may be found. The conservative elements are the domains: the parts that fold to compact secondary structures. Among the hundreds of thousands of human proteins, the number of distinct domains is only about 600 to 8,000. Consequently, proteins that may seem altogether different are quite similar when viewed structurally, but diversity lies in the precise details since similar domains may have very different amino acid sequences (Kirkpatrick, 2003).

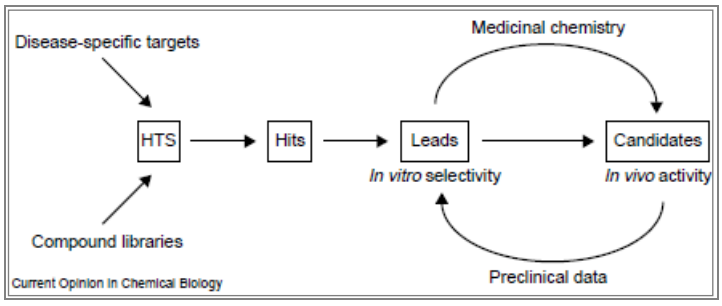

Fig. 7. The current lead-discovery process

A number of bioactive plant compounds have been recently tested for their antiangiogenic potential. Among the known angiogenesis inhibitors compounds derived from natural sources, like flavonoids, sulphated carbohydrates, or triterpenoids are playing a prominent role. The underlying mechanisms are complex and in part unknown. In this regard, we should recall the recent work by Tarallo et al which proved an interesting antiangiogenic activity of amentoflavone. This biflavonoid can bind to VEGFs preventing the interaction and phosphorylation of VEGF receptor 1 and 2 (VEGFR-1,VEGFR-2) and to inhibit endothelial cell migration and capillary-like tube formation induced by VEGF-A or placental growth factor 1 (PlGF-1) at low μm concentration. In vivo, amentoflavone is able to inhibit VEGF-A-induced chorioallantoic membrane neovascularization as well as tumor growth and associated neovascularization, as assessed in orthotropic melanoma and xenograft colon carcinoma models (Tarallo et al., 2011).

Finally, ASA404, a flavonoid compound, is a “vascular disrupting agent” capable of induction of apoptosis in tumor associated endothelial cells, resulting in the inhibition blood flow in tumor mass. ASA404 is currently in advance stage of clinical development in combination with chemotherapic drugs in NSCLC patients.

For all these reasons natural products are considered: a valid source for investigational new antiangiogenic agents to treat many disorders.

CHAPTER 3:

Results and discussion

3.1 Proteomic study

In order to identify differentially expressed proteins both in endothelial cells and tumor cells stimulated by VEGF, PlGF and VEGF/PlGF, separation and quantification of relative protein extracts have been performed by a gel-based proteomic approach.

At the outset of this work, no comparative proteomic analysis of the selected cells expressing one or both VEGF receptors and treated with PlGF and VEGF/PlGF had been produced, while few works can be found on VEGF-treated cells (such as HUVECs). Data produced by others, as discussed below, report some findings corroborating our data.

3.1.1 Electrophoretic separation of proteins

In the present study, alterations in the cellular proteome induced by VEGF, PlGF, and heterodimer treatments have been investigated using HUVECs and HEK-293 cells stably overexpressing hFlt-1 (HEK-293-Flt-1). Both cell lines underwent serum-starvation, followed by incubation with the selected growth factors for 24 hours. Total protein extracts were separated by 2-D electrophoresis (2DE) in order to obtain consistently well-separated protein profiles. For HEK-293Flt-1 protein extracts, it has been necessary to optimize the classical protocol of sample preparation, a crucial step for a successful 2 DE. Replacing sulphydryl reductants dithiothreitol DTT, the most common reductant agent, with tris (2-carboxyethyl) phosphine TCEP, we were able to solubilize the samples more effectively to get 2D maps better resolved and more easily analyzable (figure 8).

Silver staining compatible with mass spectrometry have been used for a sensitive detection of separated proteins (figures 9, 10).

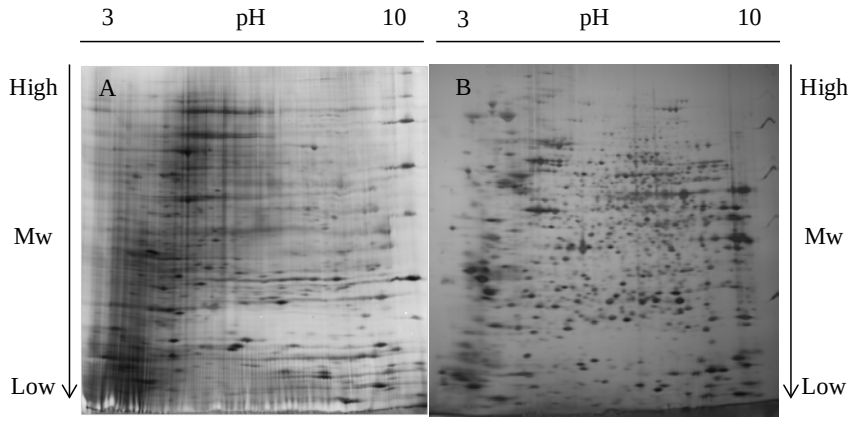

Fig. 8. 2D gel of HEK-293Flt-1 protein extracts; a) Gel obtained with utilization of DTT; b) Gel obtained with utilization of TCEP.

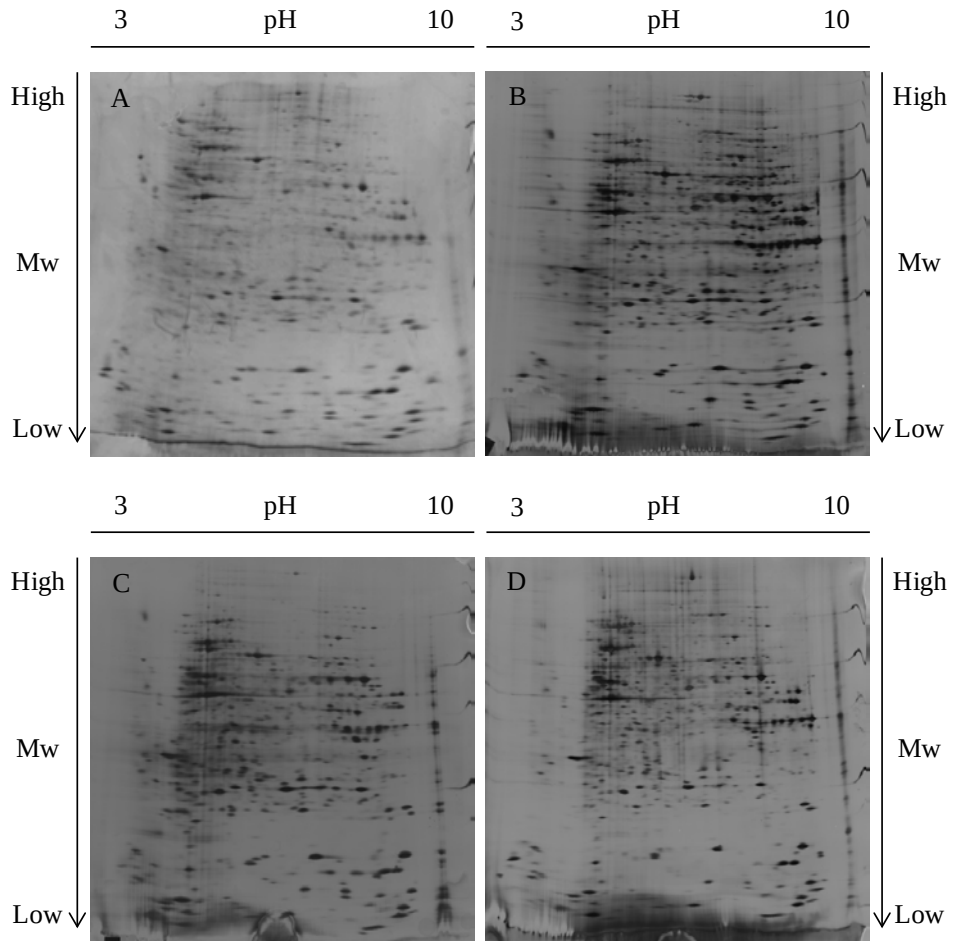

Fig. 9. 2D gel of protein extracts of HEK-293Flt-1, following the treatment with: b) VEGF, c) PlGF, d) heterodimer; a) represents the control (not induced). Each gel has been produced in triplicate.

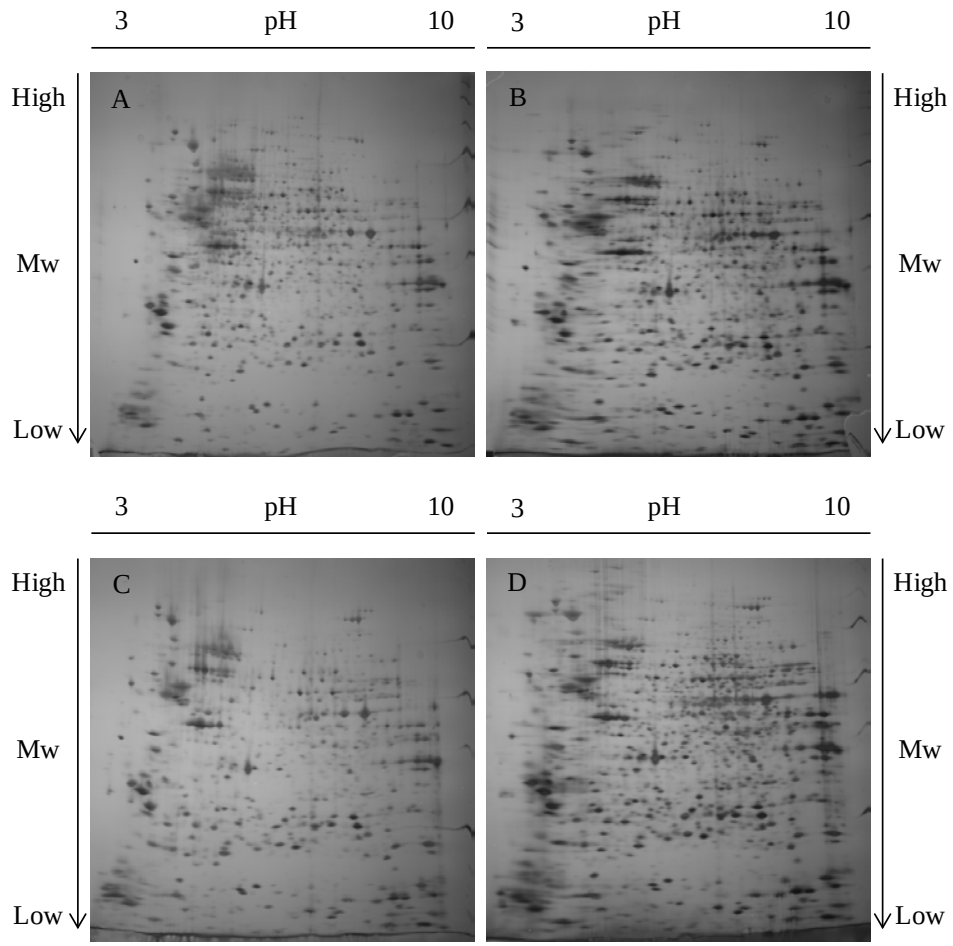

Fig. 10. 2D gel of protein extracts of HUVECs, following the treatment with: b) VEGF, c) PlGF, d) heterodimer; a) represents the control (not induced). Each gel has been produced in triplicate.

3.1.2 Image analysis and statistics

In order to perform image analysis, 2D gel images must be converted into digital data. This has been addressed acquiring images by charge-coupled device (CCD) camera systems and then analyzing them using commercial image processing software.

Schematically, workflow approach to 2D image analysis was:

- ✓ Step 1. 2D gel images, once loaded, had automatically examined from "quality control" application of the software. In general, the output of

this operation is a description of the properties of the image and of the problems (for example: saturation of the image, due to a wrong staining of the gel) associated with it. Thanks to the high quality of resolution of our gels, no problems were revealed.

- ✓ Step 2. The most appropriate reference image to which align all the other images was selected.
- ✓ Step 3. In this phase a mask of disinterest was placed on the image to exclude specific areas from the analysis (figure 11). In our work only the extremely lateral margins of the gels had been masked.

Fig. 11.Page of Progenesis SameSpots. Masked area are evidenced in pink

- ✓ Step 4. Image alignment was the process of matching gel images with the reference image. In order to achieve the best possible results, it was crucial that the alignment was highly accurate. Even if the gels showed very good resolution in the separation of proteins, as a starting point we needed to align a few spots manually. These spots, acting as "guide

vectors" for the subsequent automatic alignment, contributed to a very consistent global matching among gels (figura 12).

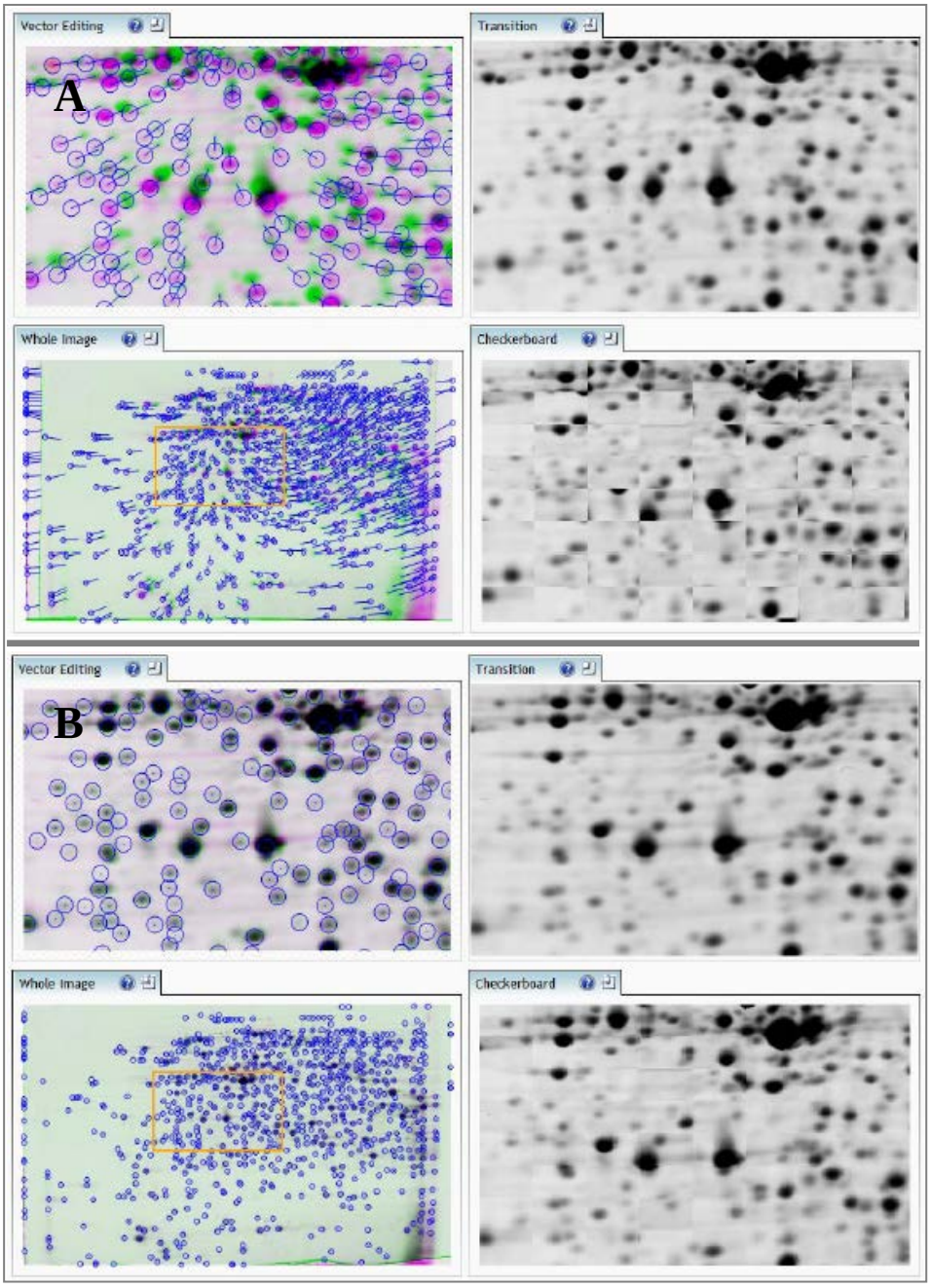

Fig 12 Alignment with Progenesis SameSpots. Vectors are colored in blu. A) Gels are not aligned; B) Gels are perfectly aligned.

- ✓ Step 5. After reviewing the alignment quality, all spots in every gel were detected and quantified. Among these, some were removed based on position, area, normalized volume and combinations of these spot properties. Anyway, the most important process of this step, essential to determine the volume of the protein in the spot, was the background subtraction and normalization. Background subtraction was performed by software, subtracting the lowest intensity value of the image pixels outside the spot's outline from the intensity value of every pixel inside the spot outline. Normalization was performed using the "total spot volume" method, which results in all spot volumes being expressed as a fraction of the total spot volume within a gel (figura 13). This allowed to correct for protein loading differences between gels and to identify any differences in expression due to only biological change.

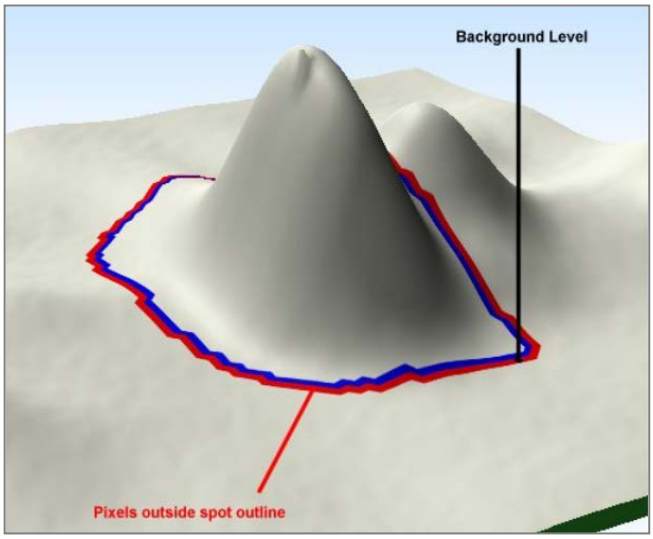

Fig. 13. Background subtraction performed by

- ✓ Step 6. At this phase one or more groups for analyzed images were built up. For this study, we grouped the gel images to reflect the biological groupings (figure 14); thus we assembled the group of three gels, representing a specific treatment (VEGF, PlGF, Heterodimer),

and that relating the control (CN). After selecting two groups (control vs treatment), software calculated the data of differential protein expression (Fold-change and relative p-value).

- ✓ Step 7. At this stage results had been revised, changing detection zones, using a set of tools, such as editing, splitting, merging of spots. This software permits to process a single image, but the effects are applied across all images in the experiment.

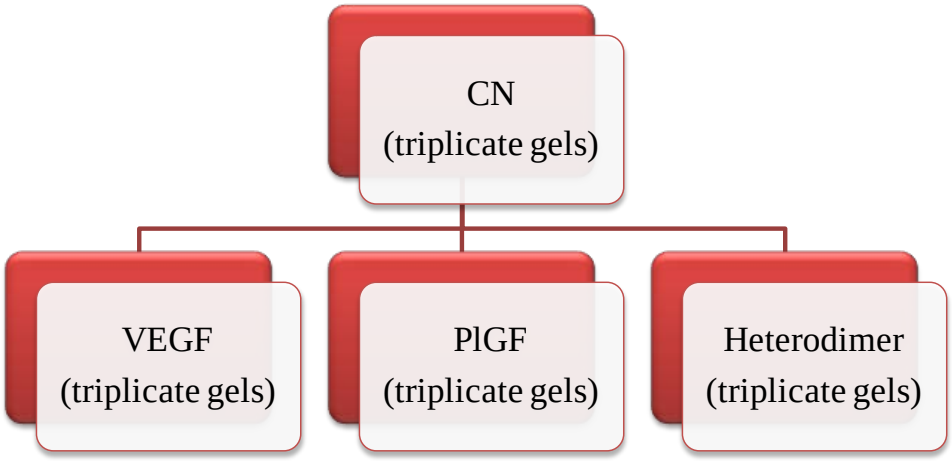

Fig. 14. Scheme: every block represents a group of three gels relateve to a specific biological condition. We compared each specific treatment block to control. This strategy have been applied to both cell cultures.

- ✓ Step 8. Finally it was possible to perform multivariate statistics on selected spots. The statistical analysis of the differentially expressed proteins (only statistically significant spots, $p<0.05$) was presented in a form of interactive graphical representations. In particular, for "Principal Component Analysis" (PCA), the software used spot expression levels across gels to determine the principle axes of expression variation. Transforming and plotting the most significant

expression data in principle component space, gels were separated according to expression variation. PCA plot allowed us to observe if gels group according to the experimental conditions and to identify gel outliers.

In this study, protein spots showing a fold change higher than 1.3 and statistically significant (p value < 0.05), were considered as differentially expressed proteins. Achieved data (tables 2, 3) showed that following the VEGF treatment, HUVECs exhibit significantly altered expression, compared to the control, of a total of 23 protein spots (figure 15); in particular, 2 protein spots are down-regulated and 21 up-regulated. Instead, in HEK-293Flt-1, after the same treatment, 24 protein spots show a significant variation of their abundance (figure 16) and specifically 19 proteins were down-regulated and 5 proteins showed up-regulated expression. PlGF modifies the expression of 61 protein spots (17 down-regulations and 44 up-regulation) in HUVECs (figure 17) and of 30 protein spots (18 down-regulations and 12 up-regulation) in HEK-293Flt-1 (figure 18). Finally, due to VEGF/PlGF treatment, 43 protein spots were found to show markedly altered expression in HUVECs (figure 19); among these regulated protein spots, 8 were down-regulated and 35 up-regulated; in HEK-293Flt-1 instead, 36 protein spots modify their abundance (figure 20), with 30 spots showing a significative down-regulation and 6 spots a significative down-regulation.

Examples of some spot patterns are shown in figures 21, 22:

- ✓ in HUVECs spot 5, spot 20 and spot 33 decrease their abundance after the treatment with VEGF, PlGF or the heterodimer, respectively, while spot 29, spot 56 and spot 46 show a significantly higher abundance.
- ✓ in HEK-293Flt-1 spot 40, spot 63 and spot 75 decrease their abundance after the treatment with VEGF, PlGF or the heterodimer, respectively, while spot 37, spot 17 and spot 68 show a significantly higher abundance.

Some of the protein level changes observed for specific protein spots is shared by multiple treatments.

HUVEC														
Rank	P value	Fold	Average Normalised		Rank	P value	Fold	Average Normalised		Rank	P value	Fold	Average Normalised	
			CN	VEGF				CN	PlGF				CN	VEGF/PlGF
5	**0.004**	**5.01**	5221312113	1019143857	80	**0.022**	**2.01**	28536186308	13850683947	16	**0.013**	**3.07**	6431815198	1753089077
33	**0.033**	**1.09**	8068445302	4201902896	30	**0.041**	**3.07**	16175038112	4420831300	17	**0.030**	**3.06**	5211441366	1433141000
39	**0.043**	**1.07**	779700292	1305002985	44	**0.008**	**3.00**	14472161855	4860457281	8	**0.011**	**5.05**	4435373552	812796104
681	**0.053**	**1.03**	2020118703	2701230422	87	**0.007**	**1.09**	17186702012	8878096989	885	**0.052**	**1.03**	17157293792	13583287960
25	**0.013**	**2.00**	999552990	2007538163	99	**0.039**	**1.07**	15161367569	8694770874	2	**0.006**	**8.05**	3730514070	439157393
36	**0.030**	**1.07**	2235486608	3780236673	51	**0.003**	**2.07**	10035207662	3686625029	33	**0.012**	**2.04**	1623874624	679648122
34	**0.028**	**1.07**	2392299756	4073039087	35	**0.015**	**3.03**	8614290880	2611661437	78	**0.009**	**1.04**	2530726210	1834369304
41	**0.005**	**1.05**	3324597956	5106738530	8	**0.002**	**7.02**	6444567768	897532726	52	**0.050**	**1.09**	1305275681	692822993
510	**0.051**	**1.05**	3813154970	5726218664	75	**0.029**	**2.02**	7974807175	3705474970	168	**0.053**	**2.07**	534812165	1452820330
27	**0.028**	**1.09**	2102707342	4073860829	20	**0.008**	**5.00**	5221477422	1050544977	59	**0.027**	**1.07**	1354185885	2363380582
43	**0.031**	**1.03**	7130582286	9121489132	58	**0.050**	**2.05**	6479529317	2556780590	24	**0.030**	**2.07**	697102088	1860900285
35	**0.042**	**1.07**	3212604106	5442152459	27	**0.011**	**4.01**	4636528914	1134034552	42	**0.050**	**2.02**	1407069646	3095098403
20	**0.006**	**2.05**	1990072466	4908389151	108	**0.026**	**1.06**	9294300617	5817516048	40	**0.047**	**2.02**	1437262657	3163097840
32	**0.047**	**1.08**	3817382728	6789537272	29	**0.030**	**3.07**	4444745863	1197448131	57	**0.049**	**1.08**	2373594192	4194915401
42	**0.007**	**1.04**	8469146596	11553274432	40	**0.030**	**3.00**	1546627446	509104966	21	**0.049**	**2.09**	1018322725	2990337531
17	**0.040**	**2.06**	2323569767	6061386360	90	**0.014**	**1.09**	1626661062	854041105	41	**0.039**	**2.02**	1692555014	3724217547
29	**0.008**	**1.09**	4191314066	8085409914	77	**0.041**	**2.01**	1307793115	613700864	65	**0.034**	**1.06**	3207412620	5252416692
31	**0.006**	**1.09**	4535150890	8439979891	109	**0.046**	**1.05**	2020179004	3076214823	51	**0.006**	**1.09**	2398839248	4561143760
33	**0.023**	**1.07**	5824188335	10042146218	102	**0.024**	**1.07**	1855754814	3143909291	46	**0.009**	**2.01**	2087801330	4331730851
22	**0.026**	**2.02**	5857082107	12623371415	97	**0.012**	**1.08**	1695406067	3018162586	62	**0.001**	**1.07**	3318937259	5630018997
45	**0.032**	**1.03**	27991344970	35117926843	31	**0.001**	**3.06**	535685083	1914408825	44	**0.030**	**2.01**	2425824963	5047159262
26	**0.020**	**1.09**	9419505341	18341655494	56	**0.013**	**2.06**	993943102	2577475892	32	**0.014**	**2.04**	1986412542	4760706222
24	**0.008**	**2.00**	16350948960	33492385430	61	**0.037**	**2.05**	1409562552	3484745315	15	**0.005**	**3.08**	991948812	3767081320
					22	**0.003**	**4.07**	612958841	2850894720	30	**0.017**	**2.06**	1921922083	4939513723
					85	**0.028**	**1.09**	2488146176	4840545208	19	**0.034**	**3.03**	1348637815	4423078809
					104	**0.020**	**1.07**	3736479226	6167661187	71	**0.036**	**1.06**	6203067956	9717110610
					101	**0.007**	**1.07**	3324680403	5766282352	73	**0.009**	**1.05**	7118344591	10693088461
					112	**0.019**	**1.04**	6213977409	8885835542	64	**0.016**	**1.06**	6966139668	11490992360
					62	**0.042**	**2.04**	1918976052	4688112083	39	**0.003**	**2.02**	3806735477	8434842634
					105	**0.049**	**1.07**	4386004190	7238344936	79	**0.011**	**1.02**	22550100531	27269700813
					88	**0.036**	**1.09**	3212687113	6191388292	70	**0.004**	**1.06**	8454637917	13286995902
					68	**0.005**	**2.02**	2403021174	5392026540	11	**0.031**	**4.05**	1439723032	6447730061
					483	**0.052**	**1.06**	5544892634	9092002288	56	**0.039**	**1.08**	6920297470	12250432396
					100	**0.023**	**1.07**	5013379644	8724404150	72	**0.045**	**1.05**	10702480055	16493294238
					43	**0.032**	**3.00**	1924772893	5818801397	54	**0.020**	**1.08**	6923412896	12780674518
					81	**0.014**	**2.00**	3813260348	7782188211	47	**0.026**	**2.01**	5847918550	12000033513
					103	**0.021**	**1.07**	6978302698	11818595239	77	**0.029**	**1.04**	16097043889	22569081081
					430	**0.052**	**1.07**	7088683962	12220337884	29	**0.026**	**2.06**	4184574377	10795803396
					66	**0.039**	**2.03**	4531274824	10496936421	35	**0.038**	**2.03**	5018921013	11740990026
					71	**0.048**	**2.02**	5028835961	11187916957	28	**0.017**	**2.06**	9404219418	24407027838
					94	**0.008**	**1.08**	8469393484	15257796751	45	**0.022**	**2.01**	15211403716	31645600421
					84	**0.005**	**2.00**	6935396073	13842519200	48	**0.038**	**2.00**	16322091586	33341498598
					83	**0.037**	**2.00**	6932636338	13969462068	58	**0.010**	**1.08**	23959921660	42069179094
					52	**0.016**	**2.07**	4191363322	11401686061					
					59	**0.035**	**2.05**	5149400842	12983975451					
					57	**0.017**	**2.06**	5857202727	15096237413					
					356	**0.051**	**1.09**	10719786669	20206510933					
					91	**0.024**	**1.08**	11581500463	21225242953					
					111	**0.047**	**1.05**	23854329328	34623604556					
					89	**0.015**	**1.09**	13151922821	25091045727					
					92	**0.026**	**1.08**	15238877215	27924116232					
					93	**0.004**	**1.08**	16125259415	29501571057					
					107	**0.035**	**1.06**	22589823492	36485344108					
					110	**0.021**	**1.05**	27939484984	41959419292					
					63	**0.040**	**2.04**	9825314072	23871691399					
					55	**0.005**	**2.07**	9419793510	25034580571					
					46	**0.014**	**2.09**	8136825687	23954467323					
					106	**0.042**	**1.06**	29977839775	48991151810					
					72	**0.023**	**2.02**	16351589716	36272533025					
					95	**0.020**	**1.08**	26280340428	47312000316					
					96	**0.041**	**1.08**	34528943083	62021250865					

Tab. 2. 2DE analysis of VEGFs treated HUVECs

293-hFlt-1														
Rank	P value	Fold	Average Normalised		Rank	P value	Fold	Average Normalised		Rank	P value	Fold	Average Normalised	
			CN	VEGF				CN	PlGF				CN	VEGF/PlGF
48	**0.003**	**1.06**	12292924338	7698563805	57	**0.038**	**1.09**	4841037870	2572130694	15	**0.027**	**3.04**	18910728760	5641557319
44	**0.011**	**1.07**	9084545885	5360950790	41	**0.004**	**2.02**	4073979987	1894115654	121	**0.038**	**1.03**	25958130382	19398805015
52	**0.041**	**1.05**	8435926721	5654328757	52	**0.045**	**2.00**	4198121558	2090067969	62	**0.011**	**2.01**	9084545885	4248264077
761	**0.053**	**1.05**	6895054959	4471725954	54	**0.033**	**2.00**	4273289323	2182600405	63	**0.004**	**2.01**	8210711480	3852930654
39	**0.049**	**1.09**	5084195645	2707187733	40	**0.007**	**2.02**	3006710314	1397855328	80	**0.008**	**2.00**	8435926721	4305659363
26	**0.049**	**2.02**	4198121558	1882233522	47	**0.023**	**2.01**	3066168162	1486958995	92	**0.003**	**1.07**	8496199374	4869744797
51	**0.019**	**1.05**	6097278510	4004767350	62	**0.035**	**1.09**	3151397231	1699582512	27	**0.021**	**2.08**	5084195645	1807099860
59	**0.002**	**1.03**	7432565355	5628679160	89	**0.018**	**1.06**	3307510668	2022500902	119	**0.002**	**1.03**	11746243268	8751290847
25	**0.002**	**2.02**	3006710314	1346286949	25	**0.004**	**2.05**	1939044808	774689396	78	**0.049**	**2.00**	5861043021	2955175865
32	**0.032**	**2.00**	2594300824	1269101826	65	**0.047**	**1.08**	2594300824	1434265662	111	**0.010**	**1.05**	8441694889	5636494529
46	**0.026**	**1.07**	2884147939	1746398820	95	**0.007**	**1.05**	3406194278	2336548699	75	**0.005**	**2.00**	5271920569	2642525111
53	**0.004**	**1.05**	3259108389	2201454862	63	**0.012**	**1.08**	2293076840	1255884382	35	**0.011**	**2.05**	4273289323	1718195000
50	**0.013**	**1.06**	2756787554	1768240707	69	**0.003**	**1.09**	2090677030	1127504572	609	**0.053**	**1.07**	5784973179	3401834089
34	**0.041**	**2.00**	1531249554	759150895	63	**0.014**	**1.09**	1857780276	977952029	107	**0.036**	**1.05**	5319421704	3495674760
60	**0.004**	**1.02**	4990504607	4283560153	72	**0.019**	**1.07**	1707606050	991855372	116	**0.045**	**1.04**	5942181008	4154195489
49	**0.026**	**1.06**	1595426359	1006819308	50	**0.025**	**2.00**	1335239438	652008130	118	**0.023**	**1.04**	6045003985	4445969375
58	**0.024**	**1.03**	2216859648	1657433245	53	**0.012**	**2.00**	861023213	435709110	125	**0.036**	**1.02**	8015140758	6571155138
55	**0.014**	**1.04**	1707606050	1223456665	55	**0.044**	**1.09**	751847640	388233401	108	**0.034**	**1.05**	4198121558	2775298578
33	**0.047**	**2.00**	861023213	424849355	90	**0.018**	**1.04**	673945398	918980067	599	**0.055**	**1.07**	3259108389	1910810725
16	**0.024**	**2.06**	1493577132	3949371220	26	**0.002**	**2.05**	496273303	1228329366	21	**0.026**	**3.01**	1813369880	590401020
37	**0.476**	**2.00**	3334026541	6527826514	89	**0.050**	**1.04**	2059798028	2817597376	1159	**0.051**	**1.03**	5001364669	3799197010
41	**0.011**	**1.08**	4521357507	8085647270	88	**0.037**	**1.04**	2990994526	4140147507	96	**0.043**	**1.06**	2913007777	1774785884
13	**0.022**	**2.08**	4489650296	12550477313	44	**0.002**	**2.01**	1159572141	2451804746	91	**0.022**	**1.07**	2334192941	1334731149
30	**0.016**	**2.01**	8123401719	16762143124	70	**0.005**	**1.07**	1946042058	3380387775	53	**0.049**	**2.02**	1621411424	728259006
					91	**0.025**	**1.04**	4330889838	5895711332	109	**0.026**	**1.05**	2419110925	1610822582
					68	**0.032**	**1.08**	2073010140	3649009781	39	**0.027**	**2.04**	1258488887	522987142
					69	**0.017**	**1.07**	2792594546	4868946840	122	**0.006**	**1.03**	2960013073	2234316012
					86	**0.005**	**1.04**	8497137479	12002488658	124	**0.029**	**1.03**	2966860580	2337296993
					77	**0.049**	**1.07**	8149199967	13773092914	99	**0.028**	**1.06**	1595426359	993818339
					17	**0.004**	**2.07**	4521357507	12411291016	123	**0.035**	**1.03**	2216859648	1701937503
										95	**0.048**	**1.07**	1598785230	2655116531
										105	**0.005**	**1.06**	2139371105	3322346578
										113	**0.017**	**1.05**	4330889838	6388156554
										68	**0.002**	**2.01**	3334026541	7009196258
										106	**0.012**	**1.06**	12010889459	18640771150
										29	**0.011**	**2.07**	4521357507	12374089314

Tab. 3. 2DE analysis of VEGFs treated HEK-293Flt-1

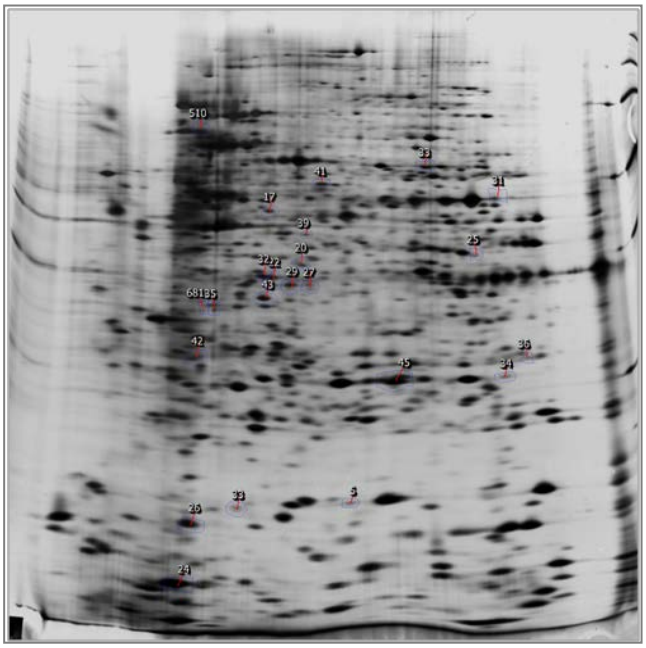

Fig. 15. 2DE gel of VEGFs-reated HUVECs

Fig. 16. 2DE gel of VEGF-treated HEK-293hFlt-1

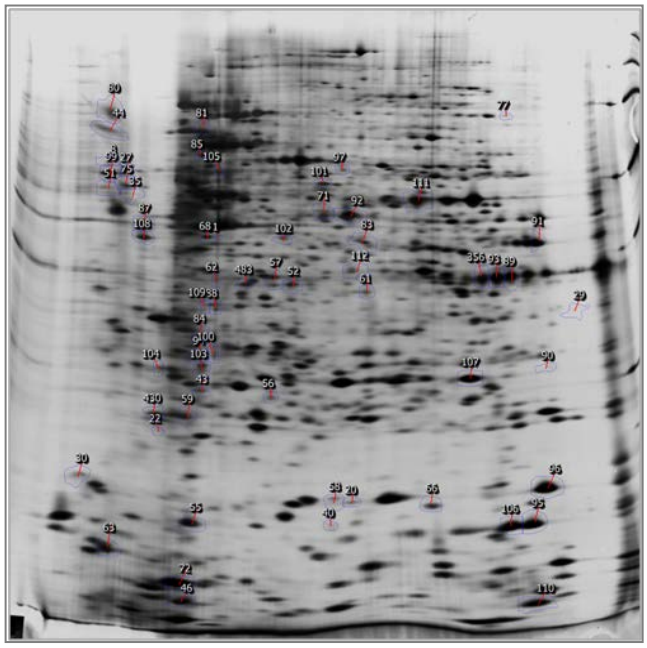

Fig. 17. 2DE gel of PlGF-treated HUVECs

Fig. 18. 2DE gel of PlGF-treated HEK-293hFlt-1

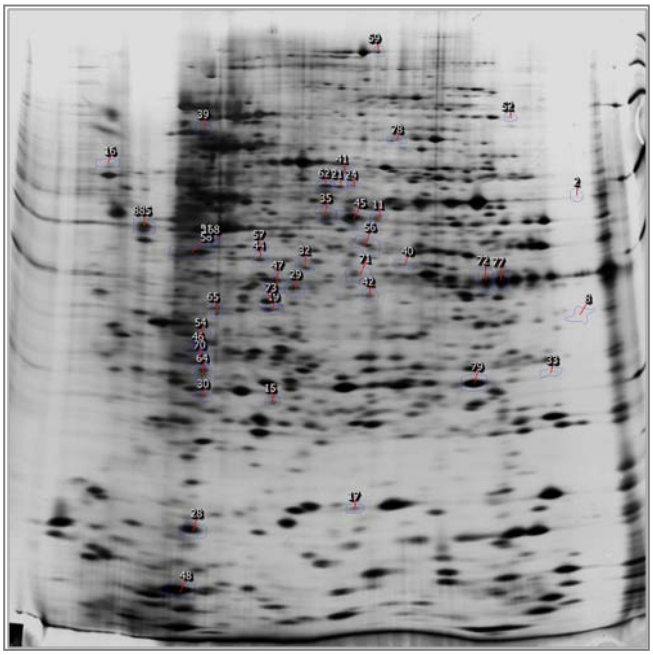

Fig. 19. 2DE gel of heterodimer-treated HUVECs

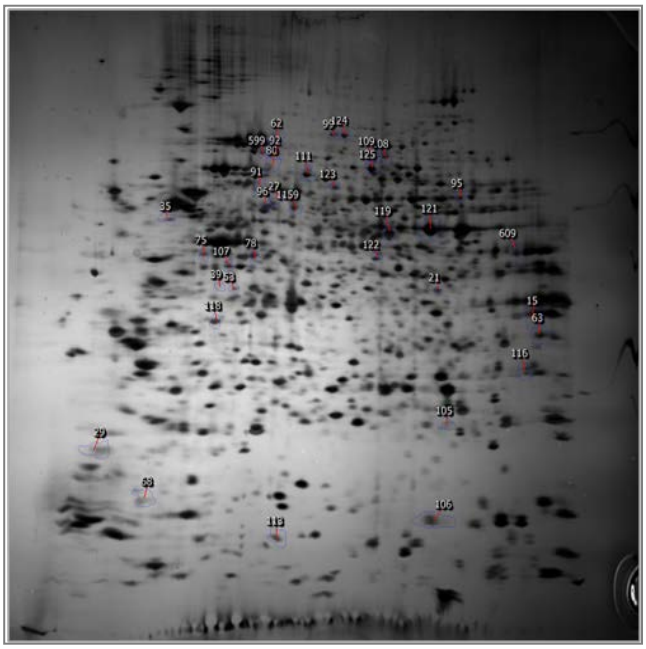

Fig. 20. 2DE gel of heterodimer-treated HEK-293hFlt-1

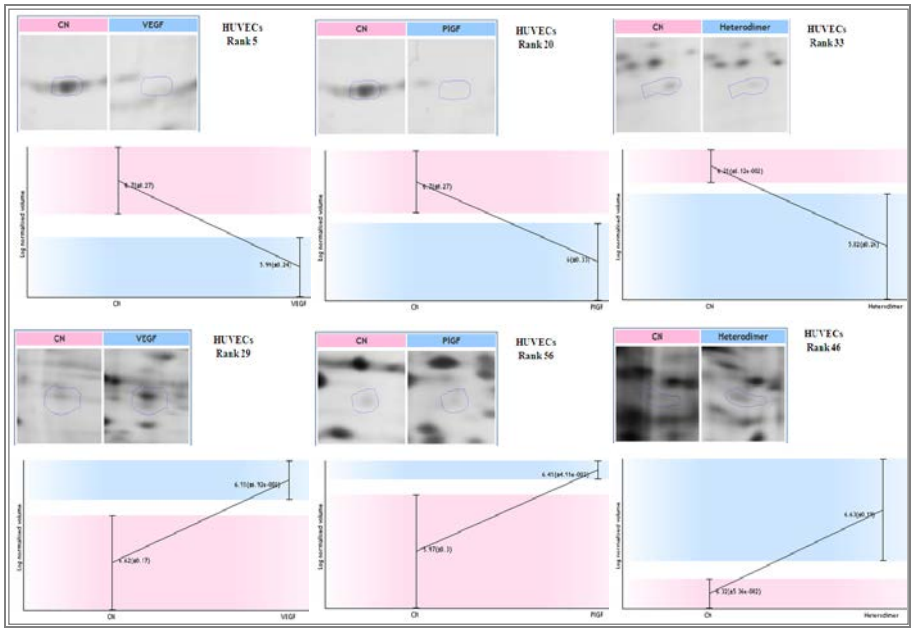

Fig. 21. HUVECs: Examples of some spot patterns

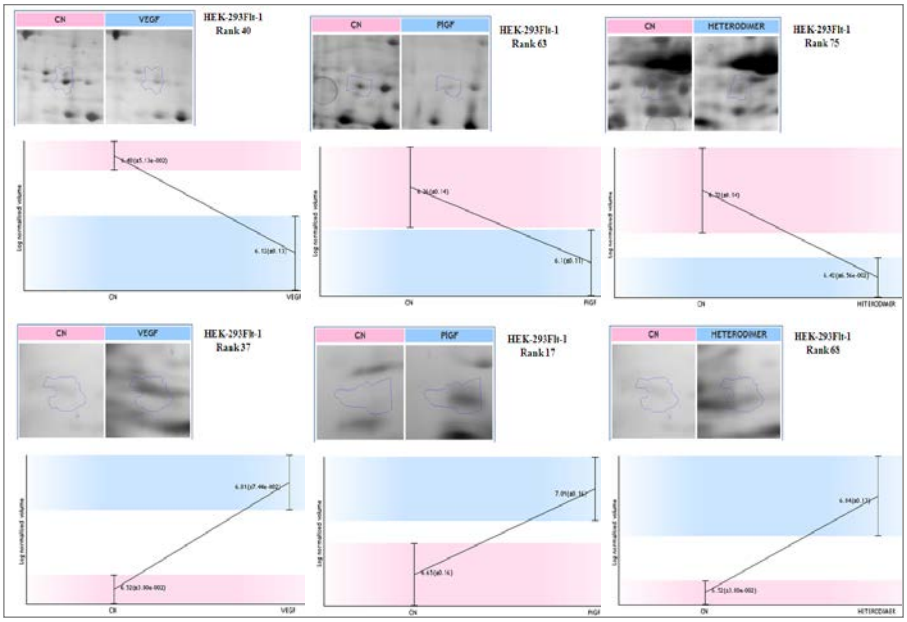

Fig. 22. HEK-293Flt-1: Examples of some spot patterns

A “principal component analysis” (PCA) of the 2DE results has been used to determine whether there are any outliers in the data and also look at how well the samples group. PCA reduces the complexity of a multidimensional

analysis into two principal components, PC1 and PC2, which orthogonally divide the samples based on the two largest sources of variation in the dataset (figure 23). Each data point in our PCA plot represents the global expression value for all spots with a significant statistic value ($p \leq 0.05$).

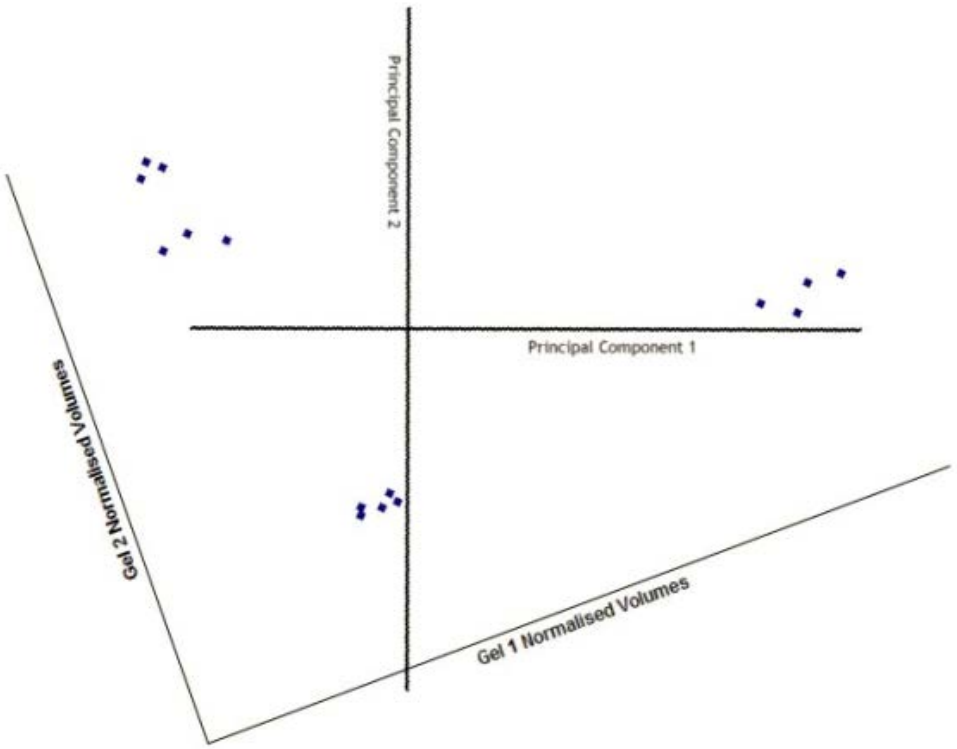

Fig. 23. Simplified representation of a PCA plot

For each comparison group, PCA plot (figures 24, 25) shows that 2D gel images cluster into two discrete groups, differentiated by two principal components (PC1 and PC2).

This means that there is:

- ✓ a clear differentiation between the expression of every specific treatment and that in the control
- ✓ a lack of outliers.

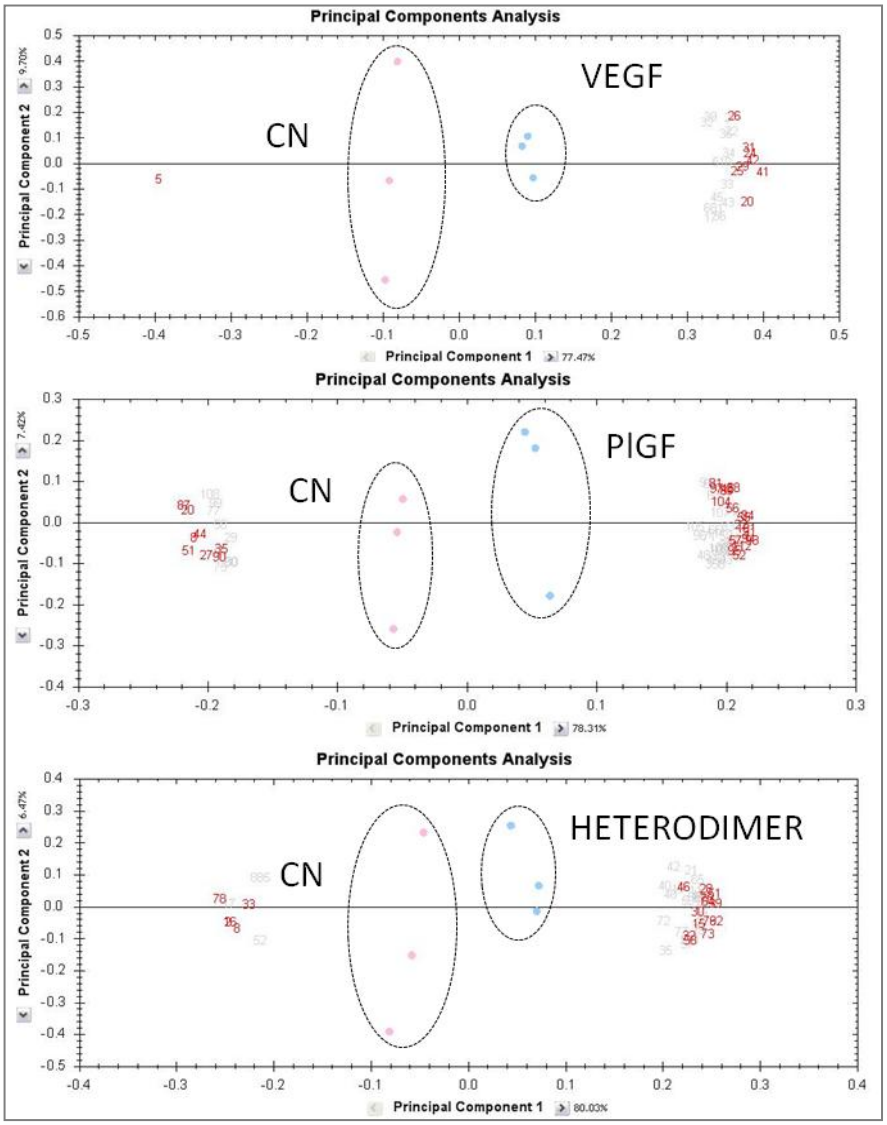

Fig. 24. Clustering of VEGFs treated HUVECs according to their protein profile.

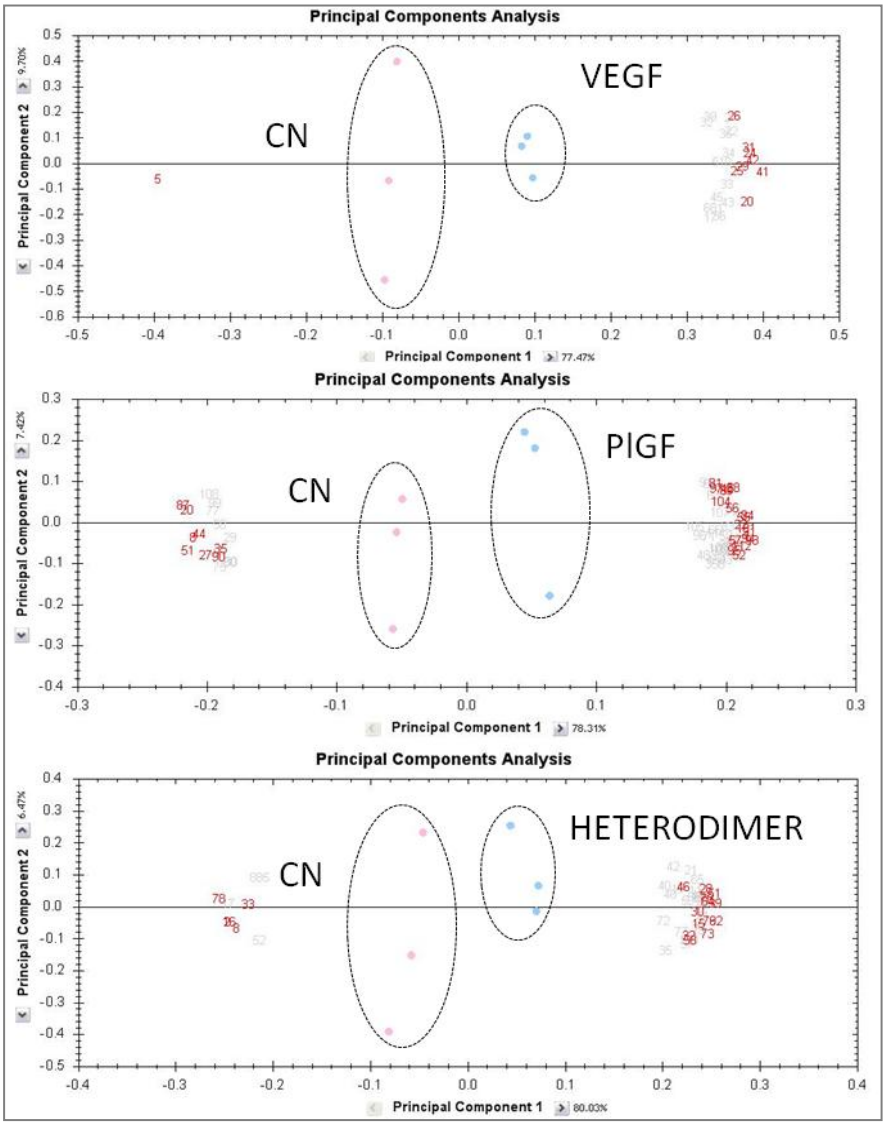

Fig. 25. Clustering of VEGFs treated HEK-293Flt-1cells according to their protein profile.

3.1.3 Protein identification

Triple replicates of 217 spots were manually cut, trypsin digested and processed for nano-LC-ESI-MS/MS analysis, allowing us to obtain both peptide mass mapping and amino acid sequencing for the more abundant peptides. The sets of peptide masses or peptide sequences obtained were used

to query biological sequence data banks, with the aim of identifying the corresponding protein or DNA sequence entries.

With this approach, we were able to identify the 13, 43, 30 unique proteins for VEGF, PlGF and heterodimer treated-HUVECs (table 4) and 15, 8, 23 proteins for VEGF, PlGF and heterodimer treated-HEK-293Flt-1 cells (table 5), respectively.

HUVECs: CV vs VEGF								
Rank	**SwissProt Code**	**Score**	**Mass**	**Matches**	**pI**	**Regulation**	**Sequence Coverage (%)**	**Name**
41	HNRH1_HUMAN	99	49484	4	5,89	up	10	Heterogeneous nuclear ribonucleoprotein H
510	GRP78_HUMAN	178	72402	5	5,07	up	11	78 kDa glucose-regulated protein
	HS71L_HUMAN	75	70730	2	5,76		4	Heat shock 70 kDa protein 1-like
	HNRPK_HUMAN	75	51230	2	5,39		7	Heterogeneous nuclear ribonucleoprotein K
35	ANXA5_HUMAN	158	35971	2	4,94	up	9	Annexin A5
42	PSA3_HUMAN	69	28643	3	5,19	up	14	Proteasome subunit alpha type-3
17	PDIA6_HUMAN	94	48490	3	4,95	up	10	Protein disulfide-isomerase A6
29	G3P_HUMAN	77	36201	3	8,57	up	12	Glyceraldehyde-3-phosphate dehydrogenase
31	ENOA_HUMAN	177	47481	8	7,01	up	22	Alpha-enolase
	ENOG_HUMAN	88	47581	2	4,91		7	Gamma-enolase
26	IF5A1_HUMAN	106	17049	4	5,08	up	23	Eukaryotic translation initiation factor 5A-1
24	LEG1_HUMAN	67	15048	9	5,34	up	57	Galectin-1
	THIO_HUMAN	67	12015	2	4,82		12	Thioredoxin

HUVECs: CV vs PlGF								
Rank	**SwissProt Code**	**Score**	**Mass**	**Matches**	**pI**	**Regulation**	**Sequence Coverage (%)**	**Name**
30	GFAP_HUMAN	69	49907	2	5,42	down	7	Glial fibrillary acidic protein
87	RCN3_HUMAN	88	37470	3	4,74	down	8	Reticulocalbin-3
	PLAK_HUMAN	82	82434	2	5,75		2	Junction plakoglobin
8	CALR_HUMAN	65	48283	2	4,29	down	6	Calreticulin
75	BASP1_HUMAN	83	22680	5	4,64	down	29	Brain acid soluble protein 1
58	NDKA_HUMAN	112	17309	12	5,83	down	48	Nucleoside diphosphate kinase A
108	RCN1_HUMAN	76	38866	3	4,84	down	10	Reticulocalbin-1

29	VDAC1_HUMAN	79	30868	4	8,62	down	19	Voltage-dependent anion-selective channel protein 1
77	FUBP1_HUMAN	76	67690	2	7,18	down	2	Far upstream element-binding protein 1
109	G3P_HUMAN	139	36201	4	8,57	up	20	Glyceraldehyde-3-phosphate dehydrogenase
	PLAK_HUMAN	110	82434	8	5,57		15	Junction plakoglobin
	DESP_HUMAN	108	334021	9	6,44		5	Desmoplakin
	1433S_HUMAN	87	27871	3	4,68		14	14-3-3 protein sigma
	H2B1B_HUMAN	69	13942	2	10,3		11	Histone H2B type 1-B
	CALL5_HUMAN	67	15883	2	4,34		23	Calmodulin-like protein 5
	FILA_HUMAN	67	435036	3	9,24		0	Filaggrin
97	ANXA1_HUMAN	66	38918	2	6,57	up	4	Annexin A1
31	ACTB_HUMAN	191	42052	17	5,29	up	49	Actin, cytoplasmic 1
	G3P_HUMAN	179	36201	13	8,57		41	Glyceraldehyde-3-phosphate dehydrogenase
	POTEE_HUMAN	110	122882	7	5,83		6	POTE ankyrin domain family member E
	UBXN1_HUMAN	134	33149	3	5,23		13	UBX domain-containing protein 1
56	PSB4_HUMAN	80	29242	2	5,72	up	12	Proteasome subunit beta type-4
61	G3P_HUMAN	91	36201	3	8,57	up	12	Glyceraldehyde-3-phosphate dehydrogenase
	PDIA6_HUMAN	73	48490	3	4,95		6	Protein disulfide-isomerase A6
101	HNRH1_HUMAN	99	49484	4	5,89	up	10	Heterogeneous nuclear ribonucleoprotein H
105	TBA1B_HUMAN	78	50804	3	4,94	up	10	Tubulin alpha-1B chain
	TBA1A_HUMAN	69	50788	3	4,94		10	Tubulin alpha-1A chain
68	PLAK_HUMAN	66	82434	2	5,75	up	2	Junction plakoglobin
81	PDIA1_HUMAN	265	57480	10	4,76	up	25	Protein disulfide-isomerase
	GRP78_HUMAN	178	72402	5	5,07		11	78 kDa glucose-regulated protein
	HS71L_HUMAN	75	70730	2	5,76		4	Heat shock 70 kDa protein 1-like
	HNRPK_HUMAN	75	51230	2	5,39		7	Heterogeneous nuclear ribonucleoprotein K
71	TBB5_HUMAN	84	50095	8	4,78	up	28	Tubulin beta chain
83	TPIS_HUMAN	415	31057	20	5,65	up	57	Triosephosphate isomerase
	GALK1_HUMAN	91	42702	6	6,04		16	Galactokinase
52	G3P_HUMAN	77	36201	3	8,57	up	12	Glyceraldehyde-3-phosphate dehydrogenase
356	G3P_HUMAN	341	36201	14	8,57	up	25	Glyceraldehyde-3-phosphate dehydrogenase
	ANXA2_HUMAN	155	38808	6	7,57		23	Annexin A2
91	ALDOA_HUMAN	315	39851	19	8,3	up	48	Fructose-bisphosphate aldolase A
111	ENOA_HUMAN	236	47481	13	7,01	up	34	Alpha-enolase
92	TBB5_HUMAN	944	50095	38	4,78	up	58	Tubulin beta chain
	TBB4B_HUMAN	569	50255	28	4,79		51	Tubulin beta-4B chain

	TBB3_HUMAN	317	50856	14	4,83		22	Tubulin beta-3 chain
	G3P_HUMAN	392	36201	14	8,57		17	Glyceraldehyde-3-phosphate dehydrogenase
93	ANXA2_HUMAN	97	38808	3	7,57	up	8	Annexin A2
	IGHA1_HUMAN	69	38486	2	6,08		9	Ig alpha-1 chain C region
63	RLA2_HUMAN	107	11658	3	4,42	up	26	60S acidic ribosomal protein P2
55	IF5A1_HUMAN	106	17049	4	5,08	up	23	Eukaryotic translation initiation factor 5A-1
106	PPIA_HUMAN	113	18229	10	7,68	up	65	Peptidyl-prolyl cis-trans isomerase A
72	LEG1_HUMAN	67	15048	9	5,34	up	57	Galectin-1
	THIO_HUMAN	67	12015	2	4,82		12	Thioredoxin
95	PPIA_HUMAN	120	18229	13	7,68	up	65	Peptidyl-prolyl cis-trans isomerase A
96	COF1_HUMAN	261	18719	18	8,22	up	60	Cofilin-1

HUVECs: CV vs HETERODIMER

Rank	SwissProt Code	Score	Mass	Matches	pI	Regulation	Sequence Coverage (%)	Name
16	CALR_HUMAN	65	48283	2	4,29	down	6	Calreticulin
8	VDAC1_HUMAN	79	30868	4	8,62	down	19	Voltage-dependent anion-selective channel protein 1
885	RCN3_HUMAN	88	37470	3	4,74	down	8	Reticulocalbin-3
	PLAK_HUMAN	82	82434	2	5,75		2	Junction plakoglobin
2	ENOA_HUMAN	95	47481	2	7,01	down	6	Alpha-enolase
52	FUBP1_HUMAN	76	67690	2	7,18	down	2	Far upstream element-binding protein 1
42	G3P_HUMAN	91	36201	3	8,57	up	12	Glyceraldehyde-3-phosphate dehydrogenase
	PDIA6_HUMAN	73	48490	3	4,95		6	Protein disulfide-isomerase A6
	AK1A1_HUMAN	226	36892	7	6,32		15	Alcohol dehydrogenase [NADP(+)]
40	ANXA1_HUMAN	192	38918	5	6,57	up	22	Annexin A1
	G3P_HUMAN	68	36201	4	8,57		17	Glyceraldehyde-3-phosphate dehydrogenase
57	ALDH2_HUMAN	215	56859	10	6,63	uo	19	Aldehyde dehydrogenase, mitochondrial
	TBA1B_HUMAN	148	50804	4	4,94		10	Tubulin alpha-1B chain
41	ANXA1_HUMAN	66	38918	2	6,57	uup	22	Annexin A1
65	ANXA5_HUMAN	158	35971	8	4,94	up	9	Annexin A5
51	PDIA1_HUMAN	265	57480	10	4,76	up	25	Protein disulfide-isomerase
46	GRP78_HUMAN	282	72402	13	5,07	up	15	78 kDa glucose-regulated protein
62	HNRH1_HUMAN	99	49484	4	5,89	up	10	Heterogeneous nuclear ribonucleoprotein H
15	PSB4_HUMAN	80	29242	2	5,72	up	12	Proteasome subunit beta type-4
39	GRP78_HUMAN	178	72402	5	5,07	up	11	78 kDa glucose-regulated protein
	HS71L_HUMAN	75	70730	2	5,76		4	Heat shock 70 kDa protein 1-like

	HNRPK_HUMAN	75	51230	2	5,39		7	Heterogeneous nuclear ribonucleoprotein K
70	PSA3_HUMAN	69	28643	3	5,19	up	14	Proteasome subunit alpha type-3
11	G3P_HUMAN	145	36201	8	8,57	up	30	Glyceraldehyde-3-phosphate dehydrogenase
	TBB5_HUMAN	121	50095	9	4,78		21	Tubulin beta chain
56	TPIS_HUMAN	415	31057	20	5,65	up	57	Triosephosphate isomerase
	GALK1_HUMAN	91	42702	6	6,04		16	Galactokinase
72	G3P_HUMAN	341	36201	14	8,57	up	25	Glyceraldehyde-3-phosphate dehydrogenase
	ANXA2_HUMAN	155	38808	6	7,57		23	Annexin A2
77	G3P_HUMAN	392	36201	14	8,57	up	17	Glyceraldehyde-3-phosphate dehydrogenase
	ANXA2_HUMAN	97	38808	3	7,57		8	Annexin A2
	IGHA1_HUMAN	69	38486	2	6,08		9	Ig alpha-1 chain C region
29	G3P_HUMAN	77	36201	3	8,57	up	12	Glyceraldehyde-3-phosphate dehydrogenase
35	TBB5_HUMAN	84	50095	8	4,78	up	28	Tubulin beta chain
28	IF5A1_HUMAN	106	17049	4	5,08	up	23	Eukaryotic translation initiation factor 5A-1
	TBB5_HUMAN	944	50095	38	4,78		58	Tubulin beta chain
45	TBB4B_HUMAN	569	50255	28	4,79	up	51	Tubulin beta-4B chain
	TBB3_HUMAN	317	50856	14	4,83		22	Tubulin beta-3 chain
48	LEG1_HUMAN	67	15048	9	5,34	up	57	Galectin-1
	THIO_HUMAN	67	12015	2	4,82		12	Thioredoxin
58	PDIA1_HUMAN	161	57480	13	4,76	up	28	Protein disulfide-isomerase

Tab. 4. List of identified proteins in HUVECs

HEK-293hFlt-1: CV vs VEGF								
Rank	**SwissProt Code**	**Score**	**Mass**	**Matches**	**pI**	**Regulation**	**Sequence Coverage (%)**	**Name**
48	CH60_HUMAN	1077	61187	37	5,7	down	50	60 kDa heat shock protein, mitochondrial
	HNRPK_HUMAN	418	51230	13	5,39		32	Heterogeneous nuclear ribonucleoprotein K
	GRP75_HUMAN	359	73920	12	5,87		22	Stress-70 protein, mitochondrial
44	TCPG_HUMAN	111	61066	2	6,1	down	4	T-complex protein 1 subunit gamma
	HSP71_HUMAN	86	70294	4	5,48		8	Heat shock 70 kDa protein 1A/1B
52	HNRPK_HUMAN	103	51230	4	5,39	down	15	Heterogeneous nuclear ribonucleoprotein K
	INO1_HUMAN	98	61542	4	5,52		10	Inositol-3-phosphate synthase 1
	TCPE_HUMAN	77	60089	5	5,45		14	T-complex protein 1 subunit epsilon
761	CH60_HUMAN	75	61187	2	5,7	down	7	60 kDa heat shock protein, mitochondrial
	EF2_HUMAN	109	96246	11	6,41		16	Elongation factor 2

26	DHSA_HUMAN	359	73672	19	7,06	down	40	Succinate dehydrogenase [ubiquinone] flavoprotein subunit, mitochondrial
51	SERA_HUMAN	328	57356	16	6,29	down	40	D-3-phosphoglycerate dehydrogenase
50	IDH3A_HUMAN	112	40022	4	6,47	down	15	Isocitrate dehydrogenase [NAD] subunit alpha, mitochondrial
49	SYG_HUMAN	96	83854	5	6,61	down	8	Glycine--tRNA ligase
37	ACTB_HUMAN	79	42052	3	5,29	down	12	Actin, cytoplasmic 1
	IMB1_HUMAN	200	98420	10	4,68		13	Importin subunit beta-1
13	HS90B_HUMAN	135	83554	7	4,97	up	10	Heat shock protein HSP 90-beta
	HS90A_HUMAN	107	85006	7	4,94		10	Heat shock protein HSP 90-alpha

HEK-293hFlt-1: CV vs PlGF

Rank	SwissProt Code	Score	Mass	Matches	pI	Regulation	Sequence Coverage (%)	Name
41	TCPD_HUMAN	151	58401	5	7,96	down	11	T-complex protein 1 subunit delta
52	DHSA_HUMAN	359	73672	19	7,06	down	40	Succinate dehydrogenase [ubiquinone] flavoprotein subunit, mitochondrial
47	TCPD_HUMAN	169	58401	8	7,96	down	18	T-complex protein 1 subunit delta
54	SC23A_HUMAN	104	87018	5	6,64	down	9	Protein transport protein Sec23A
88	RAN_HUMAN	210	24579	15	7,01	up	43	GTP-binding nuclear protein Ran
	ES1_HUMAN	147	28495	9	8,5		36	ES1 protein homolog, mitochondrial
70	PIMT_HUMAN	66	24792	3	6,7	up	18	Protein-L-isoaspartate(D-aspartate) O-methyltransferase
91	PDCD5_HUMAN	199	14276	6	5,5	up		Programmed cell death protein 5
69	PFD2_HUMAN	91	16695	3	6,2	up	33	Prefoldin subunit 2

HEK-293hFlt-1: CV vs HETERODIMER

Rank	SwissProt Code	Score	Mass	Matches	pI	Regulation	Sequence Coverage (%)	Name
15	ALDOA_HUMAN	113	39851	9	8,3	down	29	Fructose-bisphosphate aldolase A
	GRP75_HUMAN	359	73920	12	5,87		22	Stress-70 protein, mitochondrial
62	TCPG_HUMAN	111	61066	2	6,1	down	4	T-complex protein 1 subunit gamma
	HSP71_HUMAN	86	70294	4	5,48		8	Heat shock 70 kDa protein 1A/1B
63	LDHA_HUMAN	136	36950	8		down		L-lactate dehydrogenase A chain
	ROA2_HUMAN	93	37464	6		down		Heterogeneous nuclear ribonucleoproteins A2/B1
	HNRPK_HUMAN	103	51230	4	5,39		15	Heterogeneous nuclear ribonucleoprotein K
80	INO1_HUMAN	98	61542	4	5,52	down	10	Inositol-3-phosphate synthase 1
	TCPE_HUMAN	77	60089	5	5,45		14	T-complex protein 1 subunit epsilon

	CH60_HUMAN	75	61187	2	5,7		7	60 kDa heat shock protein, mitochondrial
78	EIF3M_HUMAN	115	42932	7		down		Eukaryotic translation initiation factor 3 subunit M
35	SC23A_HUMAN	104	87018	5	6,64	down	9	Protein transport protein Sec23A
107	GLRX3_HUMAN	67	37693	6	5,31	down	24	Glutaredoxin-3
116	DX39A_HUMAN	83	49611	8	5,46	down	18	ATP-dependent RNA helicase DDX39A
	KAD2_HUMAN	82	26689	6	7,67	down	27	Adenylate kinase 2, mitochondrial
118	SPEE_HUMAN	193	34373	9	5,3	down	44	Spermidine synthase
108	DHSA_HUMAN	359	73672	19	7,06	down	40	Succinate dehydrogenase [ubiquinone] flavoprotein subunit, mitochondrial
122	SEPT2_HUMAN	323	41689	12		down		Septin-2
99	SYG_HUMAN	96	83854	5	6,61	down	8	Glycine--tRNA ligase
105	PRDX1_HUMAN	65	22324	3	8,27	up	15	Peroxiredoxin-1
113	PDCD5_HUMAN	199	14276	6	5,5	up		Programmed cell death protein 5
68	ACTB_HUMAN	79	42052	3	5,29	up	12	Actin, cytoplasmic 1
106	PPIA_HUMAN	451	18229	22	7,68	up	72	Peptidyl-prolyl cis-trans isomerase A

Tab. 5. List of identified proteins in HEK-293hFlt-1

For the majority of the identified proteins, the molecular masses and isoelectric points determined by 2D gel were consistent with the theoretical values. In some cases, the same protein was identified in different spots across the 2D gel with different molecular mass and isoelectric point suggesting the presence of post-translational modifications and/or protein isoforms. In certain spots, more than one protein was identified. Sometimes, MS/MS data allowed the identification of a particular protein isoform (for example Annexin A1, A2 and A5) or subunit (for example Proteasome subunit alpha type-3, Proteasome subunit beta type-4).

The sharing of some proteins by the different groups of analysis is shown schematically in the figure 26, that allows to immediately note how the numbers related to the HEK-293Flt-1 system are more reduced, compared to those detected in HUVEC. This would implies that, while in HEK-293Flt-1 only the proteomic profiles modulated by phosphorylation and activation of a

single receptor by the three different VEGFs dimers can be appreciated, in HUVEC, other more complex situations should be covered, such as:

- ✓ Activation of KDR
- ✓ Transfosphorilation between Flt-1 and KDR
- ✓ Receptor heterodimerization between Flt-1 and KDR

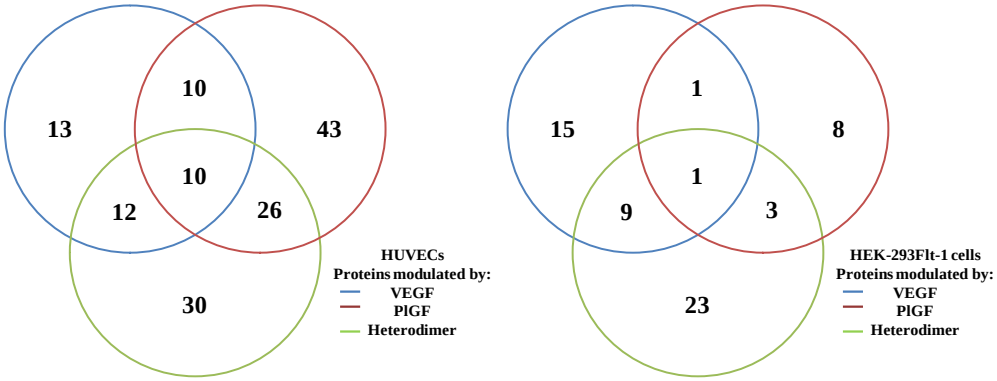

Fig. 26. VENN diagrams of proteins identified for HUVECs a) and HEK-293hFlt-1 b), with areas drawn to represent number of identified proteins. Numbers of proteins identified in each experiment, as well as number of common proteins

The differentially expressed proteins in VEGF treated HUVEC are: HNRH1_HUMAN, GRP78_HUMAN, HS71L_HUMAN, HNRPK_HUMAN, ANXA5_HUMAN, PSA3_HUMAN, PDIA6_HUMAN, G3P_HUMAN, ENOA_HUMAN, ENOG_HUMAN, IF5A1_HUMAN, LEG1_HUMAN, THIO_HUMAN; these proteins are all up-regulated. Some of these data have already been reported in the literature. For example, the up-regulation of ANXA5 and ENOA_HUMAN in HUVECs after 48 hours of incubation with VEGF have been descripted by Katanasaka et collaborators in 2007.

Pawlowska et *al*. through analysis of two-dimensional gel patterns of human endothelial cells before and after stimulation with $VEGF_{165}$, revealed differences in 85 protein spots, including heat shock proteins (HSPs; HSP-27, HSP-60, HSP-70p5, HSP-70p8, HSP-90, and HSP-96), proteins showing either chaperone activity or which participate in assembly of multimolecular

structures (TCP-1, desmoplakins, junction plakoglobin, GRP-94, thioredoxin related protein, and peptidylprolyl isomerase), components of the proteolytic machinery for the degradation of misfolded proteins (ER-60, cathepsin-D, proteasome subunits, and protease inhibitor-6), structural proteins (T-plastin, vimentin, α tubulin, actin, and myosin) that could account, at least in part, migration of endothelial cells. Authors rationalized these data explaining that VEGF induce a number of genes and multiple endogenous pathways that seem to be engaged in restoring cellular homeostasis (Pawlowska et al., 2005).. These findings fit partially with our data. In fact, as displayed in the previous tables, some of the proteins just described, seem to be modulated rather by PlGF or by heterodimer.

3.1.4 Data validation

2D-gel analysis results were then validated performing western blotting experiments using Ab against some of the proteins identified by MS. As an example, in fig. 27 results achieved using the anti-Annexin 1 antibody are shown, confirming the protein over-expression following exposure to each growth factor.

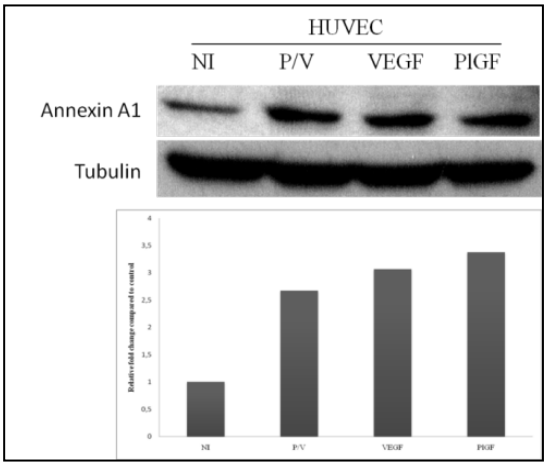

Fig. 27 Relative fold change of Annexin A1 in HUVEC compared to control

3.1.5 Functional annotation clustering of differentially regulated proteins

In gel-based proteomics, data generated from global expression and differential expression profiles can be explored by application of Gene Ontology (GO; http://www.geneontology.org/), for functional characterization of the cells. Gene Ontology is a part of the Open Biomedical Ontologies (OBO), which is the most widely used ontology in biomedical research community (Smith et al., 2007). The major aim of GO is to create a controlled and unified vocabulary for genes and gene products, such as proteins. GO annotation categorizes genes or gene products into hierarchical order based on 3 categories:

- ✓ cellular component (that describes the localization of gene products in the cells or its extracellular environment)
- ✓ biological process (that describes the biochemical reaction of gene products in the cells)
- ✓ molecular function (that describes the elemental activities of gene products at molecular levels)

By using the Database for Annotation, Visualization and Integrated Discovery (DAVID) v6.7 Bioinformatics Resource (http://david.abcc.ncifcrf.gov/home.jsp) we performed a "functional annotation clustering" of the proteins modulated by VEGFs dimers. DAVID, indeed uses many tools with which it can recognize enriched biological themes (mainly GO terms), determine enriched functional-related gene groups and cluster redundant annotation terms. A typical output of a functional annotation clustering is done as in figure 28.

With the highest classification stringency, we found 4, 14 and 15 principal functional clusters for HUVECs and 9, 1 and 7 functional clusters for HEK-293Flt-1cells, following the treatments with VEGF, PlGF and heterodimer, respectively. These data have been organized in tables (tables 6, 7), in which clusters are listed with the most enriched at top. To represent each cluster, it

has been reported the GO term with the lowest p value and the number of identified proteins related to it, useful to evaluate the reliability of the modulation of a specific cellular function. For example, in the case of HUVEC cells exposed to VEGF, 3 of the 13 proteins detected in the proteomic analysis (i.e. ENOA_HUMAN, ENOG_HUMAN and G3P_HUMAN) belong to the cluster "glycolysis". The p value at 6.4E-4 indicates that this function is significantly over represented among the 13 proteins analyzed. Similarly, also the other identified clusters ("intracellular organelle lumen", "regulation of apoptosis", "cytosolic part") were significant. Some of the identified proteins belong to more than one category since they possess multiple functions.

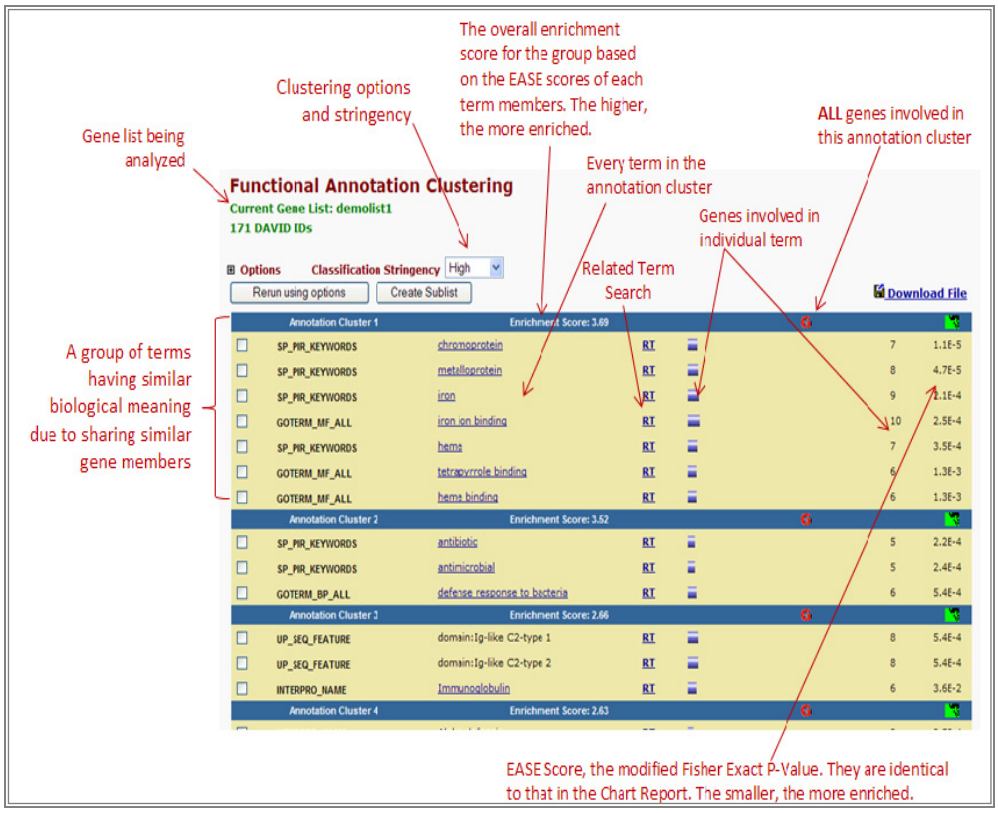

Fig.28. Output of a functional annotation clustering performed by DAVID

Likewise, the clusters "endoplasmic reticulum lumen", "glycolysis", "protein polymerization",… or "phospholipase inhibitor activity", "cell redox

homeostasis", "endoplasmic reticulum lumen",… resulted to be modulated in HUVEC following PlGF or VEGF/PlGF heterodimer treatment, respectively.
Comparing the results obtaining in this clusters analysis, some indication can be deduced: first of all, the treatments with the three different VEGF dimers stimulates some common clusters , such as "intracellular organelle lumen" and "regulation of apoptosis" in HUVECs, whereas "glycolysis" is common to with VEGF and PlGF treatment.
However, the effect of heterodimer treatment on HUVEC functions appears to be more similar to that induced by PlGF; indeed in both PlGF and VEGF/PlGF the terms "endopalsmic reticulum lumen", "protein polymerization", "cell redox homeostasis", "regulation of apoptosis", "intracellular organelle lumen", "proteinaceous extracellular matrix" are present, whereas these functions were not significantly affected by VEGF.
Due to the binding properties of the heterodimer these data indicate that also if it may induce VEGF receptor heterodimerization, the main activity is due to activation of VEGFR-1, as normally do PlGF in a specific way.

HUVEC: CN vs VEGF			
Funct Ann Clust	**Cluster**	**N of Involved Prot**	**P_Value**
GOTERM_BP_FAT	glycolysis	3	6.4E-4
GOTERM_CC_FAT	intracellular organelle lumen	4	1.2E-1
GOTERM_BP_FAT	regulation of apoptosis	3	1.4E-1
GOTERM_CC_FAT	cytosolic part	3	4.8E-3
HUVEC: CN vs PlGF			
Funct Ann Clust	**Cluster**	**N of Involved Prot**	**P_Value**
GOTERM_CC_FAT	endoplasmic reticulum lumen	6	2.7E-6

GOTERM_BP_FAT	glycolysis	4	2.4E-4
GOTERM_BP_FAT	protein polymerization	4	2.7E-4
GOTERM_BP_FAT	cell redox homeostasis	3	1.2E-2
GOTERM_BP_FAT	keratinocyte differentiation	4	6.5E-4
GOTERM_BP_FAT	regulation of apoptosis	8	4.0E-3
GOTERM_CC_FAT	intracellular organelle lumen	12	7.8E-3
GOTERM_MF_FAT	GTP binding	5	2.3E-2
GOTERM_CC_FAT	sarcomere	3	3.1E-2
GOTERM_BP_FAT	negative regulation of apoptosis	4	6.3E-2
GOTERM_MF_FAT	ribonucleotide binding	10	7.9E-2
GOTERM_CC_FAT	proteinaceous extracellular matrix	3	2.3E-1
GOTERM_MF_FAT	ATP binding	6	4.4E-1
GOTERM_BP_FAT	apoptosis	3	4.7E-1

HUVEC: CN vs VEGF/PlGF

Funct Ann Clust	Cluster	N of Involved Prot	P_Value
GOTERM_MF_FAT	phospholipase inhibitor activity	3	2.1E-4
GOTERM_BP_FAT	cell redox homeostasis	3	5.5E-3
GOTERM_CC_FAT	endoplasmic reticulum lumen	5	9.6E-6
GOTERM_CC_FAT	ribonucleoprotein complex	3	2.2E-1
GOTERM_CC_FAT	intracellular organelle lumen	10	1.7E-3
GOTERM_BP_FAT	protein complex assembly	6	1.7E-3
GOTERM_BP_FAT	cellular protein complex assembly	4	2.8E-3

GOTERM_BP_FAT	regulation of apoptosis	6	1.2E-2
GOTERM_BP_FAT	protein polymerization	3	3.4E-3
GOTERM_CC_FAT	melanosome	4	4.6E-4
GOTERM_BP_FAT	anti-apoptosis	3	5.1E-2
GOTERM_BP_FAT	negative regulation of cellular protein metabolic process	3	4.0E-2
GOTERM_CC_FAT	proteinaceous extracellular matrix	3	1.0E-1
GOTERM_MF_FAT	purine ribonucleotide binding	6	2.5E-1
GOTERM_MF_FAT	calcium ion binding	6	2.4E-2

Tab. 6. Functional annotation clustering of data obtained for HUVECs

A similar approach of functional clusters analysis was also applied to VEGFs dimers treated-HEK-293Flt-1 cells.

Contrary to what we observed in HUVEC, in this case VEGF and VEGF/PlGF heterodimer activate common cellular function, differently from PlGF. This indicate that when cells express only VEGFR-1, the activity of VEGF shifts to other targets if compared to cellular function activated when both VEGF receptors are expressed on cell surface. These differences are expected due to the diverse origin of cell line used in this study, HEK-293Flt-1is a transformed cell line while HUVECs are primary endothelial cells.

HEK-293Flt-1: CN vs VEGF			
Funct Ann Clust	**Cluster**	**N of Involved Prot**	**P_Value**
GOTERM_MF_FAT	purine ribonucleotide binding	10	5.0E-5
GOTERM_MF_FAT	adenyl nucleotide binding	10	1.4E-5

GOTERM_MF_FAT	ATP binding	9	8.5E-5
GOTERM_BP_FAT	response to unfolded protein	4	6.0E-5
GOTERM_CC_FAT	intracellular organelle lumen	8	7.9E-4
GOTERM_CC_FAT	cytoplasmic membrane-bounded vesicle	4	1.6E-2
GOTERM_MF_FAT	coenzyme binding	3	1.8E-2
GOTERM_BP_FAT	cellular protein complex assembly	3	1.4E-2
GOTERM_BP_FAT	negative regulation of apoptosis	3	5.7E-2

HEK-293Flt-1: CN vs PlGF

Funct Ann Clust	Cluster	№ of Involved Prot	P_Value
GOTERM_CC_FAT	cytoplasmic membrane-bounded vesicle	3	2.5E-2

HEK-293Flt-1: CN vs VEGF/PlGF

Funct Ann Clust	Cluster	№ of Involved Prot	P_Value
GOTERM_MF_FAT	purine ribonucleotide binding	9	5.8E-3
GOTERM_MF_FAT	adenyl nucleotide binding	9	2.2E-3
GOTERM_MF_FAT	ATP binding	8	6.7E-3
GOTERM_BP_FAT	regulation of apoptosis	5	2.8E-2
GOTERM_BP_FAT	negative regulation of apoptosis	3	9.5E-2
GOTERM_CC_FAT	mitochondrial inner membrane	3	7.5E-2
GOTERM_BP_FAT	positive regulation of apoptosis	3	1.3E-1

Tab. 7. Functional annotation clustering of data obtained for HEK-293hFlt-1

3.2 Searching for natural compounds with antiangiogenic activities

In order to identify new compounds able to interfere in Flt-1 recognition by PlGF and VEGF-A, we employed a highly sensitive competitive ELISA to screen plant extracts, fractions and pure compounds, performing a target based High Throughput Screening (HTS).

To carry out this study, a small library of plant extracts to be tested in HTS was built up. The plants were selected on the basis of their reported use in traditional folk medicine. The creation of a library of crude natural product extracts has several advantages: inexpensive to prepare, minimal sample preparation time, moderate overall size, high degree of diversity.

In our ELISA based approach, drug targets were exposed to crude extracts and, when some evidence of an inhibitory activity of the sample occurred, the extract was fractionated leading to the isolation of pure compounds which were singularly tested again. The active compounds then underwent to complete structural characterization by spectroscopic and spectrometric techniques.

The fractionation process adopted for the deconvolution of active extracts was chosen on the basis of the number of compounds in the original crude extract, the resulting fractions can differ widely in complexity from a mixture of multiple compounds to a single major compound of > 90% purity. Each extract was subjected to different separation techniques, such as solid-phase extraction, liquid-liquid partitioning, and column chromatography methods like silica gel flash chromatography and sephadex, resulting in several sub-fractions. These sub-fractions were then tested again and, when a hit notification is shown, the active sub-fraction are further fractionated. Finally, if one of these fractions is found to be active, the individual components were separated by HPLC and the resulting pure compounds were tested. This

process is attractive because only compound structures from the active fractions are elucidated.

3.2.1 Screening of a small library of plant extracts

An ELISA-based assay has been used to identify molecules able to inhibit the interaction of VEGFs with the immobilized Flt-1 receptor (De Falco, et al. 2001). In the first step we tested some plant extracts (table 6)

Plants	Abb.	Plant part	Extracts
Feretia apodanthera Del. (Rubiaceae)	FA	aerial parts	FA-H (Ex *n* Hexane) FA-C (Ex $CHCl_3$) FA-CM (Ex $CHCl_3$:MeOH 9:1) FA-M (Ex MeOH)
Campsiandra guayanensis B. Stergios (Caesalpiniaceae)	CAG	aerial parts	CAG-H (Ex *n* Hexane) CAG-C (Ex $CHCl_3$) CAG-CM (Ex $CHCl_3$:MeOH 9:1) CAG-M (Ex MeOH)
Vernonia nigritiana Oliv. & Hiern (Compositae)	VN	aerial parts	VN-H (Ex *n* Hexane) VN-C (Ex $CHCl_3$) VN-CM (Ex $CHCl_3$:MeOH 9:1 VN-M (Ex MeOH)
Salvia palaestina Bentham (Lamiaceae)	SPA	aerial parts	SPA-H (Ex *n* Hexane) SPA-C (Ex $CHCl_3$) SPA-CM (Ex $CHCl_3$:MeOH 9:1) SPA-M (Ex MeOH)
Astronium graveolens Jacq (Anacardiaceae)	AG	leaves	AG-H (Ex nHexane) AG-C (Ex $CHCl_3$) AG-M (Ex MeOH)
Cachrys ferulacea (L.) Calest. (Apiaceae)	CFU	aerial parts	CFU-H (Ex *n* Hexane) CFU-C (Ex $CHCl_3$) CFU-CM (Ex $CHCl_3$:MeOH 9:1) CFU-M (Ex MeOH)
Salvia multicaulis Vahl. (Lamiaceae)	SMU	aerial parts	SMU-H (Ex nHexane) SMU-C (Ex $CHCl_3$) SMU-M (Ex MeOH)
Salvia sclarea L., (Lamiaceae)	SS	roots	SS-H (Ex nHexane) SS-C (Ex $CHCl_3$) SS-M (Ex MeOH)

Tab. 8. The small library of natural extracts screened in this study.

The plant material was extracted with solvents at increasing polarity by using classical techniques, such as maceration at room temperature, and/or

instrumental approaches, such as ASE (Accelerated Solvent Extraction) and Naviglio, which are less time and solvent consuming.

We selected an increasing polarity extraction to obtain extracts with compound at similar polarity. This is important when fractions with wide range of polarities are going to be tested.

A critical point in a screening program is the amount of sample consumed by the assay process. For our ELISA assay, only small amounts of sample (200 μg) is required for the initial screening, while the dose-response curves required approximately 120 μg of sample, depending on chemical-physical sample characteristics and its activity range.

Preliminary, the binding of VEGF-A and PlGF in presence of 1 mg/mL of each plant extract was evaluated. Results were expressed as % of binding respect to the positive control, which is the binding of the growth factor without plant extract. Peptide 4-23-23, a previously described VEGFs/Flt-1 inhibitor (Ponticelli, et al., 2008), was used as negative control at 30 mg/L.

The extracts which caused a reduction of the binding percentage below 20% were assayed in a dose-dependent competition test at the concentrations of 500, 100, 20 mg/L. Therefore the most active extracts were further fractionated through chromatographic methods as LPLC, MPLC, HPLC in order to isolate the main components. Specific purification techniques were chosen upon the nature of the compounds to be isolated. The structural determinations were carried out using spectroscopic methods.

Below, we discuss the deconvolution of the extracts that gave the best results in a greater detail.

3.2.2 Bioassay-guided isolation of natural compounds with antiangiogenic activities

By ELISA assay, the $CHCl_3$-MeOH extract of *C. guyanensis* (aerial parts) and the MeOH extract of *F. apodanthera* (aerial parts) exhibited activity in the inhibition of both PlGF/Flt-1 and VEGF-A/Flt-1 interactions (Figure 29).

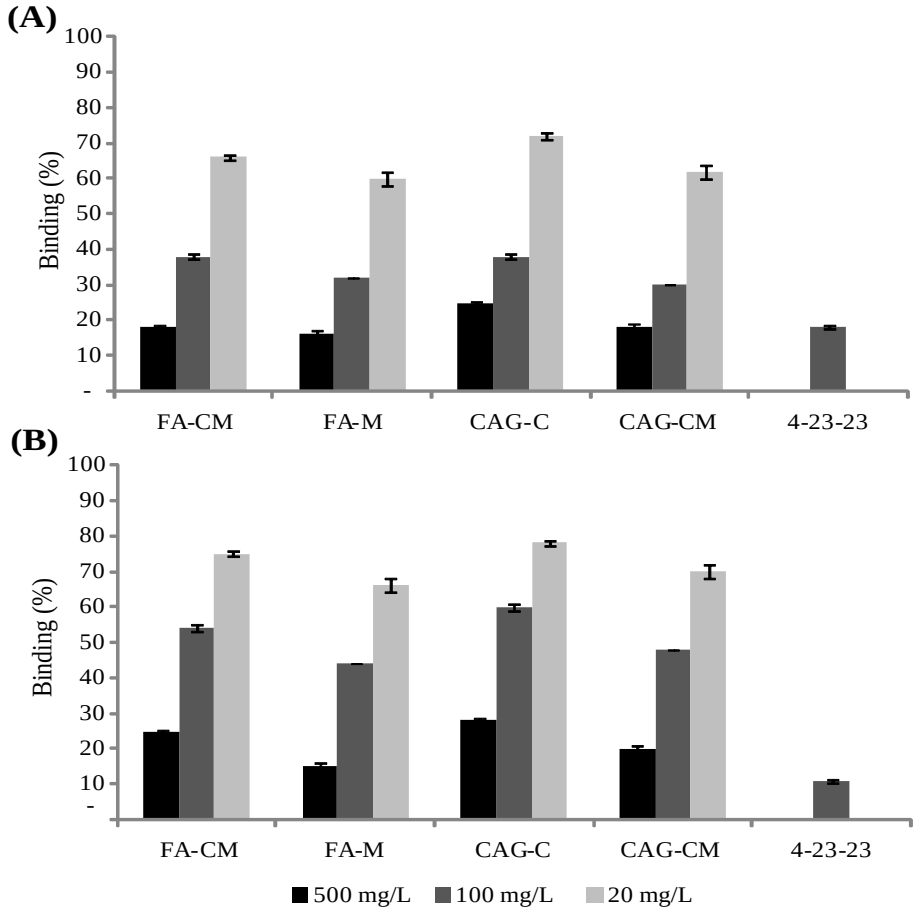

Fig. 29. Inhibitory effect of *F. apodanthera* and *C. guyanensis* extracts on PlGF/Flt-1 (A) and VEGF/Flt-1 interaction (B). The extracts were tested at 500 mg/L, 100 mg/L and 20 mg/L. A specific inhibiting peptide (4-23-23) was used as control.[7] Each experiment was performed three times and average values ± SD were reported. FA-CM = *F. apodanthera* $CHCl_3$-MeOH extract. FA-M = *F. apodanthera* MeOH extract. CAG-C = *C. guayanensis* $CHCl_3$ extract. CAG-CM = *C. guayanensis* $CHCl_3$-MeOH extract.

Therefore, these extracts were submitted to a bioassay-oriented fractionation using Sephadex LH-20. The fractions were tested on both PlGF/Flt-1 and VEGF-A/Flt-1. Only fraction 10 of the *C. guayanensis* $CHCl_3$-MeOH extract

and fractions 10 and 11 of the *F. apodanthera* MeOH extract showed inhibitory activity (data not shown). Chromatographic separation of active fractions led to the isolation of five proanthocyanidins (figure 30), the new (2*S*)-4',5,7-trihydroxyflavan-(4β→8)-afzelechin (**1**) and (2*S*)-4',5,7-trihydroxyflavan-(4β→8)-epiafzelechin (**2**) from *C. guayanensis* and the known compounds geranin B (**3**), proanthocyanidin A2 (**4**), and proanthocyanidin A1 (**5**), from *F. apodanthera* (Calzada et al 1999)

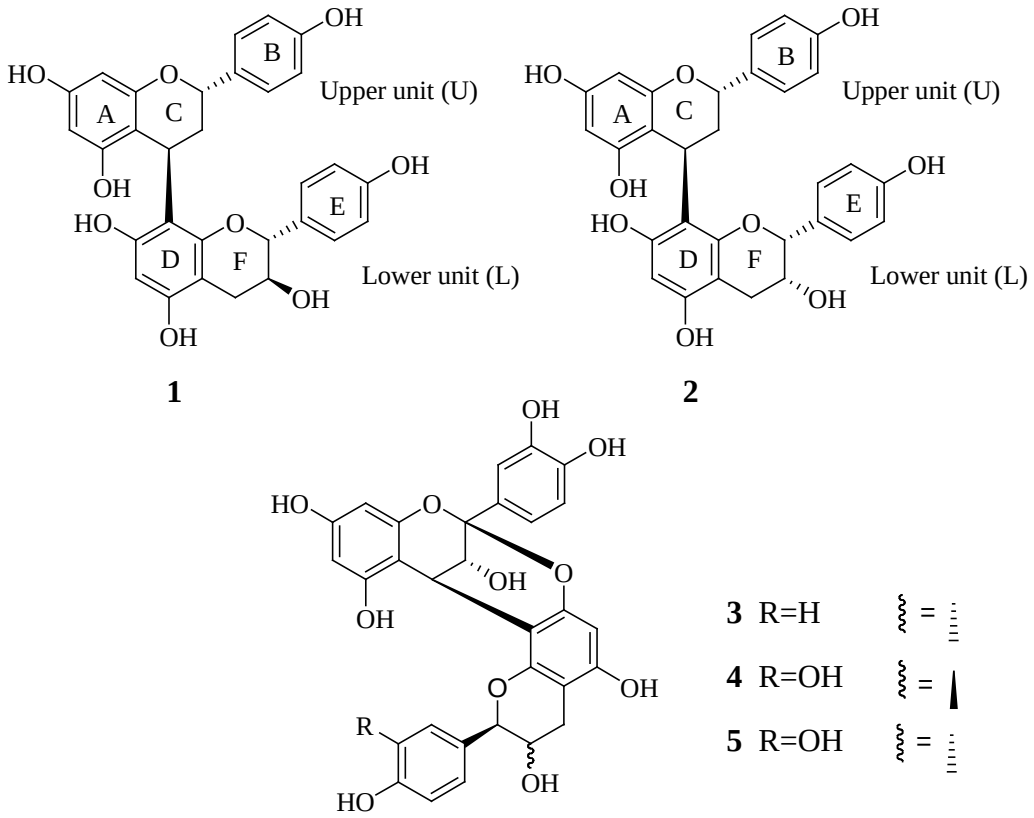

Fig. 30. Active proanthocyanidins, isolated from *F. apodanthera* and *C. guayanensis.*

Compound **1** was assigned a molecular formula, $C_{30}H_{26}O_9$, as determined by its positive HRESIMS data (*m/z* 529.1485, $[M - H]^-$). The ESIMS of **1** showed an $[M - H]^-$ ion at *m/z* 529 and prominent fragments at *m/z* 511 $[M - H - 18]^-$ and 289 $[M - H - 240]^-$. The ^1H NMR spectrum of **1** (table 9)

suggested its structural similarity to dimeric proanthocyanidins. Resonances of seven aromatic protons comprised two A_2X_2 spin systems of 1,4-disubstituted benzene rings (δ 7.11, d, *J* = 8.0 Hz, H-2'/H-6' (U and L), 6.77, d, *J* = 8.0 Hz, H-3'/H-5' (L), 6.72, d, *J* = 8.0 Hz, H-3'/H-5' (U)), ascribable to the B- and E-rings of the dimeric structure, two *meta*-coupled doublets at δ 6.24 and 6.17 (*J* = 1.8 Hz) attributed to the A-ring, and one singlet of a pentasubstituted benzene ring (δ 6.04) ascribed to the D-ring. 1D TOCSY and DQF-COSY spectra suggested the presence of two 4-spin systems attributable to a -CH-CH_2-CH- moiety (δ 5.30 [(1H, dd, *J* = 6.0, 2.5 Hz, H-2 (U)], 4.45 [1H, dd, *J* = 7.0, 6.0 Hz, H-4 (U)], 2.40 [1H, br dd, *J* = 12.0, 2.0 Hz, H-3a (U)], and 2.24 [1H, ddd, *J* = 12.0, 7.0, 6.0 Hz, H.3b (U)] and to a -CH-CHOH-CH_2- group [δ 4.30 (1H, d, *J* = 8.0 Hz, H-2 (L)], 4.02 [1H, ddd, *J* = 8.5, 8.0, 4.0 Hz, H-3 (L), 2.95 (1H, dd, *J* = 16.0, 4.0 Hz, H-4a (L)], and 2.53 [1H, dd, *J* = 16.0, 8.0 Hz, H-4b (L)]. The methylene protons of the latter 4-spin system are assignable to those of the terminal flavan-3-ol unit, and therefore, the former 4-spin system was attributed to the upper flavan unit. Direct evidence of the substituent sites was derived from the HSQC and HMBC correlations, which also allowed the assignment of all the resonances in the ^{13}C NMR spectrum (table 9). The configuration of the stereogenic carbons was obtained by means of chemical shifts, multiplicity, values of the coupling constants, in the ^{1}H NMR spectrum, and Electronic Circular Dicroism (ECD) analyses. A 2,4-*trans* C-ring configuration was deduced by the shielded C-2 signal (76.8 ppm) compared to the carbon chemical shifts of analogues with 2,4-*cis* configuration. The ECD spectrum of **1** exhibited a high-amplitude positive Cotton effect near 240 nm, indicating a 4β C-ring substituent and supported the 2*S*,4*R* absolute configuration. The ^{1}H and ^{13}C NMR values of H-2 (F-ring) (δ_H 4.30, d, *J* = 8.0 Hz, δ_C 82.6) indicated 2,3-*trans* configuration of the lower flavan-3-ol moiety. Moreover, the ECD negative Cotton effect near 280 nm supported 2*R*

configuration and hence an afzelechin moiety (i.e. 2*R*,3*S* configuration in ring F). Thus, compound **1** was identified as (2*S*)-4',5,7-trihydroxyflavan-(4β→8)-afzelechin.

The molecular formula of compound **2** ($C_{30}H_{26}O_9$) was established by ^{13}C NMR and ESIMS spectra (*m/z* 529 for $[M - H]^-$). In the ESIMS spectrum one main fragment was observed at *m/z* 289 $[M - H - 240]^-$, suggesting that **2** was an isomer of **1**. Its NMR data (table 9) suggested that the structure of **2** resembled that of **1**, but differed in the F-ring chemical shifts of the lower flavan-3-ol unit. Comparison of the chemical shifts of **2** with those of **1** suggested a 2,3-*cis* F-ring relative configuration [δ 4.64, br s, H-2 (L)]. The positive Cotton effect near 240 nm again was reminiscent of a 4β C-ring substituent and supported the 2*S*, 4*R* absolute configuration of the upper flavan unit. Again, the high-amplitude negative Cotton effect near 280 nm in the ECD spectrum supported 2*R* configuration and hence an epiafzelechin moiety (i.e. 2*R*,3*R* configuration in ring F). Thus, compound **2** was determined as (2*S*)-4',5,7-trihydroxyflavan-(4β→8)-epiafzelechin.

position	**1**		**2**	
	δ_H	δ_C	δ_H	δ_C
Upper unit				
2	5.30 dd (6.0, 2.5)	76.8	5.41 dd (6.0, 2.5)	76.7
3a	2.40 br dd (12.0, 2.0)	36.3	2.57 br dd (12.0, 2.0)	35.6
3b	2.24 ddd (12.0, 7.0,		2.22 ddd (12.0, 7.0,	
4	4.45 dd (7.0, 6.0)	29.5	4.50 m	28.7
5		156.4		155.7
6	6.24 d (1.8)	108.7	6.22 *d* (1.8)	108.6
7		157.5		157.4
8	6.17 d (1.8)	104.0	6.27 d (1.8)	103.6
9		153.8		153.4
10		119.6		119.7

1'		134.0		134.6
2'/6'	7.11 d (8.0)	128.6	7.16 d (8.0)	128.2
3'/5'	6.72 d (8.0)	115.9	6.72 d (8.0)	115.8
4'		156.0		155.8
Lower unit				
2	4.30 d (8.0)	82.6	4.64 br s	79.5
3	4.02 ddd (8.5, 8.0, 4.0)	68.4	4.22 br m	66.6
4a	2.95 dd (16.0, 4.0)	28.8	2.92 br d (16.0)	29.5
4b	2.53 dd (16.0, 8.0)		2.77 dd (16.0, 2.0)	
5		155.0		155.0
6	6.04 s	96.3	6.03 s	96.7
7		156.8		156.8
8		111.8		111.5
9		155.0		156.5
10		101.0		100.5
1'		132.0		129.9
2'/6'	7.11 d (8.0)	128.6	7.16 d (8.0)	128.2
3'/5'	6.77 d (8.0)	115.8	6.72 d (8.0)	115.8
4'		156.0		155.8

Tab. 9**.** ^{1}H and ^{13}C NMR Data of Compounds **1-2** (Methanol-d_4, 600 MHz)[a]

[a] *J* values are in parentheses and reported in Hz; chemical shifts are given in ppm; assignments were confirmed by DQF-COSY, 1D-TOCSY, HSQC, and HMBC experiments.

The pure compounds were tested in a dose dependent manner on VEGFs/Flt-1. Compounds **1**-**5** showed antiangiogenic activity in the Elisa assay on both PlGF-1/VEGFR-1 and VEGF-A/VEGFR-1. As shown in figure 31, compound **1** inhibited in a dose-dependent manner PlGF-1/VEGFR-1 interaction with an IC_{50} of 15 ±0.6 μM; **1** was also capable of inhibiting the VEGF-A/VEGFR-1 interaction but with reduced efficacy (IC_{50} = 50 ± 4.3 μM). As negative control, an inactive fraction from the same extract was used. An inhibitory activity was also shown by compound **3** with an IC_{50} of 28 ± 3.0 μM and 65 ± 5.4 μM in PlGF-1/VEGFR-1 and VEGF-A/VEGFR-1 interactions, respectively.

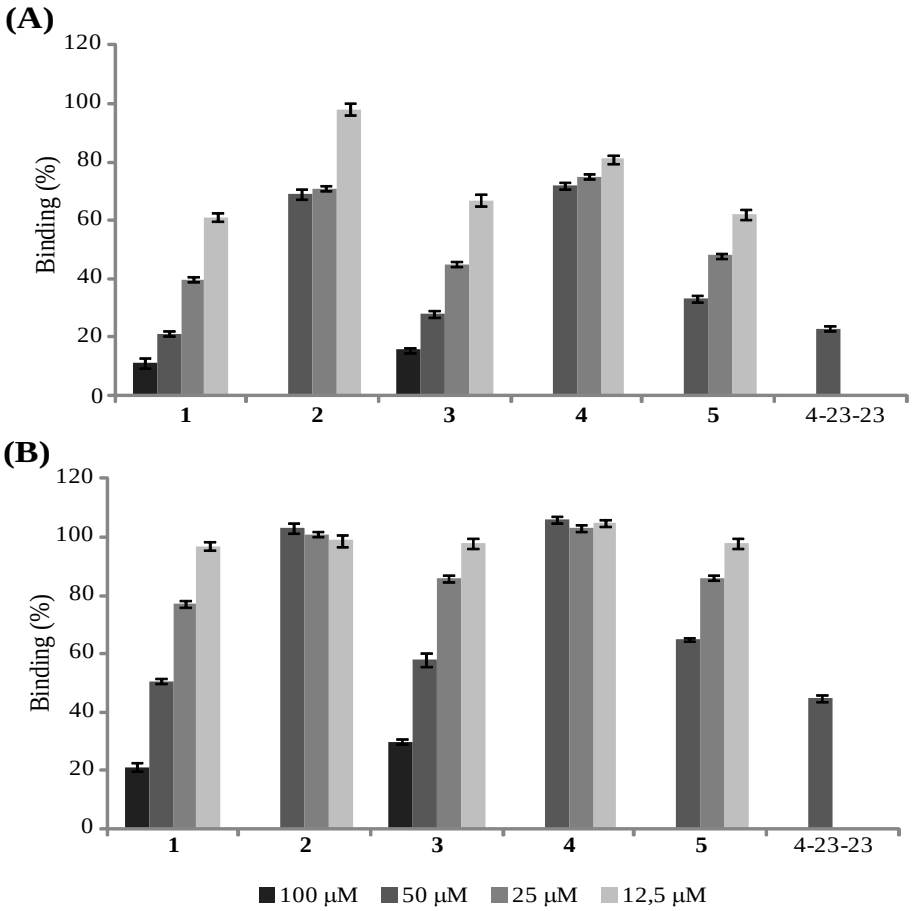

Fig. 31. Inhibitory effect of compounds **1**-**5** on PlGF/Flt-1 (A) and VEGF/Flt-1 interaction (B). Compound **1** was tested at 12.5 μM, 25 μM, 50 μM, and 100 μM while compounds **2**-**5** at 25 μM, 50 μM, and 100 μM. A specific inhibiting peptide (4-23-23) was used as control. Each experiment was performed three times and average values ± SD were reported.

3.2.3 SPR experiments

A surface plasmon resonance (SPR) based binding assay was used to investigate the interactions between the VEGRFs/VEGFs and compounds **1**-**5**. SPR allowed the measurement of kinetic and thermodynamic parameters of ligand-protein complex formation (Cooper, 2003). Amentoflavone, a potent VEGRFs/VEGFs inhibitor, was used as positive control (Tarallo et al., 2011). Recombinant PlGF-1, VEGF-A Fc-VEGFR-1 chimera, and tubulin and human serum albumin (HSA), as controls, were coated to a Biacore chip and

incubated with increasing concentrations of compounds **1**-**5**, starting from 0.025 to 4 µM, measuring the association and dissociation to the coated proteins. Compound **1** interacted with PlGF-1 and VEGF-A, as demonstrated by the concentration dependent responses and the clear exponential curves during both the association and dissociation phases (figure 32). Thermodynamic dissociation constants (K_D ± SD) of 11 ± 0.3 nM and 16 ± 0.2 nM were measured for the PlGF-1/**1** and VEGF-A/**1** interactions, respectively (table 10). Interestingly, thermodynamic dissociation constants measured for **1** were similar to those previously observed for the well known antiangiogenic compound amentoflavone (Tarallo et al., 2011). No significant interaction was detected with HSA or other controls (data not shown). Since compounds **1** and **3** have in their skeleton an afzelechin or catechin moiety, respectively, we also assayed these compounds, but no interaction was observed with the PlGF-1 or VEGF-A in SPR experiments (data not shown).

Compound	K_D (nM) vs PlGF	K_D (nM) vs VEGF
1	11 ± 3	16 ± 2
2	NB[a]	NB[a]
3	23 ± 5	48 ± 8
4	NB[a]	NB[a]
5	394 ± 86	476 ± 98
Amentoflavone	8.2 ± 0.3	16.5 ± 0.6

Tab. 10. Thermodynamic Constants Measured by SPR for the Interaction of Compounds **1**-**5** with Immobilized PlGF or VEGF

[a] For this compound no interaction with the immobilized protein was observed

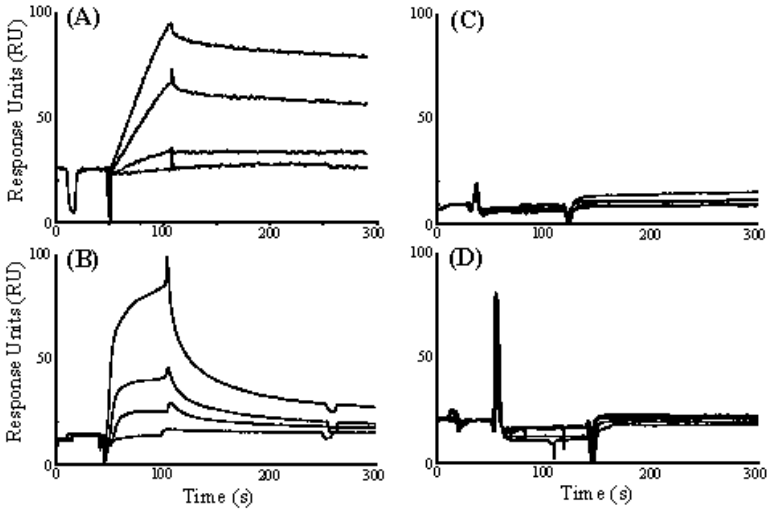

Fig. 32. Sensorgrams obtained injecting different concentration (25nM, 100 nM, 500 nM, 2 μM) of compounds **1** (A-B) or **2** (C-D) on immobilized PlGF (A-C) or VEGF (B-D).

3.2.4 Cytotoxic activity

Compounds **1-5** were tested for their cytotoxic activity against human lymphocyte cells T (Jurkat) and human breast adenocarcinoma (MCF7) cell lines. All compounds showed IC_{50} values higher than 70 μM.

3.2.5 Chicken embryo chorioallantoic membrane (CAM) assay

The antiangiogenic activity of **1** was investigated in vivo in the chicken embryo chorioallantoic membrane (CAM) assay model. The CAM of chicken eggs is a biological model to study the angiogenic and antiangiogenic activity of molecules, which interfere with physiological angiogenesis (Ribatti et al., 1996; Ribatti et al., 2001) The antiangiogenic activity, expressed as the percentage of inhibition, is reported in figure 33; compound **1** showed the highest inhibitory effects on the growth of CAM blood vessels at 10 μg with a significant inhibition percentage (56.19%, $p < 0.05$). The dose required for half-maximal inhibition (IC_{50}) was determined to be 9.79 μg. Retinoic acid (2 μg/egg), used as positive standard, confirmed its anti-angiogenesis activity ($p < 0.01$) with 75.47% inhibition. figure 34 shows the images of representative

microscopical observations of the CAMs exposed to different treatments. After four days of incubation, the CAM of control eggs showed the presence of a clear vascular network with large vessels converging towards the embryo. When the CAMs were treated with **1** (10µg/egg), a marked decrease in the number, length, size, and junctions was observed as compared with the controls. A strong inhibitory effect on capillary formation was evidenced in the CAM treated with retinoic acid (2 µg/egg) (figure 34).

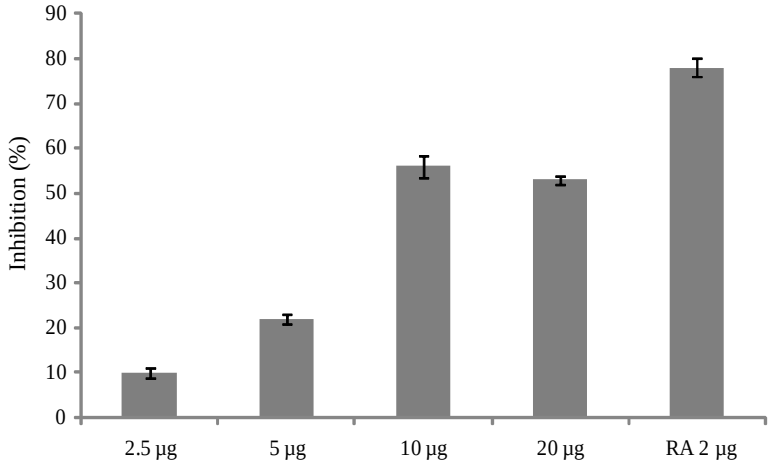

Fig. 33**.** Antiangiogenic activity of compound **1** in the chick embryo chorioallantoic membrane (CAM) assay. Retinoic acid (RA) was used as positive control. Each group contained at least 5 eggs. Each column represent mean ± SD of three experiments. **P*< 0.05 and ***P*< 0.01 compared with control group (Student's *t*-test).

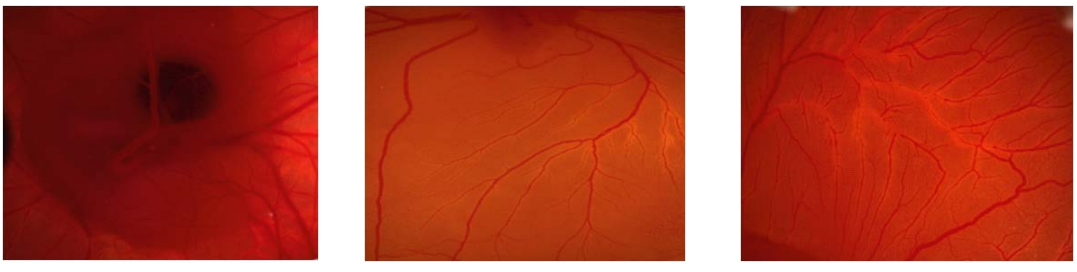

(A) **(B)** **(C)**

Fig. 34. Antiangiogenic activity of compound **1** in CAM assay. (A) = CAM vehicle control. (B) = CAM treated with retinoic acid at dose of 2 µg/egg.(C) = CAM treated with **1** at dose of 10 µg/egg.

CHAPTER 4:

Conclusions

4.1 Conclusions

Angiogenesis is a complex biological process, important for the embryonic development and the post-natal growth. In adult life, it is a tightly regulated event and occurs only during the menstrual cycle or after prolonged and sustained physical exercise, in heart and skeletal muscles. Angiogenesis is also re-activated during several pathological conditions, such as cancer, atherosclerosis, arthritis, diabetic retinopathy and age-related macular degeneration. The proangiogenic members of the vascular endothelial growth factor (VEGF) family and related receptors play a central role in the modulation of both physiological and pathological angiogenesis In the last years they have been validated as diagnostic and prognostic markers, other than as therapeutic targets. Despite the many positive responses, nowadays anti-angiogenesis therapy is facing some challenges, such as inherent/acquired resistance, enhanced invasiveness during the treatment, lack of validated predictive biomarkers to select patient population and to monitor tumors responses to the therapy.

The aim of the present study was to produce data that could be useful for the future development of new antiangiogenic drugs or treatment strategies. Thus, we focused on the following objectives:

- Producing an expression proteomic study of cell coltures (HUVECs and HEK-293hFlt-1), following their treatment with VEGFA, PlGF and VEGFA/PlGF.
- Identifying natural compounds acting as inhibitors of angiogenesis, by the inhibition of the interaction between the proangiogenic members of VEGF family and related receptors.

For the realization of the first point, gel-based proteomics was confirmed as a very effective strategy. Both in HUVECs and in HEK-293hFlt-1 cellswe were able to detect a discrete number of differentially expressed proteins, correlated to treatment with each specific VEGFs dimer selected for this study. Gels variability was also determined by principal component analysis (PCA). PCA plot showed that produced gels grouped according to the set experimental conditions. Only statistically significant spots ($p<0.05$) were manually cut, trypsin digested and processed for nano-LC-ESI-MS/MS analysis, allowing us to obtain protein identifications. The Mw and pI determined by 2D gel were consistent with the theoretical values, confirming the protein identity. In some cases, the same protein was identified in different spots across the 2D gel: this suggests the occurrence of post-translational modifications and/or protein isoforms. In certain spots, more than one protein was identified. In any cell culture, different treatments had in common the modulation of a number of proteins This phenomenon was less marked in HEK-293Flt-1 compared to the HUVEC. This would implies that, while in HEK-293Flt-1 only the proteomic profiles modulated by phosphorylation and activation of a single receptor by the three different VEGFs dimers can be appreciated, in HUVEC a complex situations occurs due to the presence of both VEGF receptors . Some of identified proteins were already reported in the literature; this represents a further confirmation of the reliability of all the data produced. By using the DAVID Bioinformatics Resource we performed a functional annotation clustering of the identified proteins for both cell culture. The partly different functions identified in the two different kind of cells may partly explain the different physiology of these cells, but above the different endothelial roles exerted by the selected VEGF dimers and related receptors. The achieved data will facilitate future studies on understanding of endothelial cells functions in response to different vascular endothelial growth factors. This aspect is extremely interesting, especially if we consider that literature gives us even

very few informations for the heterodimer. This proteomic profiling study will help researchers to elucidate connections between broad cellular pathways/molecules that were neither apparent nor predictable through traditional biochemical analysis in the past.

To achieve the second objective, we screened a small libraries of plant extracts with the aim of identifying small molecules with the capability to prevent the initial event required for the pro-angiogenic activity of the VEGF family members, the binding and activation of related receptor. As a result, we isolated two proantocyanidins, (2*S*)-4',5,7-trihydroxyflavan-(4β→8)-afzelechin (Compound **1**) and geranin B (Compound **3**), as antiangiogenic bioactive molecules. Indeed, we demonstrated that both are able to bind VEGF-A and PlGF-1, preventing the interaction with VEGFR-1. The antiangiogenic activity of Compound **1** was also confirmed in vivo by the chicken chorioallantoic membrane (CAM) assay. Compound **1** inhibited chorioallantoic membrane neo-vascularization. Monomeric flavan-3-ols like catechin and afzelechin did not interact with the VEGFs as determined by SPR assays. Taking into account these results and our previous reported data on the potent antiangiogenic activity of the biflavone amentoflavone, the antiangiogenic activity of compounds **1** and **3** may depend on dimeric and stereochemical features. Therefore, these compounds could be a promising scaffold to develop by medicinal chemistry approaches new antiangiogenic small molecules. We also reported for the first time the antiangiogenic activity of proanthocyanidins (Pesca et al,. 2012)

CHAPTER 5:

Experimental section

5.1 Proteomic study

5.1.1 Cell cultures and protein extracts

Whole protein extracts were prepared from human embryonic kidney 293 (HEK-293) (American Type Culture Collection) cells that stably overexpress hVEGFR-1 (HEK-293hFlt-1) and from human umbilical vein endothelial cells (HUVECs) (American Type Culture Collection) that express both VEGFR-1 and VEGFR-2. HEK-293hFlt-1cells were grown in Dulbecco's modified Eagle medium (DMEM) supplemented with 10% inactivated fetal bovine serum (FBS) (Euroclone) and antibiotics, while HUVECs were cultured in EBM supplemented with EGM2. Both cell lines were maintained at 37°C and at a fixed concentration of CO_2 (5%) in a humidified atmosphere. They were starved 16 hours at 37°C in serum free medium (1% FBS defined for HUVEC). After starvation, cells were incubated for 24 hours at 37°C with 100 ng/ml of PlGF-1, 100 ng/ml of VEGF-A and 100 ng/ml of VEGF-A /PlGF-1. Then they were lysed in a buffer containing 2 mM Tris-HCl at pH 8, 5 mM EDTA, 150 mM NaCl, 1% Triton-X 100, 10% glycerol, 10 mM zinc acetate, 100μM Na_3VO_4 and a protease inhibitor cocktail (Sigma-Aldrich) for 1 hr at 4°C in agitation. Then the samples were centrifuged for 10 min at 12000 x g and supernatants were recovered and stored at -80°C. The protein concentration was determined by the Bradford method using the BioRad reagent.

5.1.2 2-DE and image analysis

200 μg of protein extracts from HUVECs were resuspended in a buffer containing urea (8 M), CHAPS (4% w/v), DTT (65 mM) (Sigma–Aldrich),

bromophenol blue (0.05%) (BioRad), and carrier ampholytes (1.7% v/v IPG buffer 3–10 NL) (GE Healthcare). Mixtures were applied to 18 cm IPG strips pH 3-10 NL (GE Healthcare), by active in-gel rehydration. Focusing was performed with an IPGphor system (Amersham Biosciences) at 50 mA max, programming a gradient voltage (8000 V max) for a total of 70 kVh. Instead 250 µg of proteins extracts from HEK-293hFlt-1 were first precipitated by acetone. The obtained dry residue was dissolved in the rehydration solution containing 8M urea, 2M thiourea (Sigma–Aldrich), 4% CHAPS, 0,05% Zwittergent (Calbiochem) and 40mM TRIS and reduced with TCEP 5mM (Sigma-Aldrich) for 1 hour at room temperature. Subsequently, DeStreak Reagent (GE Healthcare), 2% IPG buffer 3-10NL (GE Healthcare) and 0.05% bromophenol blue were added. Samples were applied on 18 cm 3-10 NL Immobiline Dry Strip gels (GE Healthcare) through passive rehydration overnight at room temperature. After rehydration, the first dimension was performed with Ettan IPGphor Manifold (GE Healthcare) proceeding with a gradient voltage (8000 V max) for a total of 90 kVh. All strips were then equilibrated for 15 min in 50mM pH 8.8 Tris-HCl buffer containing 6 M urea, 30% glycerol, 2% SDS and 2% DTT, then for 15 min in the same buffer replacing DTT by 2.5% iodoacetamide (Sigma–Aldrich). Afterwards they were transferred onto 9–16% gradient acrylamide SDS-PAGE gels (20 x 20 cm) to run the second-dimension separation (60 mA/gel for 5 h). Electrophoretically separed proteins were visualized by high sensitive and MS compatible silver stain (Hochstrasser et al., 1988; Mortz et al., 2001). Gel images were acquired using a ProXpress scanner (Perkin Elmer), in a 16-bit TIF format, and 2-DE protein patterns were analyzed using Progenesis SameSpots (Nonlinear Dynamics). Each analytic experiment was carried out in triplicate.

5.1.3 Protein identification.

Differentially expressed protein spots were excised and trypsin-digested (Shevchenko et al., 2007); resulting peptide mixtures underwent high resolution nano-LC/MS-MS analysis. Chromatographic separation was achieved using a nano Acquity LC system (Waters Corporation): on a 1.7 μm BEH C-18 column (Waters Corporation) at a flow rate of 200 nl/min. A linear gradient (Solution A: 0.1% formic acid, solution B: 0.1% formic acid, 100% ACN) from 5% to 50% B over 55 min was used. MS and MS/MS data were acquired using a Q-TOF Premier mass spectrometer (Waters Corporation, Micromass). Doubly and triply charged peptide-ions were automatically chosen by the MassLynx software and fragmented. MS data were automatically processed and peaklists for protein identifications by database searches were generated by the ProteinLynx software. Database searches were carried out with MASCOT server using the SwissProt protein database (http://www.matrixscience.com/search_form_select.html). The SwissProt human database (514212 sequences; 180900945 residues) was searched allowing 2 missed cleavages, carbamidomethyl (C) as fixed modification, oxidation (M) as variable modifications. The peptide tolerance was set to 80 ppm and the MS/MS tolerance to 0.8 Da.

5.1.4 Western blot analysis

Some proteins were also detected and quantified by western blotting. Protein extracts (80μg) were resolved on 12 or 15% SDS-PAGE, electrotransferred onto polyvinylidene fluoride (PVDF) (GE Healthcare) membranes (100 V for 1 h) and incubated with Abs against some of the proteins identified by MS at the concentrations indicated by related data sheets in no fat milk 5% in Tris buffered saline (overnight at 4°C), followed by incubation with the secondary antibody, conjugated to HRP, diluted 1:10,000. Immunoreactive bands were detected using ECL reagents (GE Healthcare). Densitometry analysis to

evaluate the degree of protein expression was performed using NIH ImageJ software, using β-tubulin as house-keeping.

5.1.5 Protein categorization

The identified proteins were classified into groups according to cellular compartmentalization, biological process, and molecular function based on the information annotated in the Gene Ontology (GO) Consortium databases (http://www.geneontology.org/). This classification analysis was performed using the DAVID functional annotation tool (http://david.abcc.ncifcrf.gov/).

5.2 Bioassay oriented isolation study

5.2.1 General Experimental Procedures

Optical rotations were measured on a Perkin-Elmer 241 polarimeter equipped with a sodium lamp (589 nm) and a 1 dm microcell. UV spectra were recorded on a Perkin-Elmer-Lambda spectrophotometer. ECD spectra were measured on a JASCO J-810 spectropolarimeter with a 0.1 cm cell in DMSO at room temperature under the following conditions: speed 50 nm/min, time constant 1 s, bandwidth 2.0 nm. NMR experiments were performed on a Bruker DRX-600 spectrometer at 300 K. All the 2D NMR spectra were acquired in methanol-d_4 in the phase-sensitive mode with the transmitter set at the solvent resonance and TPPI (Time Proportional Phase Increment) used to achieve frequency discrimination in the ω_1 dimension. Standard pulse sequences and phase cycling were used for DQF-COSY, TOCSY, HSQC, HMBC, and ROESY experiments. NMR data were processed on a Silicon Graphic Indigo2 Workstation using UXNMR software. HRESIMS spectra were acquired in the positive ion mode on a Q-TOF premier spectrometer equipped with a nanoelectrospray ion source (Waters-Milford, MA, USA). Column

chromatographies were performed over Sephadex LH-20. HPLC separations were conducted on a Waters 590 series pumping system equipped with a Waters R 401 refractive index detector and U6K injector on a C_{18} μ-Bondapak column (30 cm x 7.8 mm, 10 μm Waters, flow rate 2.0 mL/min). TLC analyses were carried out using glass-coated silica gel 60 F_{254} (0.20 mm thickness) plates (Merck).

5.2.2 Plant Materials

The aerial parts of *C. guayanensis* were collected in August 2001 near Rio Cuao, Municipio Autana, in the Amazonian Region of Venezuela, and were identified by Prof. Anibal Castillo, Universidad Central de Venezuela, Caracas, Venezuela. A voucher specimen (No. VEN 299.338) was deposited at the Herbario Nacional de Venezuela, Caracas, Venezuela

The aerial parts of *F. apodanthera* were collected in March 2007 in Kolokanì (Koulikoro region, Mali), and were identified by Mr. Mamadou S. Dembele of the Departement Medicine Traditionelle (DMT), Bamako, Mali, where a voucher specimen (No. 1000) has been deposited.

5.2.3 Extraction and Bioassay-guided Isolation Procedures

All plants were extracted as previously reported (Braca et al. 2006)

The $CHCl_3$-MeOH extract of dried powdered aerial parts of *C. guayanensis* (560 g) showed a moderate inhibitory activity on VEGFs/Flt-1 interaction at a 100 mg/L concentration. Part of the $CHCl_3$-MeOH residue (10.0 g) was chromatographed on Sephadex LH-20 using MeOH as eluent; fractions of 8 mL were collected and grouped into 10 major fractions. The obtained fractions were assayed at 100-20 mg/L on VEGFs/Flt-1 complex and only fraction 10 showed inhibitory activity (100 mg/L, 70% of binding reduction). Thus, fraction 10 (276.4 mg) was separated through RP-HPLC with MeOH-H_2O

(2:3) as eluent to yield pure compounds 1 (14 mg, t_R = 25 min) and 2 (20 mg, t_R = 28 min).

Dried powdered aerial parts of *F. apodanthera* (300 g) were successively extracted for 48 h with *n*-hexane, $CHCl_3$, $CHCl_3$-MeOH (9:1), and MeOH, by exhaustive maceration (3 x 2 L), to yield 7.0, 13.0, 8.0, and 18.0 g of the respective residues. The MeOH extract showed good inhibitory activity on VEGFs/Flt-1 interaction at a concentration of 100 mg/L. This residue was fractionated by Sephadex LH-20 column chromatography, using MeOH as eluent to obtain 12 major fractions, combined on the basis of TLC analyses. The fractions were assayed at 100-20 mg/L on both hPlGF/Flt-1 and hVEGF-A/Flt-1 complexes. Fractions 10 and 11 were the most active, provoking at 100 mg/L a reduction of 60% of the binding of both PlGF/Flt-1 and VEGF-A/Flt-1. The fractions were further separated by RP-HPLC with MeOH-H_2O (38:62) to give pure compound 3 (5 mg, t_R = 18 min) from fraction 10 and pure compounds 4 (7 mg, t_R = 15 min) and 5 (8 mg, t_R = 16 min) from fraction 11, respectively.

Compound 1: red amorphous powder; $[\alpha]_D^{25}$ +40.8 (*c* 0.03, MeOH); UV (MeOH) λ_{max} (log ε) 230 (3.85), 280 (4.36) nm; CD (MeOH) $[\theta]_{278}$ – 10145, $[\theta]_{276}$ – 8700, $[\theta]_{246}$ 11828. ^{1}H and ^{13}C NMR, see Table 1; HRESIMS *m/z* 529.1485 $[M - H]^-$ (calcd. for $C_{30}H_{25}O_9$, 529.1499); ESI-MS *m/z* 529 $[M - H]^-$, 511 $[M - H - 18]^-$, 289 $[M - H - 240]^-$.

Compound 2: red amorphous powder; $[\alpha]_D^{25}$ +219.6 (*c* 0.01, MeOH); UV (MeOH) λ_{max} (log ε) 226 (3.90), 282 (4.06) nm; CD (MeOH) $[\theta]_{276}$ – 8450, $[\theta]_{246}$ + 7440. ^{1}H and ^{13}C NMR, see Table 1; HRESIMS *m/z* 529.1480 $[M - H]^-$ (calcd. for $C_{30}H_{25}O_9$, 529.1499); ESI-MS *m/z* 529 $[M - H]^-$, 289 $[M - H - 240]^-$.

5.2.4 Competitive ELISA Assays.

The competitive ELISA based assay for the screening of plant extracts and for dose-dependent experiments was performed by coating, on 96-well plates a recombinant form of Fc/VEGFR-1 at 0.5 µg/mL, 100 µL/well (the same volume was used for all subsequent steps), 16 h at room temperature. The plate was then blocked for 3 h at RT with 1% Bovine Serum Albumin (BSA) and the recombinant form of PlGF-1 at 5 ng/mL or the VEGF-A at 10 ng/mL concentration in PBS containing 0.1% BSA, 5 mM EDTA, 0.004% Tween 20 (PBET), was added and incubated for 1 h at 37 °C followed by 1 h at RT. A biotinylated anti PlGF-1 polyclonal antibody diluted in PBET at 300 ng/mL, or biotinylated antibody anti-VEGF-A diluted at 500 ng/mL, was added to the wells and incubated for 1 h at 37°C followed by 1 h at RT. A solution containing an avidin and biotinylated HRP macromolecular complex was prepared as suggested by the manufacturer (Vectastain *elite* ABC kit, Vector Laboratories, Burlingame, CA, USA) and added to the wells and incubated for 1 hr at RT followed by the HRP substrate composed of 1 mg/mL of *o*-phenylenediamine in 50 mM citrate phosphate buffer pH 5, 0.006% of H_2O_2, incubated for 40 min in the dark at RT. The reaction was blocked by adding 30 µL/well of 4 N H_2SO_4 and the absorbance measured at 490 nm on a microplate reader (BenchMark, Biorad Hercules, CA, USA). Plant extracts, extract fractions or purified compounds dissolved in DMSO were properly diluted and added to the wells along with the ligand. Each point was done in triplicate and the experiments were repeated two times.

5.2.5 Surface Plasmon Resonance Analyses

SPR analyses were performed using a Biacore 3000 optical biosensor equipped with research-grade CM5 sensor chips (Biacore AB, Uppsala, Sweden). Using this platform, two separate recombinant Hsp90 surfaces, a BSA surface and an unmodified reference surface, were prepared for

simultaneous analyses. Proteins (100 µg/mL in 10 mM NaOAc, pH 5.0) were immobilized on individual sensor chip surfaces at a flow rate of 5 µL/min using standard amine-coupling protocols[27] to obtain densities of 8–12 kRU. Compounds 1-5, as well as 17-DMAG and shepherdin used as positive controls, were dissolved in 100% DMSO to obtain 4 mM solutions, and diluted 1:200 (v/v) in PBS (10 mM NaH_2PO_4, 150 mM NaCl, pH 7.4) to a final DMSO concentration of 0.5%. Compounds were prepared as twofold dilutions into running buffer: for each sample, the complete binding study was performed using a six-point concentration series, typically spanning 0.025–1 µM, and triplicate aliquots of each compound concentration were dispensed into single-use vials. Included in each analysis were multiple blank samples of running buffer alone. Binding experiments were performed at 25 °C, using a flow rate of 50 µL/min, with 60 s monitoring of association and 200 s monitoring of dissociation. Simple interactions were adequately fit to a single-site bimolecular interaction model (A+B=AB), yielding a single K_D. Sensorgram elaborations were performed using the Biaevaluation software provided by Biacore AB.

5.2.6 Cell Culture, Proliferation, and Viability.

MCF-7 (Human breast adenocarcinoma cell line) and human lymphocyte cells T (Jurkat) were maintained in Dulbecco's modified Eagle medium (DMEM) supplemented with 10% (v/v) fetal bovine serum (FBS), 2 mM L-glutamine and antibiotics (100 U/mL penicillin, 100 µg/mL streptomycin) at 37 °C in a humidified atmosphere with 5% CO_2. To ensure logarithmic growth, cells were subcultured every two days. Cells were seeded in 96 well-plates at a cell density of 1 x 104/well (100 µl of a 1 x 105 cells/mL) and allowed to grow in the absence and in the presence of different concentrations of compounds 1-5. At 24, 48, and 72 h, the number of cells was quantified by using an MTT conversion assay.[28]

5.2.7 Chicken Chorioallantoic Membrane (CAM) Assay

The effect of 1 on angiogenesis was evaluated using the CAM assay, following a method described previously[29] with minor modifications. Fertilized chicken eggs were kept in a humidified egg incubator at 37 °C. The eggs were positioned horizontally and rotated several times. After 4 days of incubation, a 1 cm^2 window was carefully created on the broad side of the egg to assess the extent of embryonic blood vessels. The normal development was verified and embryos with malformations or dead embryos were excluded. Then, about 2 mL of albumen was aspirated from each egg through the small window. After removement of albumen, compound 1 (2.5, 5, and 10 µg) previously suspended in albumen, was applied (100 µL/egg) directly to the CAM surface through the small window. At least five eggs were used for each dose. Control eggs were treated with albumen (100 µL/egg). Retinoic acid (2 µg/egg) was used as positive control. After treatment, the eggs were reincubated for two days. At the end of incubation, each egg was observed under a Zeiss Stemi 2000-c microscope equipped with Axiocam MRc 5 Zeiss and the blood vessels were photographed. The antiangiogenic effects of 1 on the CAMs were quantified by counting the number of blood vessel branch points which were marked using an artistic software and finally expressed as percentage of inhibition using the following equation:

$$\text{Antiangiogenic activity (\%)} = 1 - (T/C) \times 100$$

T= number of blood vessel branch points in the CAMs treated with 1.

C= number of blood vessel branch points in the CAMs treated with albumen.

Statistical Analysis. All the reported values represent the mean ± standard deviation (SD) of at least two independent experiments performed in triplicate. Where necessary, data were statistically compared by *t*-test.

CHAPTER 6:

Other activity

Based on: Olivieri et al., J. Neurosci, 2011

6.1 Premise

During my PhD course, I was also involved in a project on “Ceruloplasmin oxidation, a feature of Parkinson's disease CSF, inhibits ferroxidase activity and promotes cellular iron retention” in the proteome biochemistry laboratory (San Raffaele Scientific Institute, Milan, Italy) of Prof. Massimo Alessio. This work was focused on the analysis of the modifications induced by the pro-oxidative environment of the cerebrospinal fluid from Parkinson’s and Alzheimer’s disease on ceruloplasmin. My contribution in this work has been recognized with the co-authorship in an article published in a peer-reviewed journal of primary importance in the field of neuroscience (Olivieri et al., J. Neurosci, 2011).

6.2 Project overview

Parkinson’s disease is a neurodegenerative disorder caused by oxidative damage, excitotoxicity, and inflammation (Dawson and Dawson, 2003; Litvan et al., 2007a, 2007b).

Oxidative stress is characterized by an imbalance between reactive oxygen species (ROS) and scavenging factors. Latter are represented principally by enzymes, low molecular weight antioxidant species and metal (iron and copper) transport systems (Carri et al., 2003). In the brain substantia nigra (SN), the most vulnerable region in Parkinson’s disease, there is a high iron concentration (Gotz et al., 2004); therefore it is especially sensitive to oxidative stress. Moreover, the dopamine metabolism of nigral neurons leads

to the production of hydrogen peroxide, which in turn can convert to hydroxyl radical when ferrous iron co-occurs (Lotharius and Brundin, 2002).

In PD, SN neuronal degeneration is related to increases in protein oxidation and in iron concentration (Oakley et al., 2007). Red-ox systems, such as protein-containing metal ions, exploit cyclical changes in their red-ox status as a way to resist oxidative stress.

One of these proteins is the copper-protein ceruloplasmin, which is secreted by the liver into plasma and by cells of the choroid plexus into cerebrospinal fluid (CSF) (Vassiliev et al., 2005). It is an extracellular ferroxidase that regulates cellular iron loading and export, and hence protects tissues from oxidative damage. It is resonable to think that in CSF modification of ceruloplasmin, which affect enzymatic activity, may be correlated to Parkinson's disease neurodegeneration (Rathore et al., 2008).

Using two-dimensional electrophoresis, we investigated ceruloplasmin patterns in the cerebrospinal fluid of human Parkinson's disease patients. Parkinson's disease ceruloplasmin profiles proved more acidic than those found in healthy controls and in other human neurological diseases (peripheral neuropathies, amyotrophic lateral sclerosis and Alzheimer's disease); degrees of acidity correlated with patients' pathological grading (figure 35).

Applying an unsupervised pattern recognition procedure to the two-dimensional electrophoresis images, we identified representative pathological clusters (figure 35).

In vitro oxidation of cerebrospinal fluid in two-dimensional electrophoresis generated a ceruloplasmin shift resembling that observed in Parkinson's disease, and co-occurred with an increase in protein carbonylation.

Likewise, increased protein carbonylation was observed in Parkinson's disease cerebrospinal fluid, and the same modification was directly identified in these samples on ceruloplasmin.

These results indicate that ceruloplasmin oxidation contributes to pattern modification in Parkinson's disease. From the functional point of view, ceruloplasmin oxidation caused a decrease in ferroxidase activity, which in turn promotes intracellular iron retention in neuronal cell lines as well as in primary neurons, which are more sensitive to iron accumulation. Accordingly, the presence of oxidized-ceruloplasmin in Parkinson's disease cerebrospinal fluid might be used as a marker for oxidative damage, and might provide new insights into the underlying pathological mechanisms.

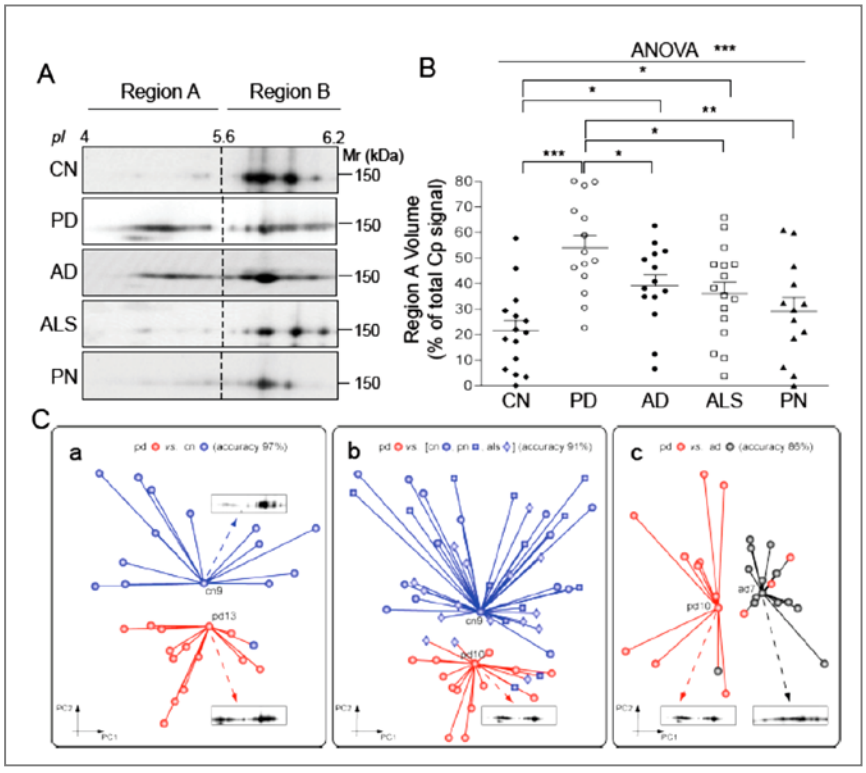

Fig.35. Cerebrospinal fluid (CSF) ceruloplasmin (Cp) 2DE profile discriminates Parkinson's disease (PD) from Alzheimer's disease (AD), amyotrophic lateral sclerosis (ALS), peripheral neuropathies (PN) and control subjects (CN). A) Representative results for Western Blot (WB) analysis performed with anti-Cp on 2DE-resolved proteins. On the basis of pI threshold value, Cp signal distribution was divided into two distinct areas, Regions A and B. B) Analysis of WB signal optical density value distribution in Region A, evaluated as a percentage of the total Cp signal. Data were analysed both by Student's t-test and by ANOVA. Single patient distributions as well as means and standard error are shown (PD n=14, CN n=15, AD n=14, ALS n= 16, PN n= 13) (*= p<0.05; **= p<0.005; ***= p<0.001). C) Unsupervised cluster

identification discriminates Cp pattern of PD patients from other groups. Dimensionality reduction of the anti-Cp WB images data set executed by Principal Component Analysis (the first two principal components, PC1 and PC2, are shown), and clusters of homogeneous subjects were identified by unsupervised affinity propagation cluster analysis. Red clusters are for PD attribution, blue and black clusters for non-PD attribution. Markers associated with sample names indicate the exemplars for the respective cluster. An original 2DE-WB image is displayed for each exemplar. a) Clustering of PD and CN. Sample cn13 proved to be misclassified. b) Clustering of PD, CN, PN, and ALS subjects. Five out of 58 samples were misclassified, from left to right, als7, als5, pn4, als10, pn6. c) Clustering of PD and AD patients. Four out of 28 samples proved to be misclassified (from left to right, ad8, pd13, pd14, pd11).

6.3 Material and methods

Patients

Having secured approval from the hospital's ethical review board, and informed consent from patients, we collected CSF samples (0.8-1 ml) by means of lumbar puncture. The analysed groups were: sporadic PD (n= 14), sporadic amyotrophic lateral sclerosis (ALS, n= 16), peripheral neuropathies (PN, n= 13), Alzheimer's disease (AD, n= 14) and healthy controls (CN, n= 15). Table 1 summarizes the demographic and clinical features of the patients and control subjects enrolled on this discovery study. All patients were at first diagnosis and drug-free. Current criteria for the diagnosis of PD (Italian-Neurological-Society, 2003), of ALS (Brooks, 1994) and of AD were used for the admission of patients into the study. PN diagnosis was as described in (Conti et al., 2005). The Unified Parkinson's Disease Rating Scale (UPDRS)) was used to grade the disease. ALS and PN samples were from aliquots collected for previous studies (Conti et al., 2005), while CSF from AD patients derived from the

Institute of Experimental Neuroscience bio-bank (INSPE, San Raffaele Scientific Institute). Exclusion criteria consisted in: HIV or HCV

seropositivity; the appearance of other neurodegenerative diseases or previous cerebral ischemic events; severe metabolic disorders (e.g. diabetes). Control CSF was obtained from patients who underwent lumbar puncture on account of a suspected neurological disease and who proved to be normal and free from pathological alterations after complete CSF analysis and thorough clinico-neuroimaging assessment. Sample selection ensured that age and gender distributions were homogeneous with those of the PD patients.

Two dimensional electrophoresis (2DE), Western blot and Image Analysis

Immediately after collection, the CSF samples were centrifuged at 4°C to eliminate cells, and protein concentrations were determined. The samples were then either immediately processed, or stored after acetone precipitation at -80°C in an N2- supplemented atmosphere in order to avoid oxidation. Protein samples (30 μg) were resuspended in 2DE buffer (8M Urea, 4% w/v CHAPS, 65 mM DTT, 0.2% v/v IPGbuffer 3-10 NL), and applied to 7cm IPG strips pH 3-10NL (GE Healthcare, Milan, Italy). The 2DE separations were performed as described in (Conti et al., 2008).

Proteins resolved by 2DE or by SDS-PAGE were electro-transferred onto nitrocellulose membranes and Western blot (WB) performed as described in (Conti et al., 2008) with an anti-human Cp antibody (Abcam, Cambridge, UK). Images were acquired by means of a laser densitometer (Molecular Dynamics, Sunnyvale, CA), and evaluation of relative abundance of Cp isoforms consisted in the analysis of optical density normalized to percentage by means of Progenesis PG240 software (Nonlinear dynamics, Newcastle, UK).

CSF oxidation by treatment with Fe-citrate and H2O2.

Proteins (100 μg) were oxidized by incubation (3 hrs at 37°C) with differing concentrations of hydrogen peroxide (1, 5 and 10 mM), and were subsequently

resolved by 2D-E or SDS-PAGE; Cp profile was identified by WB. For the assessment of correlation between specific oxidative modifications (carbonylation) and Cp *pI* shift, CSF proteins were incubated (5 hrs at 37°C) with 25 mM sodium ascorbate with or without 100 μM ferrous chloride to induce protein carbonylation (as indicated by the OxyBlot kit manufacturer) (Musci et al., 1993). Carbonylation was analyzed by means of the OxyBlot Protein Oxidation Detection Kit (Chemicon, USA) on the basis of carbonyl group derivatization with 2,4-dinitrophenilhydrazine (DNPH). Cp carbonylation was analyzed in 2 pools of CSF that were respectively harvested from all PD patients and from all CN subjects. Equal amounts (5μg) of CSF proteins were taken from each patient to generate a total 70μg of proteins per pool. After derivatization with DNPH, proteins were resolved either by 2DE or by SDS-PAGE, and carbonyl groups were detected by Western blot with an anti-DNPH antibody, while Cp profiles were detected by means of an anti-CP antibody on the same nitrocellulose membrane.

Densitometric analysis

Anti-Cp reactivity was quantified by laser densitometric analysis (Molecular Dynamics), as normalized by protein loading and total protein staining. The distribution of the Cp isoforms was evaluated by densitometric analysis of 2D spot optical density, which in turn was normalized as a percentage of total anti-Cp antibody reactivity. Signals obtained from Oxyblot were quantified by means of densitometric analysis, and normalized by total protein loading. Ferritin expression was evaluated by densitometric analysis, and normalized by β-tubulin expression for SH-SY5Y cell line, and by βIII-tubulin expression for primary neuron.

Statistical Analysis

Gender distribution was assessed by 2x2 contingency table analysis, which in turn used Fisher's exact test and two-tailed p value. Continuous data (age distribution, CSF protein concentration, and spot/band volume) were evaluated by unpaired Student's t-test, if the data passed the normality test for Gaussian distribution as assessed by the Kolmogorov-Smirnov test, or were evaluated by Mann Whitney test; two-tailed p value was used for the comparison of two means and standard error. Parametric one-way analysis of variance (ANOVA) was used to evaluate the statistical difference between three or more independent groups; post-analysis performed with Tukey's multiple comparison tests was included. The receiver operating characteristic (ROC) curve was used to define the ability of the assay to discriminate between groups, and to define the threshold value at which optical density (OD) gave the best ratio between sensitivity and specificity. Correlation analysis was evaluated as Pearson's coefficient (r). In all analyses, $p<0.05$ was considered to be statistically significant. The analysis was performed with Prism V4.03 software (GraphPad Inc., SanDiego, CA).

Image processing and unsupervised machine learning techniques for 2DEWestern

Denoising was executed by nonlinear spatial adaptive image filtering, and background removal was obtained by 3D-morphological operators (Cannistraci et al., 12 2009). After preprocessing, each 2DE-WB image was aligned by raw vectorization of its pixel intensity; each pixel intensity accordingly became a feature in a vector that characterized the Cp image sample. In order to implement the subsequent machine learning analysis, features (pixels) with small profile variance were filtered out to reduce the number of low informative features. Classification of Cp profiles was provided by the combined application of (i) unsupervised machine learning approaches

designed to reduce linear dimensionality and executed by principal component analysis (PCA), and of (ii) affinity propagation clustering as a clustering analysis tool (Cannistraci et al., 2010). Said tool was applied to the twodimensional projection space obtained as the outcome of dimensionality reduction.

References:

- Aebersold R., Mann M. Mass spectrometry-based proteomics. *Nature*, **2003,** 422, 198-207
- Ambati, B.K., Nozaki, M., Singh, N., Takeda, A., Jani, P.D., Suthar, T., Albuquerque, R.J., Richter, E., Sakurai, E., Newcomb, M.T., Kleinman, M.E., Caldwell, R.B., Lin, Q., Ogura, Y., Orecchia, A., Samuelson, D.A., Agnew, D.W., St Leger, J., Green, W.R., Mahasreshti, P.J., Curiel, D.T., Kwan, D., Marsh, H., Ikeda, S., Leiper, L.J., Collinson, J.M., Bogdanovich, S., Khurana, T.S., Shibuya, M., Baldwin, M.E., Ferrara, N., Gerber, H.P., De Falco, S., Witta, J., Baffi, J.Z., Raisler, B.J., Ambati, J. Corneal avascularity is due to soluble VEGF receptor-1. *Nature*. **2006,** 443, 993-7.
- Alitalo, K., Tammela, T., Petrova, T.V., Lymphangiogenesis in development and human disease. *Nature*. **2005**, 438, 946-53.
- Autiero M, Waltenberger J, Communi D, Kranz A, Moons L, Lambrechts D, Kroll J, Plaisance S, De Mol M, Bono F, Kliche S, Fellbrich G, Ballmer-Hofer K, Maglione D, Mayr-Beyrle U, Dewerchin M, Dombrowski S, Stanimirovic D, Van Hummelen P, Dehio C, Hicklin DJ, Persico G, Herbert JM, Communi D, Shibuya M, Collen D, Conway EM, Carmeliet P. Role of PlGF in the intra- and intermolecular cross talk between the VEGF receptors Flt1 and Flk1. *Nat Med*. **2003**, 9, 936-43.
- Bikfalvi A, Klein S, Pintucci G, Rifkin DB. The roles of proteases in angiogenesis. In: Bicknell R, Lewis CE, Ferrara N, editors. Tumor angiogenesis. *Oxford: Oxford University Press*, **1997**. p. 115–24.

- Blasi F. uPA, uPAR, PAI-1, key intersection of proteolytic, adhesive and chemotactic highways? *Immunol Today* **1997**;18:415–7.
- Braca, A.; Abdel-Razik, A. F.; Mendez, J.; De Tommasi, N. *J. Nat. Prod*. **2006**, *69*, 240-246.
- Brooks, B.R.El Escorial World Federation of Neurology criteria for the diagnosis of amyotrophic lateral sclerosis. Subcommittee on Motor Neuron Diseases/Amyotrophic Lateral Sclerosis of the World Federation of Neurology Research Group on Neuromuscular Diseases and the El Escorial "Clinical limits of amyotrophic lateral sclerosis" workshop contributors. *J Neurol Sci* , **1994**, 124, 96-107.
- Calzada F., Cerda-García-Rojas C.M., Meckes M., Cedillo-Rivera R., Bye R., Mata R. Geranins A and B, new antiprotozoal A-type proanthocyanidins from Geranium niveum. *J Nat Prod*. **1999,** 62, 705-9.
- Cannistraci CV, Montevecchi FM, Alessio M. Median-modified Wiener filter provides efficient denoising, preserving spot edge and morphology in 2-DE image processing. *Proteomics*, **2009**, 94908-4919.
- Cannistraci CV, Ravasi T, Montevecchi FM, Ideker T, Alessio M. Non-linear dimension reduction and clustering by minimun curvilinearity unfold 28 neuropathic pain and tissue embryological classes. *Bioinformatics*, **2010,** 26,i531- i539.
- Caporale, L. Darwin in the Genome: Molecular strategies in biological evolution. New York. Mc Graw Hill Companies, 2002.
- Carmeliet P. Angiogenesis in health and disease. *Nat Med*. **2003** Jun;9(6):653-60.
- Carmeliet, P. Manipulating angiogenesis in medicine. *J. Intern. Med.* **2004**, *561*, 255-538.

- Carmeliet, P. Angiogenesis in life, disease and medicine. *Nature*. **2005**, 438, 932-936.
- Carmeliet, P. and Jain, R. K. Molecular mechanisms and clinical applications of angiogenesis. *Nature*. **2011**, 473, 298–307.
- Carri MT, Ferri A, Cozzolino M, Calabrese L, Rotilio G Neurodegeneration in amyotrophic lateral sclerosis: the role of oxidative stress and altered homeostasis of metals. *Brain Res Bull*, **2003**, 61, 365-374.
- Conti A, Ricchiuto P, Iannaccone S, Sferrazza B, Cattaneo A, Bachi A, Reggiani A, Beltramo M, Alessio M. Pigment epithelium-derived factor is differentially expressed in peripheral neuropathies. *Proteomics*, 2005 5:4558-4567.
- Conti A, Iannaccone S, Sferrazza B, De Monte L, Cappa S, Franciotta D, Olivieri S, Alessio M Differential expression of ceruloplasmin isoforms in the cerebrospinal fluid of Amyotrophic Lateral Sclerosis patients. *Proteomics- Clin Appl*, **2008**, 2,1628-1637.
- Cooper M. A., Label-free screening of bio-molecular interactions *Anal Bioanal Chem* **2003**, 377, 834–842
- Cudmore, M.J., Hewett, P.W., Ahmad, S., Wang, K.Q., Cai, M., Al-Ani, B., Fujisawa, T., Ma, B., Sissaoui, S., Ramma, W., Miller, M.R., Newby, D.E., Gu, Y., Barleon, B., Weich, H., Ahmed, A. The role of heterodimerization between VEGFR-1 and VEGFR-2 in the regulation of endothelial cell homeostasis. *Nat Commun*. **2012**, 24, 3:972.
- De Falco S., Ruvoletto M.G., Verdoliva A., Ruvo M., Raucci A., Marino M,, Senatore S,, Cassani G,, Alberti A,, Pontisso P,, Fassina G. Cloning and expression of a novel hepatitis B virus-binding protein from HepG2 cells. *J Biol Chem*. **2001**, 276, 36613-23.

- De Falco, S. The discovery of placenta growth factor and its biological activity. *Exp Mol Med*. **2012,** 31, 44, 1–9.
- Di Palma, T., Tucci, M., Russo, G., Maglione, D., Lago, C.T., Romano, A., Saccone, S., Della Valle, G., De Gregorio, L., Dragani, T.A., Viglietto, G., Persico, M.G. The placenta growth factor gene of the mouse. *Mamm Genome* **1996**, 7, 6-12
- Dobson, C. M. Chemical space and biology. *Nature*. **2004**, 432, 824-828.
- Fenn, J.B., Mann, M., Meng, C.K., Wong, S.F., and Whitehouse, C.M.. Electrospray ionization for the mass spectrometry of large biomolecules. *Science* **1989**,246, 64–71.
- Ferrara, N., Gerber, H.P., LeCouter, J. The biology of VEGF and its receptors. *Nat Med*. **2003**, 9, 669-76.
- Fischer, C., Jonckx, B., Mazzone, M., Zacchigna, S., Loges, S., Pattarini, L., Chorianopoulos, E., Liesenborghs, L., Koch, M., De Mol, M., Autiero, M., Wyns, S., Plaisance, S., Moons, L., van Rooijen, N., Giacca, M., Stassen, J.M., Dewerchin, M., Collen, D., Carmeliet, P. Anti-PlGF inhibits growth of VEGF(R)-inhibitor-resistant tumors without affecting healthy vessels. Cell. **2007**, 131, 463-75.
- Fuchs, D., Winkelmann, I., Johnson, I.T., Mariman, E., Wenzel, U., Daniel, H. Proteomics in nutrition research: principles, technologies and applications. *Br J Nutr*. **2005**, 94, 302-14.
- Gevaert, K., Vandekerckhove, J. Protein identification methods in proteomics. *Electrophoresis*. **2000**, 21, 1145-54.
- Görg A, Drews O, Lück C, Weiland F, Weiss W. 2-DE with IPGs. *Electrophoresis*. **2009**, 30 Suppl 1:S122-32.

- Gotz ME, Double K, Gerlach M, Youdim MB, Riederer P The relevance of iron in the pathogenesis of Parkinson's disease. *Ann N Y Acad Sci* **2004**, 1012, 193- 208.
- Green, C.J., Lichtlen, P., Huynh, N.T., Yanovsky, M., Laderoute, K.R., Schaffner, W., Murphy, B.J. Placenta growth factor gene expression is induced by hypoxia in fibroblasts: a central role for metal transcription factor-1. *Cancer Res* **2001**, 61, 2696-703
- Henzel, W.J., Billeci, T.M., Stults, J.T., and Wong, S.C.. Identifying proteins from 2-dimensional gels by molecular mass searching of peptide-fragments in protein sequence databases. *Proc Natl Acad Sci U S A* **1993**, 90, 5011–5015
- Hochstrasser, D. F., Harrington, M. G., Hochstrasser, A. C., Miller,M. J., Merril, C. R., Anal. Biochem. 1988, 173, 424–435.
- Hsu J.Y., Wakelee H.A. Monoclonal antibodies targeting vascular endothelial growth factor: current status and future challenges in cancer therapy. *BioDrugs.* **2009**, 23, 289-304.
- Italian-Neurological-Society, The diagnosis of Parkinson's disease. Neurol Sci 2003, 24 Suppl 3:S157-164.
- Katanasaka, Y., Asai, T., Naitou, H., Ohashi, N., Oku, N., Proteomic Characterization of Angiogenic Endothelial Cells Stimulated with Cancer Cell-Conditioned Medium *Biological and Pharmaceutical Bulletin* **2007**, 30, 2300-2307
- Kirkpatrick, P. Guided by nature. Nature Reviews Drug Discovery. **2003** 2, 607.
- Koch S, Tugues S, Li X, Gualandi L, Claesson-Welsh L. Signal transduction by vascular endothelial growth factor receptors. *Biochem J.* **2011**, 437,169-83.

- Kubota Y. Tumor Angiogenesis and Anti-angiogenic Therapy *Keio J Med* **2012**; 61, 47–56.
- Liekens, S., De Clercq, E., Neyts, J. Angiogenesis: regulators and clinical applications. *Biochem Pharmacol*. **2001**, 61, 253-70.
- Lotharius J, Brundin P Pathogenesis of Parkinson's disease: dopamine,
- vesicles and alpha-synuclein. *Nat Rev Neurosci*, **2002**, 3,932-942.
- Luttun, A., Tjwa, M., Moons, L., Wu, Y., Angelillo-Scherrer, A., Liao, F., Nagy, J.A., Hooper, A., Priller, J., De Klerck, B., Compernolle, V., Daci, E., Bohlen, P., Dewerchin, M., Herbertm J.M., Fava, R., Matthys, P., Carmeliet, G., Collen, D., Dvorak, H.F., Hicklin, D.J., Carmeliet, P. Revascularization of ischemic tissues by PlGF treatment, and inhibition of tumor angiogenesis, arthritis and atherosclerosis by anti-Flt1. *Nat Med* **2002**, 8, 831-40
- Maglione, D., Guerriero, V., Viglietto, G., Ferraro, M.G., Aprelikova, O., Alitalo, K., Del Vecchio, S., Lei, K.J., Chou, J.Y., Persico, M.G. Two alternative mRNAs coding for the angiogenic factor, placenta growth factor (PlGF), are transcribed from a single gene of chromosome 14. *Oncogene* **1993a**; 8, 925-31
- Maglione, D., Guerriero, V., Rambaldi, M., Russo, G., Persico, M.G. Translation of the placenta growth factor mRNA is severely affected by a small open reading frame localized in the 5' untranslated region. *Growth Factors* **1993b**, 8, 141-52
- Mann, M., Jensen, O.N. Proteomic analysis of post-translational modifications. *Nat Biotechnol*. **2003**, 21, 255-61.
- Mignatti P, Rifkin DB. Plasminogen activators and matrix metalloproteinases in angiogenesis. *Enzyme Protein* **1996**;49:117–37.

- Mole, D.R., Maxwell, P.H., Pugh, C.W., Ratcliffe, P.J. Regulation of HIF by the von Hippel-Lindau tumour suppressor: implications for cellular oxygen sensing. *IUBMB Life*. **2001**, 52, 43-7.
- Monteoliva L., Albar J.P., Differential proteomics: an overview of gel and non-gel based approaches. *Brief Funct Genomic Proteomic*. **2004**, 3, 220-39.
- Mortz, E., Krogh, T. N., Vorum, H., Gorg, A., Proteomics 2001, 1, 1359–1363.
- Neufeld, G., Cohen, T., Gengrinovitch, S., Poltorak, Z. Vascular endothelial growth factor (VEGF) and its receptors. *FASEB J*. **1999**, 13, 9-22.
- Newman, D.J., Cragg, G.M. Natural Products as Sources of New Drugs over the Period 1981−2002. *J. Nat. Prod.* **2003**, 66, 1022–1037.
- Oakley AE, Collingwood JF, Dobson J, Love G, Perrott HR, Edwardson JA, Elstner M, Morris CM Individual dopaminergic neurons show raised iron levels in Parkinson disease. *Neurology* **2007**, 68,1820-1825.
- Olivieri, S., Conti, A., Iannaccone, S., Cannistraci, C.V., Campanella, A., Barbariga, M., Codazzi, F., Pelizzoni, I., Magnani, G., Pesca, M., Franciotta, D., Cappa, S.F., Alessio, M. Ceruloplasmin oxidation, a feature of Parkinson's disease CSF, inhibits ferroxidase activity and promotes cellular iron retention. *J Neurosci.* **2011**, 31, 18568-77.
- Otrock, Z.K., Makarem, J.A., Shamseddine, A.I. Vascular endothelial growth factor family of ligands and receptors: review. *Blood Cells Mol Dis*. **2007**, 38, 258-68.
- Oura H, Bertoncini J, Velasco P, Brown LF, Carmeliet P, Detmar M. A critical role of placental growth factor in the induction of inflammation and edema formation. *Blood* **2003**, 101:560-7

- Pandey, A., Mann, M. Proteomics to study genes and genomes. *Nature.* **2000**, 405, 837-46.
- Park, J.E., Keller, G.A., Ferrara, N. The vascular endothelial growth factor (VEGF) isoforms: differential deposition into the subepithelial extracellular matrix and bioactivity of extracellular matrix-bound VEGF. *Mol Biol Cell*. **1993**, 4, 1317–1326.
- Patterson, S.D., Aebersold, R.H. Proteomics: the first decade and beyond. *Nat Genet*. **2003**, 33, 311-23.
- Pavlakovic, H., Becker, J., Albuquerque, R., Wilting, J., Ambati, J. Soluble VEGFR-2: an antilymphangiogenic variant of VEGF receptors. *Ann N Y Acad Sci*. **2010,** 1207, 7-15. Rahimi, N. Vascular endothelial growth factor receptors: molecular mechanisms of activation and therapeutic potentials. *Exp Eye Res.* **2006**, 83, 1005-16.
- Pawlowska, Z, Baranska, P., Jerczynska, H., Koziolkiewicz, W,. Cierniewski, C.S., Heat shock proteins and other components of cellular machinery for protein synthesis are up-regulated in vascular endothelial cell growth factor-activated human endothelial cells. P*roteomics* **2005**, 5, 1217 - 1227
- Pesca MS., Dal Piaz F., Sanogo R., Vassallo A., Bruzual de Abreu M., Rapisarda A., Germanò M.P., Certo G., De Falco S., De Tommasi N., Braca A. Bioassay-Guided Isolation of Proanthocyanidins with Antiangiogenic Activities. *J Nat Prod.* **2012**,
- Pieroni, E., de la Fuente van Bentem, S., Mancosu, G., Capobianco, E., Hirt, H., de la Fuente, A. Protein networking: insights into global functional organization of proteomes. *Proteomics*. **2008** 8, 799-816.
- Ponticelli S., Marasco D., Tarallo V., Albuquerque R.J., Mitola S., Takeda A., Stassen J.M., Presta M., Ambati J., Ruvo M., De Falco S. Modulation of angiogenesis by a tetrameric tripeptide that antagonizes

vascular endothelial growth factor receptor 1. *J Biol Chem*. **2008,** 283, 34250-9

- Preisinger, C., von Kriegsheim, A., Matallanas, D., Kolch, W. Proteomics and phosphoproteomics for the mapping of cellular signalling networks. *Proteomics*. **2008** 8, 4402-15.
- Rabilloud T. Two-dimensional gel electrophoresis in proteomics: old, old fashioned, but it still climbs up the mountains. *Proteomics*. **2002,** 2, 3-10.
- Rathore KI, Kerr BJ, Redensek A, Lopez-Vales R, Jeong SY, Ponka P, David S Ceruloplasmin protects injured spinal cord from iron-mediated
- oxidative damage. *J Neurosci*, **2008,** 28, 12736-12747.
- Ribatti D., Vacca A., Roncali L., Dammacco F. The chick embryo chorioallantoic membrane as a model for in vivo research on angiogenesis. *Int J Dev Biol*. **1996**, 40, 1189-97
- Ribatti D., Nico B., Vacca A., Roncali L., Burri P.H., Djonov V. Chorioallantoic membrane capillary bed: a useful target for studying angiogenesis and anti-angiogenesis in vivo. *Anat Rec.* **2001** 264, 317-24.
- Roepstorff P. Mass spectrometry based proteomics, background, status and future needs. *Protein Cell.* **2012,** 3, 641-7
- Rosén, J., Gottfries, J., Muresan, S., Backlund, A., Oprea, T.I. Novel Chemical Space Exploration via Natural Products. *J. Med. Chem*. **2009**, 52, 1953–1962.
- Roy, H., Bhardwaj, S., Ylä-Herttuala, S. Biology of vascular endothelial growth factors. *FEBS Lett.* 2006, 580, 2879-87.
- Selvaraj SK, Giri RK, Perelman N, Johnson C, Malik P, Kalra VK. Mechanism of monocyte activation and expression of proinflammatory cytochemokines by placenta growth factor. *Blood* **2003**, 102, 1515-24

- Semenza G. Signal transduction to hypoxia-inducible factor 1. *Biochem Pharmacol*. **2002** 64, 993-8.
- Semenza, G.L. Vasculogenesis, angiogenesis, and arteriogenesis: Mechanisms of blood vessel formation and remodeling. *J. Cell. Biochem.* 2007, 102, 840-847.
- Shaw, M.M., Riederer, B.M. Sample preparation for two-dimensional gel electrophoresis. *Proteomics*. **2003**, 3, 1408-17.
- Shen, Y., Tolić, N., Hixson, K. K., Purvine, S. O., Paša-Tolić, L., Qian, W., Adkins, J.N., Ronald J. Moore, Smith, R. D. Proteome-wide identification of proteins and their modifications with decreased ambiguities and improved false discovery rates using unique sequence tags. *Anal Chem.* **2008**, 80, 1871–1882
- Shevchenko, A., Tomas, H., Havli, J., Olsen J.V., Mann M. In-gel digestion for mass spectrometric characterization of proteins and proteomes *Nature Protocols* **2007,** 1, 2856 - 2860
- Shibuya, M. Vascular endothelial growth factor receptor-1 (VEGFR-1/Flt-1): a dual regulator for angiogenesis. *Angiogenesis*. **2006**, 9, 225-30.
- Shibuya, M. Vascular endothelial growth factor and its receptor system: physiological functions in angiogenesis and pathological roles in various diseases. *J Biochem*. **2013,** 153, 13-9.
- Shojaei, F. Anti-angiogenesis therapy in cancer: current challenges and future perspectives. *Cancer Lett*. **2012**, 320, 130-7.
- Tammela, T., Enholm, B., Alitalo, K., Paavonen K. The biology of vascular endothelial growth factors. *j.cardiores.* **2005,** 65, 550– 563
- Tarallo, V., Vesci, L., Capasso, O., Esposito, M.T., Riccioni, T., Pastore, L., Orlandi, A., Pisano, C., De Falco, S. A placental growth factor variant unable to recognize vascular endothelial growth factor

(VEGF) receptor-1 inhibits VEGFdependent tumor angiogenesis via heterodimerization. *Cancer Res* **2010**, 70, 1804-13

- Tarallo, V., Lepore, L., Marcellini, M., Dal Piaz, F., Tudisco, L., Ponticelli, S., Wendelboe, F., Roepstorff, P. , Orlandi, A., Pisano, C., De Tommasi, N., De Falco, S. The Biflavonoid Amentoflavone Inhibits Neovascularization Preventing the Activity of Proangiogenic Vascular Endothelial Growth Factors. *The Journal of Biological Chemistry* **2011**, 286, 19641-19651.
- Tjwa, M., Luttun, A., Autiero, M., Carmeliet, P. VEGF and PlGF: two pleiotropic growth factors with distinct roles in development and homeostasis. *Cell Tissue Res*. **2003**, 314, 5-14.
- Tonra J.R., Hicklin D.J., Targeting the vascular endothelial growth factor pathway in the treatment of human malignancy. *Immunol Invest.* **2007**;36, 3-23.
- Tugues, S., Koch, S., Gualandi, L., Li X, Claesson-Welsh, L. Vascular endothelial growth factors and receptors: anti-angiogenic therapy in the treatment of cancer. *Mol Aspects Med*. **2011**, 32, 88-111.
- Vassiliev V, Harris ZL, Zatta P Ceruloplasmin in neurodegenerative diseases. *Brain Res Brain Res Rev* **2005**, 49,633-640.
- Weiss W, Görg A. High-resolution two-dimensional electrophoresis. *Methods Mol Biol.* **2009,** 564, 13-32.
- Westermarck J, Kahari VM. Regulation of matrix metalloproteinase expression in tumor invasion. *FASEB J* **1999**;13:781–92.
- Wilkins, M.R., Sanchez, J.C., Gooley, A.A., Appel, R.D., Humphery-Smith, I., Hochstrasser, D.F., Williams, K.L. Progress with proteome projects: why all proteins expressed by a genome should be identified and how to do it. *Biotechnol Genet Eng Rev*. **1996**; 13, 19-50.

- Wulfkuhle J.D., Paweletz C.P., Steeg P.S., Petricoin E.F. 3rd, Liotta L. Proteomic approaches to the diagnosis, treatment, and monitoring of cancer. *Adv Exp Med Biol*. **2003**, 532, 59-68
- Zhang H, Palmer R, Gao X, Kreidberg J, Gerald W, Hsiao L, Jensen RV, Gullans SR, Haber DA. Transcriptional activation of placental growth factor by the forkhead/winged helix transcription factor FoxD1. *Curr Biol* **2003**, 13, 1625-9